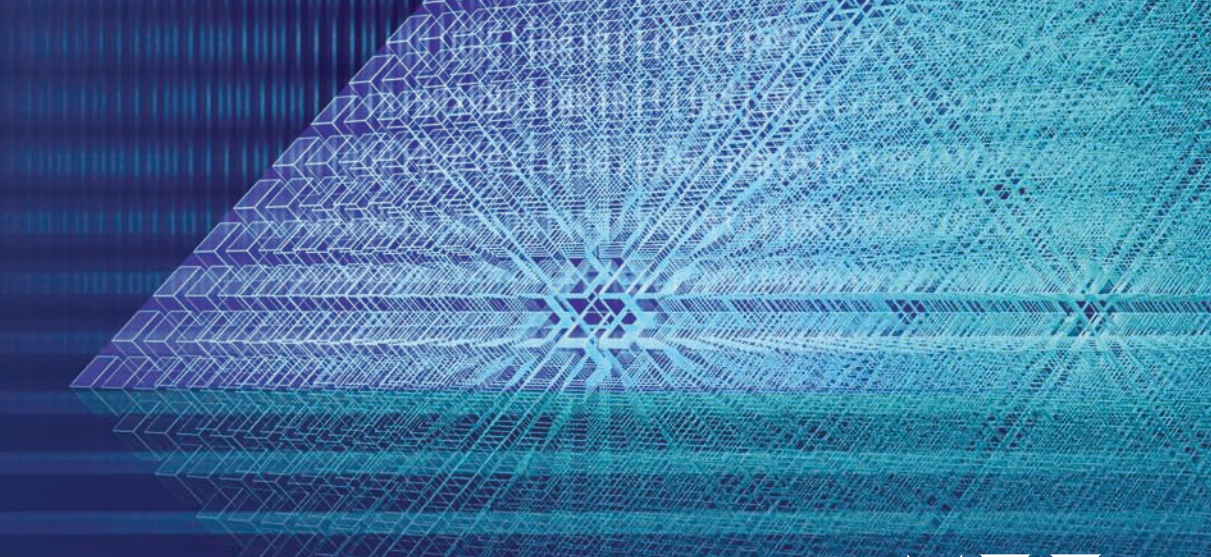

TECHNICAL REPORTS SERIES NO. 452

International Reactor Dosimetry File 2002 (IRDF-2002)

IAEA
International Atomic Energy Agency

INTERNATIONAL REACTOR DOSIMETRY FILE 2002 (IRDF-2002)

The following States are Members of the International Atomic Energy Agency:

AFGHANISTAN
ALBANIA
ALGERIA
ANGOLA
ARGENTINA
ARMENIA
AUSTRALIA
AUSTRIA
AZERBAIJAN
BANGLADESH
BELARUS
BELGIUM
BELIZE
BENIN
BOLIVIA
BOSNIA AND HERZEGOVINA
BOTSWANA
BRAZIL
BULGARIA
BURKINA FASO
CAMEROON
CANADA
CENTRAL AFRICAN REPUBLIC
CHAD
CHILE
CHINA
COLOMBIA
COSTA RICA
CÔTE D'IVOIRE
CROATIA
CUBA
CYPRUS
CZECH REPUBLIC
DEMOCRATIC REPUBLIC OF THE CONGO
DENMARK
DOMINICAN REPUBLIC
ECUADOR
EGYPT
EL SALVADOR
ERITREA
ESTONIA
ETHIOPIA
FINLAND
FRANCE
GABON
GEORGIA
GERMANY
GHANA
GREECE
GUATEMALA
HAITI
HOLY SEE
HONDURAS
HUNGARY
ICELAND
INDIA
INDONESIA
IRAN, ISLAMIC REPUBLIC OF
IRAQ
IRELAND
ISRAEL
ITALY
JAMAICA
JAPAN
JORDAN
KAZAKHSTAN
KENYA
KOREA, REPUBLIC OF
KUWAIT
KYRGYZSTAN
LATVIA
LEBANON
LIBERIA
LIBYAN ARAB JAMAHIRIYA
LIECHTENSTEIN
LITHUANIA
LUXEMBOURG
MADAGASCAR
MALAYSIA
MALI
MALTA
MARSHALL ISLANDS
MAURITANIA
MAURITIUS
MEXICO
MONACO
MONGOLIA
MOROCCO
MOZAMBIQUE
MYANMAR
NAMIBIA
NETHERLANDS
NEW ZEALAND
NICARAGUA
NIGER
NIGERIA
NORWAY
PAKISTAN
PANAMA
PARAGUAY
PERU
PHILIPPINES
POLAND
PORTUGAL
QATAR
REPUBLIC OF MOLDOVA
ROMANIA
RUSSIAN FEDERATION
SAUDI ARABIA
SENEGAL
SERBIA
SEYCHELLES
SIERRA LEONE
SINGAPORE
SLOVAKIA
SLOVENIA
SOUTH AFRICA
SPAIN
SRI LANKA
SUDAN
SWEDEN
SWITZERLAND
SYRIAN ARAB REPUBLIC
TAJIKISTAN
THAILAND
THE FORMER YUGOSLAV REPUBLIC OF MACEDONIA
TUNISIA
TURKEY
UGANDA
UKRAINE
UNITED ARAB EMIRATES
UNITED KINGDOM OF GREAT BRITAIN AND NORTHERN IRELAND
UNITED REPUBLIC OF TANZANIA
UNITED STATES OF AMERICA
URUGUAY
UZBEKISTAN
VENEZUELA
VIETNAM
YEMEN
ZAMBIA
ZIMBABWE

The Agency's Statute was approved on 23 October 1956 by the Conference on the Statute of the IAEA held at United Nations Headquarters, New York; it entered into force on 29 July 1957. The Headquarters of the Agency are situated in Vienna. Its principal objective is "to accelerate and enlarge the contribution of atomic energy to peace, health and prosperity throughout the world".

TECHNICAL REPORTS SERIES No. 452

INTERNATIONAL REACTOR DOSIMETRY FILE 2002 (IRDF-2002)

INTERNATIONAL ATOMIC ENERGY AGENCY
VIENNA, 2006

COPYRIGHT NOTICE

Sales and Promotion, Publishing Section
International Atomic Energy Agency
Wagramer Strasse 5
P.O. Box 100
1400 Vienna, Austria
fax: +43 1 2600 29302
tel.: +43 1 2600 22417
email: sales.publications@iaea.org
http://www.iaea.org/books

Printed by the IAEA in Austria
November 2006
STI/DOC/010/452

IAEA Library Cataloguing in Publication Data

International Reactor Dosimetry File 2002 : IRDF-2002 . — Vienna : International Atomic Energy Agency, 2006.
p. ; 24 cm. — (Technical reports series, ISSN 0074–1914 ; 452)
STI/DOC/010/452
ISBN 92–0–105106–9
Includes bibliographical references.

1. Neutrons — Measurement. 2. Neutron cross sections — Measurement. 3. Radiation dosimetry. I. International Atomic Energy Agency. II. Series: Technical reports series (International Atomic Energy Agency) ; 452.

IAEAL 06–00460

FOREWORD

An accurate and complete knowledge of nuclear data for reactor dosimetry is essential for improving assessments of the service life of reactor pressure vessels in nuclear power plants. This information also has important uses in other neutron metrology applications, such as boron neutron capture therapy, therapeutic uses of medical radioisotopes, nuclear physics measurements and reactor safety studies.

The International Nuclear Data Committee (INDC) is the primary advisory body to the IAEA on its nuclear data programmes. At a biennial meeting in 2000, the INDC recommended that the IAEA support a new, updated release of the International Reactor Dosimetry File. As a consequence of this recommendation, a data development project, the International Reactor Dosimetry File (IRDF-2002), was initiated in 2001. Prior to the approval of this project by the IAEA, several consultants had together defined the scope, objectives and tasks of this project. Each participant assumed responsibility for the implementation of specific tasks. The results of their research work were discussed and approved in a series of technical meetings.

The principal objective of the project was to prepare and distribute a standardized, updated and benchmarked cross-section library of neutron dosimetry reactions, with related uncertainty information, for use in the service lifetime assessment of nuclear power reactors. A substantial amount of work and effort by the participants ensured that this aim was achieved. Additionally, P.K. McLaughlin prepared and assembled the files, and A. Trkov provided significant technical advice. The IAEA officer responsible for this report and the resulting database was R. Paviotti-Corcuera of the Division of Physical and Chemical Sciences.

EDITORIAL NOTE

Although great care has been taken to maintain the accuracy of information contained in this publication, neither the IAEA nor its Member States assume any responsibility for consequences which may arise from its use.

The use of particular designations of countries or territories does not imply any judgement by the publisher, the IAEA, as to the legal status of such countries or territories, of their authorities and institutions or of the delimitation of their boundaries.

The mention of names of specific companies or products (whether or not indicated as registered) does not imply any intention to infringe proprietary rights, nor should it be construed as an endorsement or recommendation on the part of the IAEA.

Contributing authors

O. Bersillon	Commissariat à l'énergie atomique, Bruyères-le-Châtel, France
L.R. Greenwood	Pacific Northwest Laboratory, United States of America
P.J. Griffin	Sandia National Laboratories, United States of America
W. Mannhart	Physikalisch-Technische Bundesanstalt, Germany
H.J. Nolthenius	Institute of Nuclear Techniques, Budapest University of Technology and Economics, Hungary
R. Paviotti-Corcuera	International Atomic Energy Agency
K.I. Zolotarev	Institute of Physics and Power Engineering, Russian Federation
E.M. Zsolnay	Institute of Nuclear Techniques, Budapest University of Technology and Economics, Hungary

Technical assistance

P.K. McLaughlin	International Atomic Energy Agency
A. Trkov	International Atomic Energy Agency

CONTENTS

1. INTRODUCTION

R. Paviotti-Corcuera, E.M. Zsolnay

The most recently tested version of the International Reactor Dosimetry File, IRDF-90 Version 2 (IRDF-90.2), was released in 1993. Most of the evaluations used in this file were prepared in the mid-1980s, and in the meantime a large amount of new experimental data has become available, along with two new national reactor dosimetry libraries (the Russian Reactor Dosimetry File (RRDF-98) and the Japanese Evaluated Nuclear Data Library (JENDL/D-99)). The cross-sections and related uncertainties for several reactions in these libraries may be of better quality than the data in the older IRDF-90 file. These developments have resulted in different cross-section values being applied to the evaluation of experimental data, creating difficulties in comparing the results of reactor dosimetry calculations from the same types of nuclear facility. Therefore, there has been a strong demand from the reactor dosimetry community for an updated and standardized version of the IRDF.

The IAEA has in the past supported similar efforts to improve the quality of data for reactor dosimetry applications; some examples are documented in Refs [1.1–1.11]. A major objective of the present data development project was to prepare and distribute a standardized, updated and tested reactor dosimetry cross-section library accompanied by uncertainty information (IRDF-2002) for use in service life assessments of nuclear power reactors. In order to achieve this objective, two technical meetings were organized. Both meetings were held at the IAEA in Vienna. The first meeting took place from 27 to 29 August 2002, the second from 1 to 3 October 2003 [1.12, 1.13]. Recommendations were made concerning the following topics and the preparation of the library: reactions to be included, requirements for new evaluations or revisions, nuclear decay data, radiation damage data, testing of the data in benchmark fields and inclusion of computer codes.

The participants emphasized that good quality nuclear data for reactor dosimetry are essential to improve assessments of the service life of reactor pressure vessels. Accurate cross-section data are also essential in other neutron metrology applications such as boron neutron capture therapy, therapeutic uses of medical radioisotopes, nuclear physics measurements and reactor safety studies.

The work undertaken within the project included the following tasks:

(a) Detailed analyses and comparisons of the cross-section data and the related uncertainty information present in different reactor dosimetry and general purpose libraries, including IRDF-90.2, JENDL/D-99 and

RRDF-98, and the most recent releases of ENDF/B-VI, JEFF-3.0 and CENDL-2. Comparisons were also made of the calculated integral cross-section data with experimental reaction rates in standard neutron fields.

(b) Selection of the best quality cross-section information based on the above comparisons.

(c) Evaluation and testing of new reaction cross-sections, as requested by the reactor dosimetry community for extension of the library.

(d) Selection of evaluated and up to date nuclear decay characteristics and isotopic abundances.

(e) Testing of important dosimetry cross-sections in reference benchmark neutron fields.

Although the release of IRDF-2002 and publication of the related documentation occurred after 2002, participants attending the second Technical Meeting decided to retain the title IRDF-2002, since the library has been referred to as this in the open literature.

A CD-ROM containing the full contents of IRDF-2002 accompanies this report. Updated versions of this library will also be released by the IAEA on CD-ROM.

1.1. CONTENTS OF THE LIBRARY

IRDF-2002 contains the best quality data for reactor dosimetry applications available at the time of preparation. These data include cross-sections and related uncertainties, nuclear decay parameters for the reaction product nuclei and abundances of the target nuclides. This is the first time that the decay parameters and abundances have been presented in the IRDF library.

IRDF-2002 consists of three main data sets:

(a) Multigroup data:
  (i) Cross-section data for 66 neutron activation (and fission) reactions, along with uncertainties in the form of covariance information.
  (ii) Total cross-sections of three types of cover material, boron, cadmium and gadolinium, without uncertainty information.
  (iii) Radiation damage cross-sections of the following elements and compounds: iron dpa cross-section (American Society for Testing and Materials (ASTM) standard E693-01); dpa cross-section for a special steel composition (Euratom); dpa cross-sections for chromium and nickel (IRDF-90), for silicon (ASTM standard E722-94) and for GaAs displacement (ASTM standard E722-94).

(b) Pointwise data:
  (i) All dosimetry cross-sections listed above, accompanied by uncertainty information except for radiation damage cross-sections;
  (ii) Total cross-sections of all of the target nuclides present in the library.
(c) Nuclear data:
  (i) Decay data for all reaction product nuclei of interest;
  (ii) Isotopic abundances for all target nuclei of interest.

Pointwise cross-section data are given in the ENDF-6 format, while multigroup data are supplied as SAND II 640 energy group structure (simplified form of ENDF-6). The neutron temperature in both cases is 300 K. However, multigroup cross-section data were also generated for a neutron temperature of 0 K, and compared with the corresponding values obtained at 300 K; the differences between these two files were in most cases smaller than 1% and within the uncertainties of the data treatment. The multigroup cross-section data are fully characterized within this report, and all of the results presented in the various sections are based on this form of the IRDF-2002 library.

Table 1.1 lists the reactions contained in IRDF-2002, together with the origin of the corresponding cross-section data. The selection procedure applied to the cross-sections for inclusion in the library is described in Sections 3–6. The corresponding integral data for the cross-sections present in the file (e.g. cross-sections at 2200 m/s, the resonance integrals and the ^{252}Cf fission spectrum averaged cross-sections) are given in Table 6.2 in Section 6.

TABLE 1.1. CONTENTS OF IRDF-2002, AND SOURCES OF THE DATA

Reaction	Selected source	Reaction	Selected source
^{6}Li(n,t)^{4}He	IRDF-90 [a]	^{65}Cu(n,2n)^{64}Cu	IRDF-90 [a]
^{10}B(n,α)^{7}Li	IRDF-90	^{64}Zn(n,p)^{64}Cu	IRDF-90
^{19}F(n,2n)^{18}F	RRDF-98 (u)	^{75}As(n,2n)^{74}As	RRDF-98 (u)
^{23}Na(n,γ)^{24}Na [b]	IRDF-90 [a]	^{89}Y(n,2n)^{88}Y	JENDL/D-99
^{23}Na(n,2n)^{22}Na	JENDL/D-99 (u)	^{90}Zr(n,2n)^{89}Zr	IRDF-90
^{24}Mg(n,p)^{24}Na	IRDF-90	^{93}Nb(n,2n)^{92}Nb^{m}	RRDF-98
^{27}Al(n,p)^{27}Mg	RRDF-98 (n)	^{93}Nb(n,n′)^{93}Nb^{m}	RRDF-98
^{27}Al(n,α)^{24}Na	IRDF-90	^{93}Nb(n,γ)^{94}Nb [b]	IRDF-90 [a]
^{31}P(n,p)^{31}Si	IRDF-90	^{103}Rh(n,n′)^{103}Rh^{m}	RRDF-98 (n)
^{32}S(n,p)^{32}P	IRDF-90	^{109}Ag(n,γ)^{110}Ag^{m}	IRDF-90
^{45}Sc(n,γ)^{46}Sc	IRDF-90	^{115}In(n,2n)^{114}In^{m}	IRDF-90 [a]

TABLE 1.1. CONTENTS OF IRDF-2002, AND SOURCES OF THE DATA (cont.)

Reaction	Selected source	Reaction	Selected source
^{46}Ti(n,2n)^{45}Ti	RRDF-98 (u)	^{115}In(n,n′)^{115}In^{m}	RRDF-98 (n)
^{46}Ti(n,p)^{46}Sc	RRDF-98 (u)	^{115}In(n,γ)^{116}In^{m} [b]	ENDF/B-VI
^{47}Ti(n,x)^{46}Sc [c]	RRDF-98 (u)	^{127}I(n,2n)^{126}I	IRDF-90
^{47}Ti(n,p)^{47}Sc	IRDF-90	^{139}La(n,γ)^{140}La	RRDF-98 (n)
^{48}Ti(n,x)^{47}Sc [c]	RRDF-98 (u)	^{141}Pr(n,2n)^{140}Pr	RRDF-98 (u)
^{48}Ti(n,p)^{48}Sc	RRDF-98 (u)	^{169}Tm(n,2n)^{168}Tm	JENDL/D-99
^{49}Ti(n,x)^{48}Sc [c]	RRDF-98 (u)	^{181}Ta(n,γ)^{182}Ta [b]	JENDL/D-99
^{51}V(n,α)^{48}Sc	RRDF-98 (u)	^{186}W(n,γ)^{187}W	RRDF-98 (n)
^{52}Cr(n,2n)^{51}Cr	IRDF-90	^{197}Au(n,2n)^{196}Au	IRDF-90
^{55}Mn(n,γ)^{56}Mn	IRDF-90 [a]	^{197}Au(n,γ)^{198}Au	IRDF-90 [a]
^{54}Fe(n,2n)^{53}Fe	RRDF-98 (u)	^{199}Hg(n,n′)^{199}Hg^{m}	JENDL/D-99 (u)
^{54}Fe(n,α)^{51}Cr	RRDF-98 (u)	^{204}Pb(n,n′)^{204}Pb^{m}	RRDF-98 (n)
^{54}Fe(n,p)^{54}Mn	IRDF-90 [a]	^{232}Th(n,γ)^{233}Th [b]	IRDF-90
^{56}Fe(n,p)^{56}Mn	RRDF-98 (u)	^{232}Th(n,f)	IRDF-90
^{58}Fe(n,γ)^{59}Fe	JENDL/D-99 (u)	^{235}U(n,f)	IRDF-90
^{59}Co(n,2n)^{58}Co	IRDF-90	^{238}U(n,f)	JENDL/D-99
^{59}Co(n,α)^{56}Mn	RRDF-98 (u)	^{238}U(n,γ)^{239}U	IRDF-90 [a]
^{59}Co(n,γ)^{60}Co	IRDF-90 [a]	^{237}Np(n,f)	RRDF-98 (n)
^{58}Ni(n,2n)^{57}Ni	JEFF 3.0	^{239}Pu(n,f)	JENDL/D-99
^{58}Ni(n,p)^{58}Co	RRDF-98 (n)	^{241}Am(n,f)	JENDL/D-99
^{60}Ni(n,p)^{60}Co	ENDF/B-VI	^{nat}B(n,x) [d]	ENDF/B-VI
^{63}Cu(n,2n)^{62}Cu	ENDF/B-VI	^{nat}Cd(n,x) [d]	ENDF/B-VI
^{63}Cu(n,γ)^{64}Cu	IRDF-90 [a]	^{nat}Gd(n,x) [d]	ENDF/B-VI
^{63}Cu(n,α)^{60}Co	RRDF-98 (u)		

[a] ENDF/B-VI Release 8.
[b] Diagonal covariance matrix.
[c] (n,x): sum of the reactions (n,np) + (n,pn) + (n,d).
[d] Cover material; no covariance information is available.
(u): Updated data.
(n): New data.

Note: IRDF-2002 includes pointwise cross-sections; however, when the origins of these data from IRDF-90 were tracked, the source was found to be ENDF/B-VI in several cases. The corresponding data from ENDF/B-VI Release 8 were taken as the source for these particular reactions.

REFERENCES TO SECTION 1

[1.1] ZIJP, W.L., ZSOLNAY, E.M., NOLTHENIUS, H.J., SZONDI, E.J., VERHAAG, G.C., Intercomparison of predicted displacement rates based on neutron spectrum adjustments (REAL-80 exercise), Nucl. Technol. **67** (1984) 282.

[1.2] ZIJP, W.L., ZSOLNAY, E.M., CULLEN, D.E., Information Sheet for the REAL-84 Exercise, Rep. INDC(NDS)-166, IAEA, Vienna (1985).

[1.3] NOLTHENIUS, H.J., ZSOLNAY, E.M., ZIJP, W.L., SZONDI, E.J., "Nuclear data aspects encountered in the REAL80 and REAL84 intercomparisons", Nuclear Data for Radiation Damage Estimates for Reactor Structural Materials (PIKSAIKIN, V., Ed.), Rep. INDC(NDS)-179, IAEA, Vienna (1986) 95.

[1.4] ZSOLNAY, E.M., NOLTHENIUS, H.J., The Assessment of the Results of the REAL-84 Exercise, Rep. INDC(NDS)-190, IAEA, Vienna (1987).

[1.5] SZONDI, E.J., ZSOLNAY, E.M., "Nuclear data need for the covariance information used in the neutron spectrum adjustment", Covariance Methods and Practices in the Field of Nuclear Data (PIKSAIKIN, V., Ed.), Rep. INDC(NDS)-192, IAEA, Vienna (1988) 66.

[1.6] ZIJP, W.L., ZSOLNAY, E.M., NOLTHENIUS, H.J., SZONDI, E.J., Final Report on the REAL-84 Exercise, Rep. ECN-212, BME-TR-RES-18/88, Technical University Delft (1988).

[1.7] GOULO, V., "Analysis of the REAL-84 intercomparison exercise", Summary of the Specialists Meeting Held in Jackson Hole, USA, 27–29 May 1987, Rep. INDC(NDS)-198, IAEA, Vienna (1987).

[1.8] ZSOLNAY, E.M., NOLTHENIUS, H.J., SZONDI, E.J., "The role of the REAL-88 exercise in the radiation damage characterization of nuclear facilities", Nuclear Data for Radiation Damage Assessment and Related Safety Aspects 1989, IAEA-TECDOC-572, IAEA, Vienna (1990) 133–137.

[1.9] KOCHEROV, N.P., McLAUGHLIN, P.K., The International Reactor Dosimetry File (IRDF-90 Version 2), Rep. IAEA-NDS-141, Rev. 3, IAEA, Vienna (1996).

[1.10] KOCHEROV, N.P., Neutron Metrology File NMF-90, An Integrated Database for Performing Neutron Spectrum Adjustment Calculations, Rep. INDC(NDS)-347, IAEA, Vienna (1996).

[1.11] ZSOLNAY, E.M., SZONDI, E.J., NOLTHENIUS, H.J., The Neutron Metrology File NMF-90, Rep. IAEA-NDS-191, Rev. 1, IAEA, Vienna (1999).

[1.12] GREENWOOD, L.R., PAVIOTTI-CORCUERA, R., Summary Report of the Technical Meeting on International Reactor Dosimetry File: IRDF-2002, Rep. INDC(NDS)-435, IAEA, Vienna (2002).

[1.13] GRIFFIN, P.J., PAVIOTTI-CORCUERA, R. (Eds), Summary Report of the Final Technical Meeting on International Reactor Dosimetry File: IRDF-2002, Rep. INDC(NDS)-448, IAEA, Vienna (2003).

2. NEW RUSSIAN EVALUATIONS FOR IRDF-2002

K.I. Zolotarev

The contributions of the Institute of Physics and Power Engineering (IPPE), Obninsk, Russian Federation, to IRDF-2002 are summarized below.

The $^{93}Nb(n,n')^{93}Nb^{m}$ and $^{93}Nb(n,2n)^{92}Nb^{m}$ reactions were taken from RRDF-98 [2.1]. Fourteen reactions from RRDF-98 were revised and corrected following the recommendations made by Zsolnay et al. [2.2]; these reactions are: $^{19}F(n,2n)^{18}F$, $^{46}Ti(n,2n)^{45}Ti$, $^{46}Ti(n,p)^{46}Sc^{m+g}$, $^{47}Ti(n,x)^{46}Sc^{m+g}$, $^{48}Ti(n,p)^{48}Sc$, $^{48}Ti(n,x)^{47}Sc$, $^{49}Ti(n,x)^{48}Sc$, $^{51}V(n,\alpha)^{48}Sc$, $^{54}Fe(n,\alpha)^{51}Cr$, $^{54}Fe(n,2n)^{53}Fe^{m+g}$, $^{59}Co(n,\alpha)^{56}Mn$, $^{63}Cu(n,\alpha)^{60}Co^{m+g}$, $^{75}As(n,2n)^{74}As$ and $^{141}Pr(n,2n)^{140}Pr$. A further nine new evaluations were undertaken: $^{27}Al(n,p)^{27}Mg$, $^{56}Fe(n,p)^{56}Mn$, $^{58}Ni(n,p)^{58}Co$, $^{103}Rh(n,n')^{103}Rh^{m}$, $^{115}In(n,n')^{115}In^{m}$, $^{139}La(n,\gamma)^{140}La$, $^{186}W(n,\gamma)^{187}W$, $^{204}Pb(n,n')^{204}Pb^{m}$ and $^{237}Np(n,f)$.

Cross-section data were not provided in IRDF-90.2 [2.3] for the reactions $^{46}Ti(n,2n)^{45}Ti$, $^{49}Ti(n,x)^{48}Sc$, $^{54}Fe(n,2n)^{53}Fe^{m+g}$, $^{54}Fe(n,\alpha)^{51}Cr$, $^{75}As(n,2n)^{74}As$, $^{139}La(n,\gamma)^{140}La$, $^{186}W(n,\gamma)^{187}W$, $^{141}Pr(n,2n)^{140}Pr$ and $^{204}Pb(n,n')^{204}Pb^{m}$. Activation detectors based on the $^{139}La(n,\gamma)^{140}La$ and $^{186}W(n,\gamma)^{187}W$ reactions are commonly used in reactor dosimetry for determination of the neutron flux in the epithermal energy range. The $^{204}Pb(n,n')^{204}Pb^{m}$ reaction would appear to be of use for a neutron spectrum unfolding in the energy above 2.2 MeV. The $^{46}Ti(n,2n)^{45}Ti$ and $^{54}Fe(n,2n)^{53}Fe^{m+g}$ reactions appear to be useful for neutron dosimetry with $T(d,n)^{4}He$ as the sources. The $^{49}Ti(n,x)^{48}Sc$, $^{75}As(n,2n)^{74}As$ and $^{141}Pr(n,2n)^{140}Pr$ threshold reactions as well as the $^{47}Ti(n,x)^{46}Sc^{m+g}$ and $^{48}Ti(n,x)^{47}Sc$ reactions may be useful for high energy neutron dosimetry. As well as their adoption in dosimetry, the $^{75}As(n,2n)^{74}As$ and $^{141}Pr(n,2n)^{140}Pr$ reactions are also used in experimental nuclear physics as monitor reactions for the measurement of unknown cross-sections in the neutron energy range 14–15 MeV.

Three information sources were consulted in the preparation of the input data for the evaluation of cross-sections and their uncertainties: available differential and integral experimental data, results of theoretical model calculations and predictions of the systematics. Differential and integral experimental data were taken from the EXFOR library (version of May 2003) and from the original publications. As a first step in the evaluation procedure, all experimental data were thoroughly analysed and, where possible, corrected to conform to the recommended cross-section data for monitor reactions used in the measurements, and also to the recommended decay data. The correction of experimental data to conform to the new standards results in general in a decrease in the discrepancies between the experimental data and the evaluated

cross-sections, and as a consequence the uncertainties in the evaluated cross-section values are reduced.

Additional information was obtained from theoretical model calculations for the excitation functions of the dosimetry reactions ^{47}Ti(n,x)^{46}Sc^{m+g}, ^{48}Ti(n,x)^{47}Sc, ^{49}Ti(n,x)^{48}Sc, ^{139}La(n,γ)^{140}La, ^{186}W(n,γ)^{187}W, ^{204}Pb(n,n′)^{204}Pb^{m} and ^{237}Np(n,f).

The optical statistical method was used in order to obtain a theoretical description of the excitation functions of the above mentioned reactions, taking into account the contribution of the direct, pre-equilibrium and statistical equilibrium processes to the different outgoing channels. Cross-sections were calculated using modified versions of GNASH [2.4] and STAPRE [2.5]. The principal difference between the original GNASH code [2.6] and this modified version is that the latter contains a subroutine for calculation of the width fluctuation correction. Calculations of penetrability coefficients for neutrons were performed using the generalized optical model, which permits estimation of the cross-sections for the direct excitations of collective low lying levels; the ECIS coupled channel deformed optical model code was used for these calculations [2.7]. The optical coefficients of proton and alpha particle penetrabilities were determined using the SCAT2 code [2.8].

Modified GNASH was used to calculate the cross-sections from 1 keV to 20 MeV for the ^{139}La(n,γ)^{140}La and ^{186}W(n,γ)^{187}W reactions. The same data for the ^{47}Ti(n,x)^{46}Sc^{m+g}, ^{48}Ti(n,x)^{47}Sc, ^{49}Ti(n,x)^{48}Sc and ^{204}Pb(n,n′)^{204}Pb^{m} reactions were obtained from threshold to 20 MeV, and the results of the STAPRE calculations were used as supplementary information for the ^{237}Np(n,f) cross-section evaluation between 10 and 20 MeV.

Evaluations of the excitation functions for the dosimetry reactions were carried out using prepared input data, within the framework of the generalized least squares method. The rational function was used as a model function [2.9], and calculations of the recommended cross-section data and the related covariance uncertainty matrices were performed using PADE-2 [2.10].

The multi-level Breit–Wigner (MLBW) resonance parameters used for the calculation of the excitation functions in the resolved resonance region of the ^{139}La(n,γ)^{140}La, ^{186}W(n,γ)^{187}W and ^{237}Np(n,f) reactions were evaluated on the basis of data given in the compilations of Mughabghab et al. [2.11] and Sukhoruchkin et al. [2.12]. Radiative capture cross-sections for ^{139}La and ^{186}W nuclei in the unresolved resonance region were evaluated on the basis of calculations performed using EVPAR [2.13].

Three block matrices give the uncertainties in the evaluated excitation function for the ^{139}La(n,γ)^{140}La and ^{186}W(n,γ)^{187}W reactions. The first and second matrices describe the cross-section uncertainty in the resolved resonance region, while the third block matrix defines the uncertainty of the

reactions from the unresolved resonance region to 20 MeV. Both the first and third block matrices are the relative covariance matrices obtained by applying PADE-2. The cross-section uncertainties in the second block matrix are given by diagonal matrices. All three matrices were prepared using DSIGNG [2.14].

Integral experimental data for the ^{235}U fission neutron spectrum and the ^{252}Cf spontaneous fission neutron spectrum were used to test the evaluated excitation functions of the threshold reactions. Data for the ^{235}U thermal fission neutron spectrum and the ^{252}Cf spontaneous fission neutron spectrum were taken from Refs [2.15] and [2.16], respectively. The average cross-sections for the ^{235}U thermal fission neutron spectrum and the ^{252}Cf spontaneous fission neutron spectrum, as calculated from the evaluated excitation functions of IRDF-2002 (IPPE) and IRDF-90.2, are given in Tables 2.1 and 2.2; these data are also compared with the experimental values. Integral experimental data [2.17–2.29] were corrected to the new recommended cross-sections for the monitor reactions in Refs [2.30, 2.31].

Detailed descriptions of the cross-section evaluation for the ^{27}Al(n,p)^{27}Mg, ^{56}Fe(n,p)^{56}Mn, ^{139}La(n,γ)^{140}La, ^{186}W(n,γ)^{187}W, ^{204}Pb(n,n′)^{204}Pb^{m} and ^{237}Np(n,f) dosimetry reactions, as taken from the latest RRDF, are given in Refs [2.14, 2.32].

TABLE 2.1. MEASURED AND CALCULATED AVERAGED CROSS-SECTIONS IN THE CALIFORNIUM-252 SPONTANEOUS FISSION NEUTRON SPECTRUM

Reaction	Updated RRDF-98 $\langle\sigma\rangle$ (mb)	IRDF-90 $\langle\sigma\rangle$ (mb)	Experimental $\langle\sigma\rangle$ (mb)
$^{19}F(n,2n)^{18}F$	0.01615	0.01703	0.01612 ± 0.00054 [2.31]
$^{24}Mg(n,p)^{24}Na$	2.1398	2.1564	1.996 ± 0.049 [2.31]
$^{27}Al(n,p)^{27}Mg$	4.9070	—	4.880 ± 0.105 [2.31]
$^{46}Ti(n,2n)^{45}Ti$	0.01198	—	0.093 ± 0.031 [2.23]
$^{46}Ti(n,p)^{46}Sc^{m+g}$	13.818	12.313	14.07 ± 0.25 [2.31]
$^{47}Ti(n,x)^{46}Sc^{m+g}$	0.019201	—	—
$^{48}Ti(n,p)^{48}Sc$	0.42629	0.3864	0.4247 ± 0.0080 [2.31]
$^{48}Ti(n,x)^{47}Sc$	0.0042891	—	—
$^{49}Ti(n,x)^{48}Sc$	0.0026070	—	—
$^{51}V(n,\alpha)^{48}Sc$	0.038514	0.03872	0.03900 ± 0.00086 [2.31]
$^{54}Fe(n,2n)^{53}Fe^{m+g}$	0.0036219	—	—
$^{54}Fe(n,\alpha)^{51}Cr$	1.1114	—	—
$^{56}Fe(n,p)^{56}Mn$	1.4730	1.368	1.465 ± 0.026 [2.31]
$^{59}Co(n,\alpha)^{56}Mn$	0.22095	0.2159	0.2218 ± 0.0042 [2.31] 0.2208 ± 0.0014 [2.24]
$^{58}Ni(n,p)^{58}Co^{m+g}$	117.36	115.2	117.5 ± 1.5 [2.31]
$^{63}Cu(n,\alpha)^{60}Co^{m+g}$	0.6925	0.6778	0.6887 ± 0.0135 [2.31]
$^{75}As(n,2n)^{74}As$	0.61804	—	—
$^{93}Nb(n,2n)^{92}Nb^{m}$	0.7701	0.7773	0.749 ± 0.038 [2.31]
$^{93}Nb(n,n')^{93}Nb^{m}$	146.02	142.55	147.5 ± 2.5 [a]
$^{103}Rh(n,n')^{103}Rh^{m}$	724.83	714.1	620.8 ± 67.2 [2.20] 813.2 ± 24.2 [2.27]
$^{115}In(n,n')^{115}In^{m}$	191.66	189.7	197.4 ± 2.7 [2.31]
$^{141}Pr(n,2n)^{140}Pr$	1.9843	—	—
$^{139}La(n,\gamma)^{140}La$	6.650	—	—
$^{186}W(n,\gamma)^{187}W$	31.699	—	—
$^{204}Pb(n,n')^{204}Pb^{m}$	20.373	—	20.900 ± 1.202 [2.21] 20.850 ± 0.920 [2.25]
$^{237}Np(n,f)$	1359.9	1359.6	1361.0 ± 21.6 [2.31]

[a] Evaluated by the author.

TABLE 2.2. MEASURED AND CALCULATED AVERAGED CROSS-SECTIONS IN THE URANIUM-235 THERMAL FISSION NEUTRON SPECTRUM

Reaction	Updated RRDF-98 $<\sigma>$ (mb)	IRDF-90 $<\sigma>$ (mb)	Experimental $<\sigma>$ (mb)
$^{19}F(n,2n)^{18}F$	0.007299	0.00772	0.007200 ± 0.00100 [2.18] 0.008624 ± 0.00046 [2.31]
$^{24}Mg(n,p)^{24}Na$	1.5396	1.5517	1.455 ± 0.023 [2.30] 1.451 ± 0.023 [2.31]
$^{27}Al(n,p)^{27}Mg$	4.0768	—	4.133 ± 0.074 [2.28] 3.914 ± 0.070 [2.30] 3.902 ± 0.069 [2.31]
$^{46}Ti(n,2n)^{45}Ti$	0.004469	—	—
$^{46}Ti(n,p)^{46}Sc^{m+g}$	11.447	10.252	11.51 ± 0.20 [2.31]
$^{47}Ti(n,x)^{46}Sc^{m+g}$	0.008116	—	—
$^{48}Ti(n,p)^{48}Sc$	0.3043	0.2749	0.305 ± 0.020 [2.28] 0.2996 ± 0.0054 [2.31]
$^{48}Ti(n,x)^{47}Sc$	0.001656	—	—
$^{49}Ti(n,x)^{48}Sc$	0.001004	—	—
$^{51}V(n,\alpha)^{48}Sc$	0.02441	0.0246	0.02429 ± 0.00056 [2.31]
$^{54}Fe(n,2n)^{53}Fe^{m+g}$	0.001284	—	—
$^{54}Fe(n,\alpha)^{51}Cr$	0.8459	—	0.850 ± 0.050 [a]
$^{56}Fe(n,p)^{56}Mn$	1.1085	1.0297	1.130 ± 0.070 [2.28] 1.083 ± 0.017 [2.30] 1.079 ± 0.017 [2.31]
$^{59}Co(n,\alpha)^{56}Mn$	0.1582	0.1549	0.1563 ± 0.0035 [2.31]
$^{58}Ni(n,p)^{58}Co$	107.44	105.73	108.2 ± 1.4 [2.31]
$^{63}Cu(n,\alpha)^{60}Co^{m+g}$	0.5329	0.5214	0.5295 ± 0.0255 [2.29] 0.4918 ± 0.0242 [2.31]
$^{75}As(n,2n)^{74}As$	0.3092	—	0.309 ± 0.019 [a]
$^{93}Nb(n,2n)^{92}Nb^{m}$	0.4416	0.4459	0.4576 ± 0.0226 [a] 0.4645 ± 0.0117 [2.31]
$^{93}Nb(n,n')^{93}Nb^{m}$	143.46	139.97	147.6 ± 7.0 [a]
$^{103}Rh(n,n')^{103}Rh^{m}$	715.85	706.03	702.2 ± 28.1 [2.26] 721.2 ± 38.7 [2.28]
$^{115}In(n,n')^{115}In^{m}$	188.40	186.35	188.2 ± 2.3 [2.30] 187.8 ± 2.3 [2.31]

TABLE 2.2. MEASURED AND CALCULATED AVERAGED CROSS-SECTIONS IN THE URANIUM-235 THERMAL FISSION NEUTRON SPECTRUM (cont.)

Reaction	Updated RRDF-98 $<\sigma>$ (mb)	IRDF-90 $<\sigma>$ (mb)	Experimental $<\sigma>$ (mb)
$^{141}Pr(n,2n)^{140}Pr$	1.0922	—	—
$^{139}La(n,\gamma)^{140}La$	6.737	—	5.30 [2.17]
$^{186}W(n,\gamma)^{187}W$	32.267	—	—
$^{204}Pb(n,n')^{204}Pb^{m}$	17.770	—	18.900 ± 2.000 [2.19] 19.080 ± 1.524 [2.22]
$^{237}Np(n,f)$	1356.2	1355.1	1350.0 ± 24.0 [2.31]

[a] Evaluated by the author.

REFERENCES TO SECTION 2

[2.1] ZOLOTAREV, K.I., IGNATYUK, A.V., MAHOKHIN, V.N., PASHCHENKO, A.B., RRDF-98, Russian Reactor Dosimetry File, Rep. IAEA-NDS-193, Rev. 0, IAEA, Vienna (1999).

[2.2] ZSOLNAY, E.M., NOLTHENIUS, H.J., SZONDI, E.J., Nuclear Data for Reactor Dosimetry Libraries: Analysis, Intercomparison and Selection of Data, Rep. BME-NTI-251/2001, Institute of Nuclear Techniques, Budapest University of Technology and Economics, Budapest (2001).

[2.3] KOCHEROV, N.P., McLAUGHLIN, P.K., The International Reactor Dosimetry File (IRDF-90), Rep. IAEA-NDS-141, Rev. 2, IAEA, Vienna (1993).

[2.4] TRYKOV, E.L., TERTYCHNYI, G.Y., Institute of Physics and Power Engineering (IPPE), Obninsk, personal communication, 1999.

[2.5] UHL, M., STROHMAIER, B., STAPRE — A Computer Code for Particle Induced Activation Cross Section and Related Quantities, Rep. IRK 76-01, University of Vienna (1976).

[2.6] YOUNG, P.G., ARTHUR, E.D., A Pre-equilibrium Statistical Nuclear Model Code for Calculation of Cross Section and Emission Spectra, Rep. LA-6947, Los Alamos Lab., NM (1977).

[2.7] RAYNAL, J., "Optical-model and coupled-channel calculations in nuclear physics", Computing as a Language of Physics (Proc. Int. Sem. Trieste, 1971), IAEA, Vienna (1972) 281–322.

[2.8] BERSILLON, O., SCAT2 — A Spherical Optical Model Code, Rep. CEA-N-2037, Commissariat à l'énergie atomique, Bruyères-le-Châtel (1978) 111.

[2.9] BADIKOV, S., RABOTNOV, N., ZOLOTAREV, K., "Evaluation of neutron dosimetry reactions cross sections and covariance analysis with rational functions", Evaluation and Processing of Covariance Data (Proc. Specialists Mtg, Oak Ridge, TN, 1992), OECD, Paris (1993) 105.
[2.10] BADIKOV, S.A., et al., preprint FEI-1686, Institute of Physics and Power Engineering, Obninsk (1985).
[2.11] MUGHABGHAB, S.F., DIVADEENAM, M., HOLDEN, N.E., Neutron Cross Sections, Vol. 1, part A, Z = 1–60, Academic Press, New York (1981); MUGHABGHAB, S.F., Neutron Cross Sections, Vol. 1, part B, Z = 61–100, Academic Press, New York (1984).
[2.12] SUKHORUCHKIN, S.I., SOROKO, Z.N., DERIGLAZOV, V.V., Tables of Neutron Resonance Parameters, Landolt Bornstein New Series, I/16B (SCHOPPER, H., Ed.), Springer-Verlag, Berlin (1998).
[2.13] MANTUROV, G.N., et al., Vopr. At. Nauki Tekh, Jadernye Konstanty **1** (1983) 50.
[2.14] ZOLOTAREV, K.I., Evaluation and Improvement of Cross Section Accuracy for Most Important Dosimetry Reactions Including Covariance Data, Rep. INDC(CCP)-431, IAEA, Vienna (2002).
[2.15] WESTON, L.W., YOUNG, P.G., POENITZ, W.P., LUBITZ, C.R., "Evaluated neutron data file for U-235, ENDF/B-VI library, MAT=9228, MF=5, MT=18; evaluated April 1989", ENDF/B-VI Summary Documentation (ROSE, P.F., Ed.), Rep. BNL-NCS-17541 (ENDF-201), Brookhaven Natl Lab., Upton, NY (1991).
[2.16] MANNHART, W., "Evaluation of the Cf-252 fission neutron spectrum between 0 MeV and 20 MeV", Properties of Neutron Sources, IAEA-TECDOC-410, IAEA, Vienna (1987) 158.
[2.17] HUGHES, D., SHERMAN, D., Fast neutron cross sections and nuclear shells, Phys. Rev. **78** (1950) 632.
[2.18] NASYROV, F., SCIBORSKIJ, B.D., Fission-spectrum average cross-sections for (n,2n), (n,p), (n,α) reactions, At. Ehnerg. **25** (1968) 437.
[2.19] KIMURA, I., KOBAYASHI, K., SHIBATA, T., Measurements of average cross sections for some threshold reactions for neutrons with fission-type reactor spectrum, Nucl. Sci. Technol. **8** (1971) 59.
[2.20] KIROUAC, G.J., et al., Knolls Atomic Power Laboratory Rep. 4005, Knolls Atomic Power Lab., Schenectady, NY (1974).
[2.21] CSIKAI, J., "Use of californium-252 sources in Hungary for teaching and research", Some Physical, Dosimetry and Biomedical Aspects of Californium-252 (Proc. Sem. Karlsruhe, 1975), IAEA, Vienna (1976) 29–47.
[2.22] BRODSKAJA, A.K., et al., Fission neutron spectra averaged cross-sections of (n,α), (n,p), (n,2n), (n,n) reactions for some elements, Jadernyje Konstanty **4** (1976) 7610.
[2.23] DEZSO, Z., CSIKAI, J., "Average cross-sections for the Cf-252 neutron spectrum", Proc. 4th All Union Conference on Neutron Physics, Kiev, Vol. 3, CNIIA Atominform, Moscow (1977) 32–43. CSIKAI, J., DEZSO, Z., Fission neutron spectrum of ^{252}Cf, Ann. Nucl. Energy **3** (1976) 527–530.

[2.24] KOBAYASHI, K., KIMURA, I., MANNHART, W., Measurement and covariance analysis of californium-252 spectrum averaged cross sections, Nucl. Sci. Technol. **19** (1982) 341.
[2.25] KOBAYASHI, K., et al., Measurement of Average Cross Sections for Some Threshold Reactions of Ti, Cr, and Pb in the Californium-252 Spontaneous Fission Neutron Spectrum Field, Progress Report, Rep. NEANDC(J)-106/U, INDC(JPN)-92/U, Japan Atomic Energy Research Institute, Tokai-mura (1984) 41–44.
[2.26] GRIGOR'EV, E.I., et al., "Measurement of the neutron threshold reaction cross-sections for U-235 fission spectrum", Proc. 6th All Union Conference on Neutron Physics, Kiev, Vol. 3, CNIIA Atominform, Moscow (1984) 187–190.
[2.27] LAMAZE, G.P., SCHIMA, F.J., EISENHAUER, C.M., SPIEGEL, V., Spectrum-averaged cross-section measurement of ^{103}Rh(n,n′)^{103m}Rh in the ^{252}Cf fission neutron spectrum, Nucl. Sci. Eng. **100** (1988) 43.
[2.28] HORIBE, O., CHATANI, H., "Cross sections of the reactions ^{55}Mn(n,2n)^{54}Mn, ^{58}Ni(n,2n)^{57}Ni and ^{58}Ni(n,np)^{57}Co averaged over the U-235 fission neutron spectrum", Nuclear Data for Science and Technology (Proc. Int. Conf. Jülich, 1991), Springer-Verlag, Berlin (1992) 68.
[2.29] GERALDO, L.P., DIAS, M.S., KOSKINAS, M.F., Average neutron cross section measurements in U-235 fission spectrum for some threshold reactions, Radiochim. Acta **57** (1992) 63.
[2.30] MANNHART, W., Evaluation of a 'Best Set' of Average Cross Section Measurements in the ^{235}U(n_{th},f) Neutron Field, Progress Report of Nuclear Data Research in the Federal Republic of Germany for the Period 1 April 1998 to 31 March 1999, Rep. INDC(Ger)-045, Forschungszentrum Jülich (1999) 40.
[2.31] MANNHART, W., "Validation of differential cross sections with integral data", Summary Report of the Technical Meeting on International Dosimetry File: IRDF-2002, Rep. INDC(NDS)-435, IAEA, Vienna (2002) 59.
[2.32] ZOLOTAREV, K.I., Evaluation and Improvement of Cross Section Accuracy for Most Important Dosimetry Reactions Including Covariance Data, Rep. INDC(CCP)-438, IAEA, Vienna (2004).

3. SELECTION OF CANDIDATE CROSS-SECTIONS FOR IRDF-2002

E.M. Zsolnay, H.J. Nolthenius

As stated in Section 1, IRDF-2002 contains cross-section data for 66 dosimetry reactions along with their related uncertainty information [3.1]. These data have been selected from the most recently available cross-section libraries and new evaluations. The procedure for selecting the best quality data for IRDF-2002 began with detailed analyses of the contents of the cross-section files of interest.

Prior to the Technical Meeting on International Reactor Dosimetry File: IRDF-2002 (held at the IAEA in Vienna from 27 to 29 August 2002), a supplementary workshop on benchmarks took place at the 11th International Symposium on Reactor Dosimetry, Brussels, 18–23 August 2002 [3.2]. Agreement was reached that only those cross-sections accompanied with adequate uncertainty information in the form of covariance matrices would be accepted for IRDF-2002. The primary basis for the selection of the cross-sections for IRDF-2002 was comparison of the data with the experimental results obtained from four standard neutron fields (thermal Maxwellian, $1/E$, ^{252}Cf fission and 14 MeV neutron field), taking into consideration the corresponding uncertainty information.

Detailed analyses of the data were followed by comparisons of the integral values of the candidate cross-sections with the experimental data obtained in the above mentioned standard neutron fields. C/E values were determined and evaluated, together with the corresponding uncertainty data.

The original cross-section information was available in the ENDF-6 format for all the libraries investigated. These data have been converted to a SAND II type 640 group cross-section form. A neutron temperature of 300 K and a 'flat' weighting spectrum were applied in the conversion procedure. All the calculations for the cross-section and related uncertainty information were performed using the 640 energy group structure.

The following sections contain details of the work outlined above, and the results obtained.

3.1. ANALYSIS OF THE DATA FROM RECENT NATIONAL REACTOR DOSIMETRY FILES AND NEW EVALUATIONS

As part of the procedure for updating IRDF-90, data in the reactor dosimetry files JENDL/D-99 [3.3] and RRDF-98 [3.4], and new evaluations

from ENDF/B-VI Release 8, JEFF-3.0 and CENDL-2 [3.5], were assessed and analysed.

Analysis began with a survey of the plots of the relevant cross-sections in order to detect discontinuities and other obvious discrepancies in the cross-section data. The numerical characterization of the cross-sections of interest required that the spectrum averaged cross-section values be calculated for three theoretical spectrum functions (Maxwellian thermal spectrum at a neutron temperature of 293.58 K, $1/E$ spectrum from 0.5 eV to 1.05 MeV and Watt fission spectrum). A three group structure was used for the representation of the uncertainty information, with energy boundaries of 10^{-4} eV, 0.5 eV, 1.05 MeV and 20 MeV. A typical materials testing reactor (MTR) spectrum available in 640 SAND II group format [3.6] (Fig. 3.1) was used as a weighting spectrum in the input of the cross-section uncertainty processing code.

Cross-section values and the related uncertainty information were investigated (including detailed analyses of the relevant covariance matrices). Corresponding data from the different libraries were compared, along with the equivalent data of IRDF-90. The results, together with the detected errors, discrepancies and shortcomings (which could be related to the physics and/or mathematics content, or to the format of the data), were presented in the form of progress reports [3.7, 3.8] and communicated to the evaluators of the libraries via the IAEA. Some 180 different cross-sections were analysed (some several times due to revisions (see below)). For several reactions, no better quality cross-section evaluations are available in the literature than the data in IRDF-90. Only a limited number of new evaluations accompanied by uncertainty information (the majority of them for the RRDF) have been made in the energy region from thermal to 20 MeV over the previous decade.

As a result of the analysis outlined above [3.7], the evaluators revised and modified selected data from JENDL/D-99 and RRDF-98, and a number of new cross-section evaluations have been included from Refs [3.9, 3.10]. Examination of the revised data and analyses of the new data [3.8] led to the preparation of a new set of cross-sections. These cross-sections were candidates for inclusion in IRDF-2002, and are listed in Table 3.1 [3.8, 3.11].

The cross-sections and their uncertainty information (as listed in Table 3.1) were the best quality data available in the literature before the end of 2004, and therefore the cross-section data for IRDF-2002 are taken from these sources. There are some reactions that are of interest for dosimetry applications with insufficient cross-section information, while no suitable cross-section data were found in the literature for others. These reactions are also listed in Table 3.1.

3.2. PRELIMINARY SELECTION OF CROSS-SECTIONS IN THE THERMAL AND EPITHERMAL NEUTRON ENERGY REGION FOR IRDF-2002, AND CHARACTERIZATION OF THE SELECTED DATA

3.2.1. Selection procedure and results

With reference to Table 3.1, the majority of reactions with correct cross-sections and uncertainty information in the thermal and epithermal neutron energy region are found only in IRDF-90. For the other libraries considered, either no data of this type are available or the cross-sections and/or the related uncertainty information (covariance matrices) are erroneous or incomplete [3.7, 3.8].

The evaluators of the RRDF have undertaken new evaluations in the low neutron energy region for the cross-sections of the ^{139}La(n,γ) and ^{186}W(n,γ) reactions. A revision of the covariance information was made for the ^{58}Fe(n,γ)

TABLE 3.1. REACTIONS FROM THE VARIOUS LIBRARIES WITH CROSS-SECTIONS SUITABLE FOR IRDF-2002

Reactions from IRDF-90						
LI6T	B10A	MG24P	AL27P	AL27A	P31P	S32P
SC45G	TI46P	TI47NP	TI47P	TI48NP	TI48P	CR522
MN55G	FE54P	FE58G	CO592	CO59G	NI582	NI58P
CU632	CU63G	CU63A	CU652	ZN64P	ZR902	NB932 [a]
NB93N [a]	RH103N [a]	AG109G [a]	IN1152 [a]	IN115N [a]	I1272	AU1972
AU197G	TH232F	U235F	U238F	U238G	PU239F	
NA23G [b]	NB93G [b]	IN115G [a,b]	TH232G [b]			45 cross-sections
Reactions from JENDL/D-99						
F192	MG24P	AL27P	AL27A	P31P	TI0XSC46 [c]	TI0XSC48 [c]
TI462	TI46P	TI48NP	TI48P	TI49NP	CR522	MN55G
FE54P	FE58G	NI582	NI58P	CU632	CU652	Y892
ZR902	IN115N [a]	I1272	TM1692	AU1972	HG199N [a]	U238F
NP237F	PU239F	AM241F	NA232 [d]			
TA181G [b]						33 cross-sections

TABLE 3.1. REACTIONS FROM THE VARIOUS LIBRARIES WITH CROSS-SECTIONS SUITABLE FOR IRDF-2002 (cont.)

Reactions from RRDF-98						
F192	TI462	TI46P	TI47NP	TI48NP	TI48P	TI49NP
V51A	FE542	FE54A	FE56P	CO59A	CU63A	AS752
NB932 [a]	NB93N [a]	LA139G	PR1412	W186G	PB204N [a]	
AL27P [d]	NI58P [d]	RH103N [a,d]	IN115N [a,d]	NP237F		25 cross-sections
Reactions from ENDF/B-VI Release 8						
CR522	NI58P	NI60P	CU632	CU63G	CU652	
NA23G [b]	NB93G [b]	IN115G [a,b]	TH232G [b]			10 cross-sections
Reactions from JEFF-3.0						
FE56P	NI582	NI58P	NI60P			4 cross-sections
Σ = 117 cross-sections						
Problematic reactions						
NA23G [b]	TI0XSC47 [c]	CR50G	MN552	FE57NP	NB93G [b]	IN115G [a,b]
EU151G	TA181G [b]	TH232G [b]				10 cross-sections

[a] Metastable state of the reaction product nuclide.
[b] Diagonal covariance matrix.
[c] TI0XSC-46, -47 and -48 indicate the reactions on a natural titanium target leading to the products ^{46}Ti, ^{47}Ti and ^{48}Ti, respectively.
[d] New evaluations or updates, 2003.

Notes: (a) SAND type short reaction notation: chemical symbol and mass number of the target nucleus are followed by the name of the reaction product; A, G, F, 2, N, P, NP and T represent (n,α), (n,γ), (n,f), (n,2n), (n,n′), (n,p), (n,np) and (n,t) reactions, respectively. (b) No suitable cross-section data have been found in the libraries investigated for reactions ^{nat}Ti(n,x)^{47}Sc, ^{50}Cr(n,γ)^{51}Cr, ^{55}Mn(n,2n)^{54}Mn, ^{57}Fe(n,np)^{56}Mn and ^{151}Eu(n,γ)^{152}Eu. (c) Only diagonal covariance matrices were found for the following reactions: ^{23}Na(n,γ)^{24}Na, ^{93}Nb(n,γ)^{94}Nb, ^{115}In(n,γ)^{116}In^{m}, ^{181}Ta(n,γ)^{182}Ta and ^{232}Th(n,γ)^{233}Th (below 15 eV).

reaction by the Japanese evaluators [3.12] so as to substitute for earlier erroneous data in JENDL/D-99.

3.2.1.1. Selection procedure

The procedure for selecting the cross-sections for IRDF-2002 was based on comparisons with each other of the integral values of the cross-sections and related uncertainty information from the libraries of interest, and with experimental data obtained in standard neutron fields. This implies that the experimental data in a Maxwellian thermal neutron spectrum and in a $1/E$ neutron field had to be considered [3.2]. A review of the literature identified two sources that were adequate for the purpose: Mughabghab [3.13] and Holden [3.14].

The thermal neutron cross-sections in both experimental evaluations refer to a neutron energy of 0.0253 eV (v_0 = 2200 m/s), while the resonance integrals were calculated by Mughabghab with a lower energy limit of 0.5 eV and an upper energy limit corresponding to the upper resonance with known scattering width [3.15]. Holden calculated the resonance integrals from 0.5 eV to 0.1 MeV. The recommended cross-section values refer to room temperature in both cases (293.43 K and 300 K for Holden and Mughabghab, respectively). Thermal neutron cross-sections in this work refer to 0.0253 eV neutron energy (v_0 = 2200 m/s), while the resonance integrals were calculated from 0.5 eV to 1.05 MeV (preliminary analyses are found in Refs [3.7, 3.8]). In the comparison of the corresponding cross-section data, 0 K was used, while in characterizing the selected data, 300 K neutron temperature was used. The difference between the corresponding data at the two neutron temperatures was less than 1%, including the uncertainty deriving from the data processing (see below).

A similar comparison of the thermal neutron cross-sections and resonance integrals with the corresponding Mughabghab data [3.13] was made for a series of capture cross-sections from different dosimetry libraries by Trkov (Appendix III); these results agree with those presented in this report.

The uncertainty information for the cross-sections of interest is represented by their relative standard deviation values (calculated in a three energy group structure as described in Section 3.1), weighted with a typical MTR spectrum (Fig. 3.1).

3.2.1.2. Results

The results of the cross-section comparison are listed in Table 3.2. As shown for some of these reactions, the same cross-section data are given in both

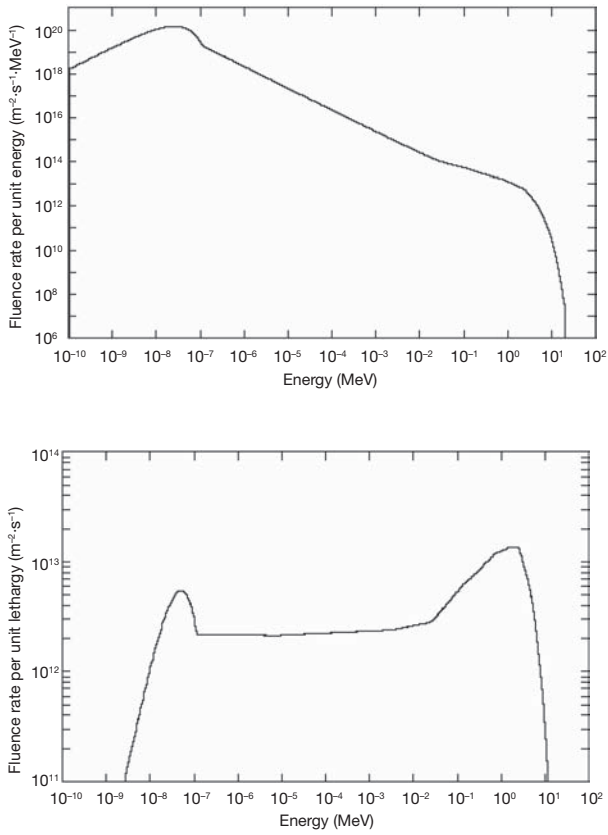

FIG. 3.1. Neutron spectrum MTR in two different representations, as used in the uncertainty calculations [3.6].

IRDF-90 and the other libraries of interest, while the related uncertainty information can vary with the source of data. Reactions exhibiting this behaviour are $^{23}Na(n,\gamma)^{24}Na$ (IRDF-90 and ENDF/B-VI), $^{55}Mn(n,\gamma)^{56}Mn$ (IRDF-90 and JENDL/D-99), $^{63}Cu(n,\gamma)^{64}Cu$ (IRDF-90 and ENDF/B-VI), $^{93}Nb(n,\gamma)^{94}Nb$ (IRDF-90 and ENDF/B-VI), $^{115}In(n,\gamma)^{116}In^{m}$ (IRDF-90 and ENDF/B-VI) and $^{232}Th(n,\gamma)^{233}Th$ (IRDF-90 and ENDF/B-VI). IRDF-90 was taken as the source of data for IRDF-2002 in these particular cases.

Considering the $^{58}Fe(n,\gamma)^{59}Fe$ reaction: the resonance integral in both cross-section files of interest (IRDF-90 and JENDL/D-99) deviates significantly from the corresponding data of Mughabghab, while the JENDL/D-99 value is in good agreement with the data of Holden (as compared with the relevant uncertainties). Further clarification is required, for example, by

TABLE 3.2. COMPARISON OF THE INTEGRAL CROSS-SECTION CHARACTERISTICS FOR SOME THERMAL AND EPITHERMAL NEUTRON REACTIONS WITH EVALUATED EXPERIMENTAL DATA

(calculated cross-section values refer to a neutron temperature of 0 K)

Reaction	Library (selected evaluation)	Calculated cross-section σ_L (2200 m/s) (m^2)	Relative standard deviation of σ_L [a] (%)	Calculated resonance integral IRL [b] (m^2)	Relative standard deviation in epithermal region [c] (%)	Thermal cross-section ratio		Resonance integral ratio	
						σ_L/σ_M	σ_L/σ_H	IR_L/IR_M	IR_L/IR_H
$^{23}Na(n,\gamma)$ [d]	IRDF-90	5.28E-29	2.00	3.16E-29	3.15	0.99	—	1.02	1.06
$^{23}Na(n,\gamma)$ [d]	ENDF/B-VI	5.28E-29	2.00	3.16E-29	3.15	0.99	—	1.02	1.06
$^{55}Mn(n,\gamma)$	IRDF-90	1.34E-27	4.18	1.18E-27	3.84	1.00	1.01	0.84	0.84
$^{55}Mn(n,\gamma)$	JENDL/D-99	1.34E-27	6.31	1.18E-27	8.04	1.00	1.01	0.84	0.84
$^{58}Fe(n,\gamma)$	IRDF-90	1.15E-28	5.07	1.51E-28	5.12	0.88	0.88	0.89	1.16
$^{58}Fe(n,\gamma)$	JENDL/D-99	1.30E-28	12.60	1.37E-28	8.75	1.00	1.00	0.81	1.05
$^{63}Cu(n,\gamma)$	IRDF-90	4.48E-28	4.11	4.96E-28	3.86	0.99	1.00	1.00	0.99
$^{63}Cu(n,\gamma)$	ENDF/B-VI	4.48E-28	4.11	4.95E-28	3.86	0.99	1.00	1.00	0.99
$^{93}Nb(n,\gamma)$ [d]	IRDF-90	1.16E-28	10.0	9.92E-28	9.49	1.01	1.05	1.17	1.17
$^{93}Nb(n,\gamma)$ [d]	ENDF/B-VI	1.16E-28	10.0	9.91E-28	9.49	1.01	1.05	1.17	1.17
$^{115}In(n,\gamma)$ [d,e]	IRDF-90	2.11E-26	6.00	3.28E-25	5.98	1.04	1.03	0.99	0.96
$^{115}In(n,\gamma)$ [d,e]	ENDF/B-VI	2.11E-26	6.00	3.28E-25	5.98	1.04	1.03	0.99	0.96
$^{232}Th(n,\gamma)$ [d]	IRDF-90	7.40E-28	4.33	8.57E-27	10.92	1.01	1.00	1.01	1.01
$^{232}Th(n,\gamma)$ [d]	ENDF/B-VI	7.40E-28	4.33	8.57E-27	10.92	1.01	1.00	1.01	1.01

TABLE 3.2. COMPARISON OF THE INTEGRAL CROSS-SECTION CHARACTERISTICS FOR SOME THERMAL AND EPITHERMAL NEUTRON REACTIONS WITH EVALUATED EXPERIMENTAL DATA (cont.)
(calculated cross-section values refer to a neutron temperature of 0 K)

Reaction	Library (selected evaluation)	Calculated cross-section σ_L (2200 m/s) (m^2)	Relative standard deviation of σ_L [a] (%)	Calculated resonance integral IRL [b] (m^2)	Relative standard deviation in epithermal region [c] (%)	Thermal cross-section ratio		Resonance integral ratio	
						σ_L/σ_M	σ_L/σ_H	IR_L/IR_M	IR_L/IR_H
^{239}Pu(n,f)	IRDF-90	7.48E-26	0.25	2.93E-26	0.26	—	0.99	—	0.98
^{239}Pu(n,f)	JENDL/D-99	7.47E-26	0.71	2.97E-26	3.823	—	0.99	—	0.99

[a] Calculated for a typical MTR spectrum from 1E-4 eV to 0.5 eV.
[b] Calculated from 0.5 eV to 1.05 MeV.
[c] Calculated for a typical MTR spectrum from 0.5 eV to 1.05 MeV.
[d] Diagonal covariance matrix.
[e] Metastable and ground state of the product nuclide.

Notes: σ_L and IR_L are calculated from the corresponding library data; σ_M and IR_M data are from Mughabghab [3.13]; σ_H and IR_H data are from Holden [3.14].
For the reaction ^{115}In (n,γ) the sum of the cross-sections for the reactions leading to the metastable states and to the ground level (σ^{m+g}) of the product nucleus ^{116}In is given.

comparing the data with experimental values from benchmark neutron fields. Better agreement was found when the experimental values were compared with JENDL/D-99 data than with IRDF-90 data. Furthermore, when taking into consideration the corresponding uncertainties, these JENDL/D-99 data appear to be more realistic, and therefore they are recommended for inclusion in IRDF-2002.

The cross-section values found in the libraries for the ^{239}Pu(n,f) reaction (Table 3.2) are almost identical. However, the uncertainties in JENDL/D-99 are considered to be more reliable than the corresponding IRDF-90 values. Therefore, JENDL/D-99 data have been selected for IRDF-2002. Uncertainty information for the cross-sections of the ^{23}Na(n,γ)^{24}Na, ^{93}Nb(n,γ)^{94}Nb, ^{115}In(n,γ)^{116}In^{m} and ^{232}Th(n,γ)^{233}Th (below 15 eV) reactions is given in the form of diagonal covariance matrices in all the libraries investigated. This situation arises because no cross-sections with more complete covariance data are at present available for these reactions. Under such circumstances, these data have been selected for IRDF-2002.

3.2.2. Characterization of the selected cross-section data

The thermal and epithermal neutron cross-sections selected for IRDF-2002 are listed in Table 3.3. Thermal cross-sections (σ_L) at 2200 m/s (0.0253 eV) and the resonance integral (IR_L) values from 0.5 eV to 1.05 MeV have been calculated (temperature 300 K) in order to obtain the numerical characterization of the data. All the cross-section and resonance integral values are compared with the evaluated experimental data recommended by Mughabghab [3.13] and Holden [3.14], as noted in Section 3.2.1.

Relative standard deviations (weighted with an MTR spectrum) were separately calculated for the thermal and the intermediate neutron energy regions. The same energy boundaries were used as for the cross-section characterization, and the results are given in Table 3.4.

Evaluation of the data in Tables 3.3 and 3.4 leads to the following observations:

(a) Thermal neutron cross-sections for the selected reactions are generally in agreement with the recommended experimental data (Mughabghab and Holden) within one standard deviation of the corresponding library and experimental data.
(b) Resonance integrals calculated from the library data deviate from the recommended values (Mughabghab and Holden) by more than one standard deviation for several reactions (details given below).
(c) List of problems by reaction (related to the data in the tables):

— $^{10}B(n,\alpha)^{7}Li$ and $^{6}Li(n,t)^{4}He$: The uncertainty of the library cross-sections in the intermediate neutron energy region is too small (not realistic) compared with the corresponding *C*/*E* values (or the library data deviate significantly from the experimental values).
— $^{23}Na(n,\gamma)^{24}Na$: The uncertainty information contains only a diagonal matrix — a new evaluation is required.
— $^{55}Mn(n,\gamma)^{56}Mn$: The *C*/*E* value for the resonance integral deviates by 16% from unity — excessive when compared with the related uncertainty values; a new cross-section evaluation is needed in the intermediate neutron energy region.
— $^{58}Fe(n,\gamma)^{59}Fe$: The *C*/*E* value for the resonance integral with the Mughabghab data deviates by 19% from unity. A large difference is also found between the recommended experimental data for the sources considered. Clarification of this discrepancy is necessary because this reaction is one of the most frequently used detectors in reactor dosimetry. A new cross-section evaluation in the intermediate neutron energy region should also be considered.
— $^{93}Nb(n,\gamma)^{94}Nb$: The *C*/*E* value for the resonance integral deviates by 17% from unity; furthermore, the uncertainty information contains only a diagonal matrix — a new evaluation is required.
— $^{109}Ag(n,\gamma)^{110}Ag^{m}$: Mughabghab data represent the sum of the reaction cross-sections leading to $^{110}Ag^{m+g}$, while the evaluated data libraries contain only cross-section data for the $^{109}Ag(n,\gamma)^{110}Ag^{m}$ reaction. Therefore, no comparison with the Mughabghab data was possible.
— $^{115}In(n,\gamma)^{116}In^{m}$: In the present library the cross-section leading to the metastable states of the product nucleus ^{116}In is given; uncertainty information contains only a diagonal matrix — a new evaluation is required.
— $^{181}Ta(n,\gamma)^{182}Ta$: The uncertainty information contains only a diagonal matrix — a new evaluation is required.
— $^{197}Au(n,\gamma)^{198}Au$: The available uncertainty information for this reaction is not reliable; similar data have been withdrawn from ENDF/B-VI. Uncertainty data in IRDF-90 were derived from the same source — a new evaluation is required.
— $^{232}Th(n,\gamma)^{233}Th$: The uncertainty information below 15 eV is defined only in terms of a diagonal matrix — a new evaluation is required.
— $^{235}U(n,f)$: The uncertainty information has been declared to be unreliable, and has been withdrawn from ENDF/B-VI. Data in IRDF-90 have the same origin — a new evaluation is required.

— ^{241}Am(n,f): No up to date experimental data are available for this reaction, therefore the corresponding *C*/*E* values could not be derived.

3.3. CONCLUSIONS

Based on the results of the cross-section selection procedure outlined above, the following principal conclusions can be drawn related to the data in Tables 3.3 and 3.4:

(a) Very few new cross-section evaluations accompanied by complete uncertainty information have been undertaken in the low neutron energy region over the previous decade, except the ^{139}La(n,γ)^{140}La and ^{186}W(n,γ)^{187}W reactions evaluated for the RRDF [3.4].
(b) Integral values of the selected cross-sections in the thermal neutron region exhibit very good agreement in most cases with the corresponding recommended experimental values.
(c) Resonance integrals of the ^{55}Mn(n,γ)^{56}Mn, ^{58}Fe(n,γ)^{59}Fe and ^{93}Nb(n,γ)^{94}Nb reactions deviate significantly (>10%) from the corresponding experimental data. Further investigation (e.g. testing the data in benchmark neutron fields) and new cross-section evaluations are required.
(d) For the ^{23}Na(n,γ)^{24}Na, ^{93}Nb(n,γ)^{94}Nb, ^{115}In(n,γ)^{116}In^{m} and ^{181}Ta(n,γ)^{182}Ta reactions and the ^{232}Th(n,γ)^{233}Th reaction below 15 eV, the uncertainty information is quantified in terms of diagonal covariance matrices only. New evaluations with complete covariance information are required.
(e) Unreliable uncertainty data are present in all the investigated cross-section libraries for the ^{197}Au(n,γ)^{198}Au and ^{235}U(n,f) reactions (withdrawn from ENDF/B-VI). New cross-section evaluations with complete covariance information are required.
(f) Selected cross-sections in Table 3.3 should be subjected to a consistency test by comparing the relevant integral data with the corresponding experimental values in benchmark neutron fields.

TABLE 3.3. THERMAL NEUTRON CROSS-SECTIONS AND RESONANCE INTEGRALS FOR REACTIONS SELECTED FOR IRDF-2002 (TEMPERATURE OF 300 K)

Reaction	Material No.	MT No.	Library (selected evaluation)	Library cross-section (2200 m/s) σ_L (m^2)	Evaluated experimental data (2200 m/s) σ_M (m^2)	Evaluated experimental data (2200 m/s) σ_H (m^2)	Cross-section ratio		Resonance integral from library data IR_L (m^2)	Evaluated resonance integral IR_M (m^2)	Evaluated resonance integral IR_H (m^2)	Resonance integral ratio	
							σ_L/σ_M	σ_L/σ_H				IR_L/IR_M	IR_L/IR_H
^{6}Li(n,t)	325	105	IRDF-90	9.42E-26	Not available	9.4(1)E-26	—	1.00	4.27E-26	Not available	4.22(4)E-26	—	1.01
^{10}B(n,α)	525	107	IRDF-90	3.84E-25	Not available	3.84(1)E-25	—	1.00	1.73E-25	Not available	1.73(1)E-25	—	1.00
^{23}Na(n,γ) [a]	1123	102	IRDF-90	5.29E-29	5.30(5)E-29	—	1.00	—	3.17E-29	3.11(10)E-29	3.0(6)E-29	1.02	1.06
^{45}Sc(n,γ)	2126	102	IRDF-90	2.73E-27	2.72(2)E-27	2.7E-27	1.00	1.01	1.20E-27	1.20(5)E-27	1.20E-27	1.00	1.00
^{55}Mn(n,γ)	2525	102	IRDF-90	1.34E-27	1.336(5)E-27	1.33(1)E-27	1.00	1.01	1.18E-27	1.40(3)E-27	1.40(3)E-27	0.84	0.84
^{58}Fe(n,γ)	2637	102	JENDL/D-99 (u)	1.30E-28	1.30(3)E-28	1.3(1)E-28	1.00	1.00	1.37E-28	1.7(1)E-28	1.3(2)E-28	0.81	1.05
^{59}Co(n,γ)	2725	102	IRDF-90	3.72E-27	3.718(6)E-27	3.72E-27	1.00	1.00	7.60E-27	7.59(2)E-27	7.4E-27	1.00	1.03
^{63}Cu(n,γ)	2925	102	IRDF-90	4.47E-28	4.52(2)E-28	4.5(2)E-28	0.99	0.99	4.96E-28	4.97(8)E-28	5.0(1)E-28	1.00	0.99
^{93}Nb(n,γ) [a]	4125	102	IRDF-90	1.16E-28	1.15(5)E-28	1.1E-28	1.01	1.05	9.91E-28	8.5(5)E-28	8.5E-28	1.17	1.17
^{109}Ag(n,γ) [b]	4731	102	IRDF-90 (u)	4.21E-28	—	4.2E-28	—	1.00	6.86E-27	—	7.0E-27	—	0.98
^{115}In(n,γ) [a,b]	4931	102	IRDF-90	1.67E-26	2.02(2)E-26	2.05E-26	—	1.04	2.59E-25	Not available	2.7E-25	—	0.96
^{139}La(n,γ)	5712	102	RRDF-98 (n)	9.04E-28	9.04(4)E-28	9.2(2)E-28	1.00	0.98	1.20E-27	1.21(6)E-27	1.2(1)E-27	0.99	1.00
^{181}Ta(n,γ) [a]	7328	102	JENDL/D-99	2.07E-27	2.05(5)E-27	2.01E-27	1.01	1.04	6.59E-26	6.60(23)E-26	6.504E-26	1.00	1.01
^{186}W(n,γ)	7452	102	RRDF-98 (n)	3.85E-27	3.85(5)E-27	3.7(2)E-27	1.00	1.04	4.80E-26	4.85(15)E-26	5.10(50)E-26	0.99	0.94
^{197}Au(n,γ) [c]	7925	102	IRDF-90	9.88E-27	9.865(90)E-27	9.87(10)E-27	1.00	1.00	1.57E-25	1.550(28)E-25	1.55(3)E-25	1.01	1.01
^{232}Th(n,γ) [a]	9040	102	IRDF-90	7.41E-28	7.35(3)E-28	7.37(4)E-28	1.01	1.00	8.56E-27	8.5(3)E-27	8.5(3)E-27	1.01	1.01
^{235}U(n,f) [d]	9228	18	IRDF-90	5.86E-26	Not available	5.86(2)E-26	—	1.01	2.72E-26	Not available	2.75(5)E-26	—	0.99
^{238}U(n,γ)	9237	102	IRDF-90	2.72E-28	2.680(19)E-28	2.7(1)E-28	1.01	1.00	2.77E-26	2.77(3)E-26	2.77(3)E-26	1.00	1.00

TABLE 3.3. THERMAL NEUTRON CROSS-SECTIONS AND RESONANCE INTEGRALS FOR REACTIONS SELECTED FOR IRDF-2002 (TEMPERATURE OF 300 K) (cont.)

Reaction	Material No.	MT No.	Library (selected evaluation)	Library cross-section (2200 m/s) σ_L (m^2)	Evaluated experimental data (2200 m/s) σ_M (m^2)	Evaluated experimental data (2200 m/s) σ_H (m^2)	Cross-section ratio		Resonance integral from library data IR_L (m^2)	Evaluated resonance integral IR_M (m^2)	Evaluated resonance integral IR_H (m^2)	Resonance integral ratio	
							σ_L/σ_M	σ_L/σ_H				IR_L/IR_M	IR_L/IR_H
^{239}Pu(n,f)	9437	18	JENDL/D-99	7.47E-26	Not available	7.52(3)E-26	—	0.99	2.97E-26	Not available	3.0(1)E-26	—	0.99
^{241}Am(n,f)	9543	18	JENDL/D-99	3.03E-28	Not available	3.15(1)E-28	—	0.99	7.83E-28	Not available	Not available	—	—

[a] Diagonal matrix (for the ^{232}Th(n,γ)^{233}Th reaction only below 15 eV).
[b] Metastable state of the product nuclide.
[c] Uncertainty information for the ^{197}Au(n,γ)^{198}Au reaction is not reliable; withdrawn from ENDF/B-VI (a similar old evaluation is also present in IRDF-90).
[d] Uncertainty information for the ^{235}U(n,f) reaction is not reliable; withdrawn from ENDF/B-VI (a similar old evaluation is also present in IRDF-90).
(u): Updated data.
(n): New data.

Notes: Evaluated experimental cross-section data: values in brackets are 'absolute uncertainties' (one standard deviation). Subscript L signifies library data; subscripts M and H denote evaluated experimental data of Mughabghab [3.13] and Holden [3.14], respectively.

TABLE 3.4. RELATIVE STANDARD DEVIATIONS AVERAGED OVER A TYPICAL MTR SPECTRUM FOR THE CROSS-SECTIONS SELECTED FOR IRDF-2002 IN THE THERMAL AND EPITHERMAL NEUTRON ENERGY REGIONS

Reaction	Library (selected evaluation)	Mat. MT No.	Relative standard deviation for the spectrum part (%)	
			Thermal [a]	Epithermal [b]
^{6}Li(n,t)	IRDF-90	0325.105	0.14	0.14
^{10}B(n,α)	IRDF-90	0525.107	0.16	0.16
^{23}Na(n,γ) [c]	IRDF-90	1123.102	2.00	3.14
^{45}Sc(n,γ)	IRDF-90	2126.102	0.73	0.76
^{55}Mn(n,γ)	IRDF-90	2525.102	4.18	3.84
^{58}Fe(n,γ)	JENDL/D-99 (u)	2637.102	12.56	8.70
^{59}Co(n,γ)	IRDF-90	2725.102	0.66	0.77
^{63}Cu(n,γ)	IRDF-90	2925.102	4.11	3.86
^{93}Nb(n,γ) [c]	IRDF-90	4125.102	10.00	9.49
^{109}Ag(n,γ) [d]	IRDF-90 (n)	4731.102	5.10	6.90
^{115}In(n,γ) [c,d]	IRDF-90	4931.102	6.00	5.98
^{139}La(n,γ)	RRDF-98 (n)	5712.102	3.87	5.50
^{181}Ta(n,γ) [c]	JENDL/D-99	7328.102	3.00	3.77
^{186}W(n,γ)	RRDF-98 (u)	7452.102	2.31	3.32
^{197}Au(n,γ) [e]	IRDF-90	7925.102	0.14	0.17
^{232}Th(n,γ) [c]	IRDF-90	9040.102	4.33	10.92
^{235}U(n,f) [e]	IRDF-90	9228.018	0.19	0.26
^{238}U(n,γ)	IRDF-90	9237.102	0.35	0.37
^{239}Pu(n,f)	JENDL/D-99	9437.018	0.71	3.82
^{241}Am(n,f)	JENDL/D-99	9543.018	2.00	1.56

[a] From 1E-4 eV to 0.5 eV.
[b] From 0.5 eV to 1.05 MeV.
[c] Diagonal covariance matrix (only below 15 eV for the ^{232}Th(n,γ)^{233}Th reaction).
[d] Metastable state of the product nuclide.
[e] Uncertainty information is not reliable for the ^{197}Au(n,γ) and ^{235}U(n,f) reactions; withdrawn from ENDF/B-VI (similar old evaluations are also present in IRDF-90).
(u): Updated data.
(n): New data.

REFERENCES TO SECTION 3

[3.1] PAVIOTTI-CORCUERA, R., et al., "International reactor dosimetry file IRDF-2002", Reactor Dosimetry in the 21st Century (Proc. Int. Symp. Brussels, 2002) (WAGEMANS, J., ABDERRAHIM, H.A., D'HONDT, P., DE RAEDT, C., Eds), World Scientific, Singapore (2003) 654.

[3.2] GREENWOOD, L.R., PAVIOTTI-CORCUERA, R., "Summary of the supplementary workshop on testing of the IRDF-2002 File", Summary Report of the Technical Meeting on International Reactor Dosimetry File: IRDF-2002, Rep. INDC(NDS)-435, IAEA, Vienna (2002) Appendix 4.

[3.3] KOBAYASHI, K., et al., JENDL Dosimetry File (JENDL/D-99), Rep. JAERI 1344, Japan Atomic Energy Research Institute, Tokai-mura (2002).

[3.4] ZOLOTAREV, K.I., IGNATYUK, A.V., MAHOKHIN, V.N., PASHCHENKO, A.B., RRDF-98, Russian Reactor Dosimetry File, Rep. IAEA-NDS-193, Rev. 0, IAEA, Vienna (1999).

[3.5] WINENDF, ENDF package: includes Release 8 of ENDF/B-VI, Release 3.3 of JENDL, Release 3.0 of JEFF, WINENDF Prepro2000 codes, WNDVER codes, utility codes, manuals, Utils, ZaLibs, Nuclear Data Section, IAEA, Vienna (2002).

[3.6] BAARD, J.H., ZIJP, W.L., NOLTHENIUS, H.J., Nuclear Data Guide for Reactor Neutron Metrology, Kluwer, Dordrecht (1989).

[3.7] ZSOLNAY, E.M., NOLTHENIUS, H.J., SZONDI, E.J., Nuclear Data for Reactor Dosimetry Libraries: Analysis, Intercomparison and Selection of Data, Rep. BME-NTI-251/2001, Institute of Nuclear Techniques, Budapest University of Technology and Economics, Budapest (2001).

[3.8] ZSOLNAY, E.M., NOLTHENIUS, H.J., SZONDI, E.J., Analysis, Intercomparison and Selection of Data for the Preliminary Version of the International Reactor Dosimetry File IRDF-2002, Rep. BME-NTI-265/2002, Institute of Nuclear Techniques, Budapest University of Technology and Economics, Budapest (2002).

[3.9] ZOLOTAREV, K.I., Evaluation and Improvement of Cross Section Accuracy for Most Important Dosimetry Reactions Including Covariance Data, Rep. INDC(CCP)-431, IAEA, Vienna (2002).

[3.10] ZOLOTAREV, K.I., Evaluation and Improvement of Cross Section Accuracy for Most Important Dosimetry Reactions Including Covariance Data: ^{27}Al(n,p), ^{56}Fe(n,p), ^{237}Np(n,f), Rep. INDC(CCP)-438, IAEA, Vienna (2004).

[3.11] ZSOLNAY, E.M., NOLTHENIUS, H.J., Selection of Cross Sections for Thermal Neutron Capture and Fission Reactions for the File IRDF-2002, and Characterization of the Selected Data, Rep. BME-NTI-269/2003, Institute of Nuclear Techniques, Budapest University of Technology and Economics, Budapest (2003).

[3.12] SHIBATA, K., Japan Atomic Energy Research Institute, Tokai-mura, personal communication, 2002.

[3.13] MUGHABGHAB, S.F., Thermal Neutron Capture Cross Sections, Resonance Integrals and g-factors, Rep. INDC(NDS)-440, IAEA, Vienna (2003).

[3.14] HOLDEN, N.E., "Neutron scattering and absorption properties (revised 2003)", CRC Handbook of Chemistry and Physics, 84th edn (LIDE, D.R., Ed.), CRC Press, Boca Raton, FL (2003) 198–213.
[3.15] MUGHABGHAB, S.F., Brookhaven Natl Lab., Upton, NY, personal communication, 2003.

4. RESPONSE OF ACTIVATION REACTIONS IN THE NEUTRON FIELD OF CALIFORNIUM-252 SPONTANEOUS FISSION

W. Mannhart

The response of evaluated cross-section data for neutron activation reactions in the reference neutron field of ^{252}Cf spontaneous fission has been calculated. The bulk of the investigated cross-section data stems from the previous version of the IRDF (IRDF-90.2) [4.1], the JENDL Dosimetry File (JENDL/D-99) [4.2] and RRDF-98 [4.3, 4.4]. A few selected data sets of the ENDF/B-VI and JEFF-3.0 libraries were also used.

The neutron field of ^{252}Cf spontaneous fission is the only neutron field for which the available data meet all the criteria of a reference field with a well established and accurate spectral distribution, valid up to 20 MeV, together with a complete description of the uncertainty. The spectral distribution $N(E)$ of the fission neutrons of ^{252}Cf is the result of an evaluation based on modern time of flight measurements of this neutron spectrum [4.5]. The numerical values and the associated covariance matrix are given in Ref. [4.6].

Calculated spectrum averaged cross-sections of

$$\int \sigma(E)\, N(E)\, \mathrm{d}E \,/ \int N(E)\, \mathrm{d}E$$

were determined for the various $\sigma(E)$ data. Associated uncertainties were obtained from the propagated uncertainties of $\sigma(E)$ and $N(E)$. The calculated data were compared with experimental data to derive C/E values, and the experimental data were obtained from a detailed evaluation of the available integral experiments [4.7, 4.8].

The results are summarized in Table 4.1. Column 1 lists the neutron reactions that were investigated, in order of increasing energy response ranges. Column 2 quantifies the mean neutron energy $E(50\%)$ of the integrated response of each neutron reaction in the specified fission neutron field. The experimental data of spectrum averaged cross-sections and the uncertainties are given in columns 3 and 4; data in square brackets are from single experiments that were not included in the evaluation. These data can be found in Ref. [4.9], and in a few cases more recent data from the EXFOR database were used. The C/E values in columns 5–7 were obtained with the IRDF-90.2, JENDL/D-99 and RRDF-98 libraries, as indicated. With the exception of the ^{24}Mg(n,p)^{24}Na and ^{93}Nb(n,2n)^{92}Nb^{m} reactions, the original $\sigma(E)$ data of the RRDF-98 library were replaced by recent updates [4.3, 4.4].

The rigorous inclusion of all uncertainty components contributing to the C/E values allows quantitative statements to be made on the quality of the evaluated $\sigma(E)$ data, which are valid for the energy response range of the reaction. Calculated C/E values that show agreement with unity within the given uncertainties are printed in bold type in Table 4.1; these data show an optimum agreement between the integral and differential data. C/E values were also accepted that were within ±5% of unity, even if the calculated uncertainties were too small to achieve the desired overlap; these values are printed in normal font in Table 4.1. For most of the investigated reactions, a suitable data set of $\sigma(E)$ is identified in one of the libraries under study. This statement is only invalid for the ^{199}Hg(n,n′), ^{24}Mg(n,p), ^{127}I(n,2n), ^{55}Mn(n,2n) and ^{63}Cu(n,2n) reactions.

Table 4.2 contains a summary of the results obtained with selected data sets of the ENDF/B-VI and JEFF-3.0 libraries. The structure of the table is identical to that of Table 4.1.

The energy response of the various reactions depends strongly upon the threshold and shape of the $\sigma(E)$ data. This response range covers 90% of the total response of a reaction in the ^{252}Cf neutron field, and is between 0.21 and 5.70 MeV for the ^{235}U(n,f) reaction and between 13.12 and 18.25 MeV for the ^{58}Ni(n,2n)^{57}Ni reaction, with mean values $E(50\%)$ of 1.70 and 14.98 MeV, respectively. Thus the C/E values in Tables 4.1 and 4.2 cover quite different energy regions and provide data only for selected portions of the cross-section curve. A complete proof of the validity of a cross-section requires additional investigation of the remaining energy regions.

Additional details of the data analysis are given in Tables 4.3–4.6. A complete list of considered reactions and all calculated spectrum averaged data are given for each of the investigated cross-section libraries, independent of the availability of appropriate experimental data. Column 4 lists numerical values for the calculated spectrum averaged cross-sections, while the corresponding uncertainties are found in column 5, and the individual uncertainty contributions of the $\sigma(E)$ data and spectral distribution $N(E)$ to the calculated values are given separately in columns 6 and 7. The original uncertainties of the $\sigma(E)$ data are often further reduced by application of the averaging process in the calculation of spectrum averaged data.

Very low uncertainties are found in column 6 of the tables for a number of reactions, indicating that the quoted uncertainties of the evaluated $\sigma(E)$ data are probably extremely small. An analysis of the covariance files for these evaluations gives uncertainty values that often approach the accuracy level of the best known reference cross-sections. When considering the experimental database of the individual reactions and the spread of the available data, only a minority of the evaluated data sets with uncertainty values of <2% will meet

TABLE 4.1. *C*/*E* VALUES IN THE CALIFORNIUM-252 NEUTRON FIELD CALCULATED WITH $\sigma(E)$ DATA FROM IRDF-90.2, JENDL/D-99 AND RRDF-98

Reaction	*E*(50%) (MeV)	Experiment		*C*/*E*		
		$<\sigma>$ (mb)	%	IRDF-90.2	JENDL/D-99	RRDF-98 (update)
Au-197(n,γ)Au-198	0.75	7.679E+1	1.59	0.966 ± 0.021	**0.977 ± 0.086**	—
Cu-63(n,γ)Cu-64	0.93	1.044E+1	3.24	**0.996 ± 0.091**	**1.005 ± 0.196**	—
In-115(n,γ) In-116m1+m2	1.06	1.256E+1	2.23	**0.969 ± 0.047**	**1.003 ± 0.047**	—
U-235(n,f)	1.70	1.210E+3	1.20	**1.007 ± 0.012**	**1.021 ± 0.024**	—
Pu-239(n,f)	1.78	1.812E+3	1.37	0.980 ± 0.014	**0.996 ± 0.025**	—
Np-237(n,f)	2.07	1.361E+3	1.59	**0.999 ± 0.093**	**0.983 ± 0.016**	**0.999 ± 0.024**
In-115(n,n′)In-115m	2.68	1.974E+2	1.37	0.961 ± 0.025	0.961 ± 0.025	0.972 ± 0.021
U-238(n,f)	2.78	3.257E+2	1.64	0.969 ±0.017	**0.980 ± 0.026**	—
Hg-199(n,n′)Hg-199m	3.10	2.984E+2	1.81	—	0.833 ± 0.067	—
Ti-47(n,p)Sc-47	3.84	1.927E+1	1.66	**1.006 ± 0.042**	0.962 ± 0.021	—
S-32(n,p)P-32	4.06	7.254E+1	3.49	**0.969 ± 0.049**	**1.033 ± 0.090**	—
Ni-58(n,p)Co-58	4.17	1.175E+2	1.30	**0.982 ± 0.026**	0.975 ± 0.016	**1.000 ± 0.023**
Zn-64(n,p)Cu-64	4.26	4.059E+1	1.65	**1.037 ± 0.054**	0.942 ± 0.023	—
Fe-54(n,p)Mn-54	4.32	8.684E+1	1.34	**1.015 ± 0.026**	1.027 ± 0.019	—
Co-59(n,p)Fe-59	5.76	1.690E+0	2.48	—	—	—
Al-27(n,p)Mg-27	5.87	4.880E+0	2.14	0.958 ± 0.039	1.058 ± 0.027	**1.007 ± 0.032**
Ti-46(n,p)Sc-46	6.08	1.407E+1	1.77	0.876 ± 0.029	0.964 ± 0.030	**0.983 ± 0.037**
V-51(n,p)Ti-51	6.44	6.488E-1	1.97	—	—	—
Cu-63(n,α)Co-60	7.28	6.887E-1	1.96	**0.986 ± 0.033**	1.059 ± 0.029	**1.007 ± 0.037**
Fe-56(n,p)Mn-56	7.56	1.465E+0	1.77	0.936 ± 0.030	**0.962 ± 0.048**	**1.007 ± 0.035**
Mg-24(n,p)Na-24	8.25	1.996E+0	2.44	1.082 ± 0.040	1.092 ± 0.034	1.073 ± 0.034
Co-59(n,α)Mn-56	8.36	2.218E-1	1.88	**0.975 ± 0.036**	**1.040 ± 0.050**	**0.997 ± 0.043**
Ti-48(n,p)Sc-48	8.38	4.247E-1	1.89	0.912 ± 0.032	0.931 ± 0.028	**1.005 ± 0.057**
Al-27(n,α)Na-24	8.66	1.016E+0	1.28	**1.022 ± 0.026**	**1.022 ± 0.026**	—
V-51(n,α)Sc-48	9.97	3.900E-2	2.21	**0.995 ± 0.044**	—	**0.989 ± 0.041**
Tm-169(n,2n)Tm-168	10.34	[6.690E+0]	6.28	—	**0.932 ± 0.065**	—
Au-197(n,2n)Au-196	10.61	5.506E+0	1.83	**1.044 ± 0.052**	1.049 ± 0.031	—
Nb-93(n,2n)Nb-92m	11.47	[7.490E-1]	5.07	**1.041 ± 0.064**	**1.011 ± 0.070**	**1.030 ± 0.058**
I-127(n,2n)I-126	11.75	2.069E+0	2.73	1.062 ± 0.045	1.096 ± 0.051	—
Cu-65(n,2n)Cu-64	12.64	6.582E-1	2.22	**1.030 ± 0.042**	1.061 ± 0.039	—

TABLE 4.1. *C*/*E* VALUES IN THE CALIFORNIUM-252 NEUTRON FIELD CALCULATED WITH $\sigma(E)$ DATA FROM IRDF-90.2, JENDL/D-99 AND RRDF-98 (cont.)

Reaction	*E*(50%) (MeV)	Experiment		*C*/*E*		
		$<\sigma>$ (mb)	%	IRDF-90.2	JENDL/D-99	RRDF-98 (update)
Mn-55(n,2n)Mn-54	12.84	4.075E-1	2.33	1.181 ± 0.115	1.237 ± 0.111	—
Co-59(n,2n)Co-58	13.06	4.051E-1	2.51	**1.044 ± 0.051**	**1.030 ± 0.045**	—
Cu-63(n,2n)Cu-62	13.75	1.844E-1	3.98	1.134 ± 0.068	1.140 ± 0.066	—
F-19(n,2n)F-18	14.02	1.612E-2	3.37	**1.065 ± 0.063**	1.151 ± 0.070	**1.009 ± 0.064**
Zr-90(n,2n)Zr-89	14.41	2.210E-1	2.89	**1.001 ± 0.061**	**0.979 ± 0.058**	—
Ni-58(n,2n)Ni-57	14.98	8.952E-3	3.57	**1.033 ± 0.079**	**1.004 ± 0.072**	—

the accuracy level quoted. Unfortunately, such low uncertainties can also originate from cross-section evaluations based on least squares principles, if the cross-correlations between the different experimental data sets or the correlations between data belonging to the same experiment are neglected or improperly handled.

The impact of unreliable uncertainty values should not be underestimated; for example, the response of a number of activation reactions in a typical neutron field is used in reactor dosimetry to derive the spectral fluence distribution with unfolding methods. The response of each of the activation reactions represents a broad resolution experiment with a strong overlap in the energy response range between the various reactions. Unfolding implicitly requires that the $\sigma(E)$ data of the various reactions be consistent within the uncertainties quoted; if this consistency is not maintained, the derived spectral fluences will exhibit strong discontinuities that will seriously distort the result of the unfolding process.

TABLE 4.2. *C*/*E* VALUES IN THE CALIFORNIUM-252 NEUTRON FIELD CALCULATED WITH SELECTED $\sigma(E)$ DATA FROM ENDF/B-VI AND JEFF-3.0

Reaction	*E*(50%) (MeV)	Experiment		*C*/*E*	
		<σ> (mb)	%	ENDF/B-VI	JEFF-3.0
Ni-58(n,p)Co-58	4.17	1.175E+2	1.30	**0.981 ± 0.028**	**0.997 ± 0.037**
Ni-60(n,p)Co-60	7.05	[2.390E+0]	5.44	**1.044 ± 0.121**	1.170 ± 0.117
Fe-56(n,p)Mn-56	7.56	1.465E+0	1.77	—	**0.981 ± 0.025**
Cu-65(n,2n)Cu-64	12.64	6.582E-1	2.22	**1.030 ± 0.044**	—
Cu-63(n,2n)Cu-62	13.75	1.844E-1	3.98	1.115 ± 0.078	—
Cr-52(n,2n)Cr-51	14.69	—	—	—	—
Ni-58(n,2n)Ni-57	14.98	8.952E-3	3.57	**1.034 ± 0.077**	**1.034 ± 0.078**

TABLE 4.3. IRDF-90.2 (<σ> DATA IN A CALIFORNIUM-252 NEUTRON FIELD)

Reaction	Experiment		Calculation		σ(E) error (%)	N(E) error (%)	C/E	E(50%) (MeV)
	<σ> (mb)	Error (%)	<σ> (mb)	Error (%)				
Sc-45(n,γ)Sc-46	—	—	4.850	9.06	9.00	1.07	—	0.56
Li-6(n,t)He-4	—	—	311.8	0.85	0.63	0.57	—	0.62
Nb-93(n,γ)Nb-94m	—	—	26.33	7.52	7.48	0.84	—	0.68
Au-197(n,γ)Au-198	76.79	1.59	74.19	1.43	1.23	0.73	0.966 ± 0.021	0.73
Ag-109(n,γ)Ag-110m	—	—	9.344	7.58	7.56	0.53	—	0.74
Mn-55(n,γ)Mn-56	—	—	2.843	11.71	11.66	1.08	—	0.80
B-10(n,α)Li-7	—	—	444.1	6.23	6.20	0.56	—	0.92
U-238(n,γ)U-239	—	—	67.97	1.06	0.94	0.48	—	0.92
Na-23(n,γ)Na-24	[0.335]	4.48	0.2696	12.92	12.90	0.85	0.805 ± 0.110	0.93
Th-232(n,γ)Th-233	[87.8]	4.56	89.68	11.83	11.82	0.42	**1.021 ± 0.129**	0.93
Cu-63(n,γ)Cu-64	10.44	3.24	10.40	8.51	8.49	0.62	**0.996 ± 0.091**	0.97
Fe-58(n,γ)Fe-59	—	—	2.469	29.17	29.17	0.60	—	1.07
Co-59(n,γ)Co-60	[6.97]	4.88	6.062	4.76	4.70	0.71	0.870 ± 0.059	1.08
In-115(n,γ)In-116m1+m2	125.6	2.23	121.7	4.35	4.33	0.33	**0.969 ± 0.047**	1.13
U-235(n,f)	1210	1.20	1218	0.32	0.32	0.06	**1.007 ± 0.012**	1.70
Pu-239(n,f)	1812	1.37	1775	0.41	0.41	0.04	0.980 ± 0.014	1.78
Np-237(n,f)	1361	1.59	1360	9.21	9.21	0.21	**0.999 ± 0.093**	2.07
Rh-103(n,n′)Rh-103m	[809]	2.97	714.4	3.08	3.07	0.25	0.883 ± 0.038	2.39

TABLE 4.3. IRDF-90.2 (<σ> DATA IN A CALIFORNIUM-252 NEUTRON FIELD) (cont.)

Reaction	Experiment		Calculation		σ(E) error (%)	N(E) error (%)	C/E	E(50%) (MeV)
	<σ> (mb)	Error (%)	<σ> (mb)	Error (%)				
In-115(n,n′)In-115m	197.4	1.37	189.8	2.19	2.16	0.37	0.961 ± 0.025	2.68
Nb-93(n,n′)Nb-93m	[146]	3.45	142.6	3.01	2.99	0.35	**0.977 ± 0.045**	2.72
U-238(n,f)	325.7	1.64	315.5	0.67	0.54	0.39	0.969 ± 0.017	2.78
Th-232(n,f)	[89.4]	3.02	78.55	5.11	5.09	0.42	0.879 ± 0.052	2.99
Ti-47(n,p)Sc-47	19.27	1.66	19.38	3.83	3.78	0.62	**1.006 ± 0.042**	3.85
P-31(n,p)Si-31	—	—	30.68	3.65	3.58	0.69	—	3.97
S-32(n,p)P-32	72.54	3.49	70.30	3.67	3.60	0.74	**0.969 ± 0.049**	4.08
Ni-58(n,p)Co-58	117.5	1.30	115.4	2.32	2.21	0.72	**0.982 ± 0.026**	4.13
Zn-64(n,p)Cu-64	40.59	1.65	42.10	4.93	4.87	0.78	**1.037 ± 0.054**	4.16
Fe-54(n,p)Mn-54	86.84	1.34	88.16	2.23	2.09	0.78	**1.015 ± 0.026**	4.28
Al-27(n,p)Mg-27	4.880	2.14	4.674	3.44	3.24	1.14	**0.958 ± 0.039**	5.85
Ti-46(n,p)Sc-46	14.07	1.77	12.33	2.74	2.47	1.17	0.876 ± 0.029	5.93
Ni-60(n,p)Co-60	[2.39]	5.44	2.495	10.14	10.05	1.37	**1.044 ± 0.120**	7.09
Cu-63(n,α)Co-60	0.6887	1.96	0.6789	2.75	2.38	1.39	**0.986 ± 0.033**	7.29
Fe-56(n,p)Mn-56	1.465	1.77	1.371	2.62	2.18	1.46	0.936 ± 0.030	7.54
Mg-24(n,p)Na-24	1.996	2.44	2.160	2.75	2.24	1.59	1.082 ± 0.040	8.25
Co-59(n,α)Mn-56	0.2218	1.88	0.2163	3.14	2.73	1.56	**0.975 ± 0.036**	8.35
Ti-48(n,p)Sc-48	0.4247	1.89	0.3872	3.02	2.58	1.57	0.912 ± 0.032	8.40

TABLE 4.3. IRDF-90.2 (<σ> DATA IN A CALIFORNIUM-252 NEUTRON FIELD) (cont.)

Reaction	Experiment		Calculation		$\sigma(E)$ error (%)	$N(E)$ error (%)	C/E	E(50%) (MeV)
	<σ> (mb)	Error (%)	<σ> (mb)	Error (%)				
Al-27(n,α)Na-24	1.016	1.47	1.038	2.12	1.36	1.62	**1.022 ± 0.026**	8.66
V-51(n,α)Sc-48	3.900E-2	2.21	3.882E-2	3.81	3.32	1.88	**0.995 ± 0.044**	9.95
Au-197(n,2n)Au-196	5.506	1.83	5.747	4.65	4.19	2.02	**1.044 ± 0.052**	10.62
Nb-93(n,2n)Nb-92m	[0.749]	5.07	0.7794	3.48	2.67	2.23	**1.041 ± 0.064**	11.35
In-115(n,2n)In-114	—	—	1.586	4.02	3.23	2.39	—	11.74
I-127(n,2n)I-126	2.069	2.73	2.197	3.30	2.28	2.38	1.062 ± 0.045	11.75
Cu-65(n,2n)Cu-64	0.6582	2.22	0.6779	3.44	1.83	2.92	**1.030 ± 0.042**	12.64
Mn-55(n,2n)Mn-54	0.4075	2.33	0.4811	9.42	8.90	3.07	1.181 ± 0.115	12.85
Co-59(n,2n)Co-58	0.4051	2.51	0.4228	4.20	2.67	3.24	**1.044 ± 0.051**	13.03
Cu-63(n,2n)Cu-62	0.1844	3.98	0.2091	4.44	1.66	4.11	1.134 ± 0.068	13.79
Y-89(n,2n)Y-88	—	—	0.3446	5.91	4.05	4.30	—	13.94
F-19(n,2n)F-18	1.612E-2	3.37	1.716E-2	4.86	2.09	4.39	**1.065 ± 0.063**	14.00
Zr-90(n,2n)Zr-89	0.2210	2.89	0.2212	5.31	1.57	5.07	**1.001 ± 0.061**	14.41
Ti-47(n,np)Sc-46	—	—	2.316E-2	30.45	30.00	5.24	—	14.61
Cr-52(n,2n)Cr-51	—	—	9.703E-2	6.23	2.72	5.60	—	14.70
Ni-58(n,2n)Ni-57	8.952E-3	3.57	9.243E-3	6.80	3.05	6.07	**1.033 ± 0.079**	14.95
Ti-48(n,np)Sc-47	—	—	4.059E-3	30.61	30.00	6.09	—	15.13

TABLE 4.4. JENDL/D-99 (<σ> DATA IN A CALIFORNIUM-252 NEUTRON FIELD)

Reaction	Experiment		Calculation		σ(E) error (%)	N(E) error (%)	C/E	E(50%) (MeV)
	<σ> (mb)	Error (%)	<σ> (mb)	Error (%)				
Eu-151(n,γ)Eu-152	—	—	360.0	2.76	2.63	0.86	—	0.62
Li-6(n,t)He-4	—	—	323.3	2.83	2.77	0.56	—	0.64
Sc-45(n,γ)Sc-46	—	—	6.023	3.51	3.40	0.86	—	0.68
Au-197(n,γ)Au-198	76.79	1.59	75.01	8.71	8.69	0.66	**0.977 ± 0.086**	0.77
Mn-55(n,γ)Mn-56	—	—	2.843	11.71	11.66	1.08	—	0.80
Fe-58(n,γ)Fe-59	—	—	1.795	3.05	2.96	0.75	—	0.80
Ta-181(n,γ)Ta-182	[106]	5.78	83.34	5.46	5.41	0.77	0.786 ± 0.062	0.82
B-10(n,α)Li-7	—	—	427.2	6.19	6.17	0.58	—	0.84
U-238(n,γ)U-239	—	—	64.68	5.74	5.72	0.51	—	0.87
Cu-63(n,γ)Cu-64	10.44	3.24	10.49	19.19	19.18	0.65	**1.005 ± 0.196**	0.88
Cr-50(n,γ)Cr-51	—	—	6.230	10.65	10.64	0.62	—	0.92
Th-232(n,γ)Th-233	[87.8]	4.56	83.48	11.92	11.91	0.43	**0.951 ± 0.121**	0.95
In-115(n,γ)In-116m1+m2	125.6	2.23	126.0	4.11	4.09	0.41	**1.003 ± 0.047**	0.99
W-186(n,γ)W-187	—	—	34.74	4.61	4.59	0.38	—	1.00
Co-59(n,γ)Co-60	[6.97]	4.88	5.591	4.58	4.52	0.74	0.802 ± 0.054	1.04
Na-23(n,γ)Na-24	[0.335]	4.48	0.2236	12.89	12.86	0.95	0.667 ± 0.091	1.08
Ag-109(n,γ)Ag-110m	—	—	6.657	9.85	9.84	0.39	—	1.09
U-235(n,f)	1210	1.20	1236	1.97	1.97	0.05	**1.021 ± 0.024**	1.70

TABLE 4.4. JENDL/D-99 (<σ> DATA IN A CALIFORNIUM-252 NEUTRON FIELD) (cont.)

Reaction	Experiment		Calculation		σ(*E*) error (%)	*N*(*E*) error (%)	*C*/*E*	*E*(50%) (MeV)
	<σ> (mb)	Error (%)	<σ> (mb)	Error (%)				
Pu-239(n,f)	1812	1.37	1804	2.04	2.04	0.05	**0.996 ± 0.025**	1.79
Np-237(n,f)	1361	1.59	1338	0.34	0.27	0.21	**0.983 ± 0.016**	2.07
Am-241(n,f)	—	—	1396	2.81	2.90	0.29	—	2.23
Rh-103(n,n′)Rh-103m	[809]	2.97	716.3	3.08	3.07	0.25	0.885 ± 0.038	2.39
In-115(n,n′)In-115m	197.4	1.37	189.8	2.19	2.16	0.37	0.961 ± 0.025	2.68
Nb-93(n,n′)Nb-93m	[146]	3.45	149.7	3.18	3.16	0.35	**1.025 ± 0.048**	2.69
U-238(n,f)	325.7	1.64	319.2	2.04	2.00	0.40	0.980 ± 0.026	2.77
Th-232(n,f)	[89.4]	3.02	82.14	5.10	5.08	0.42	0.919 ± 0.054	2.98
Hg-199(n,n′)Hg-199m	298.4	1.81	248.6	7.83	7.82	0.43	0.833 ± 0.067	3.10
Ti-47(n,p)Sc-47	19.27	1.66	18.54	1.42	1.28	0.61	0.962 ± 0.021	3.82
P-31(n,p)Si-31	—	—	32.24	1.55	1.40	0.67	—	3.83
S-32(n,p)P-32	72.54	3.49	74.97	7.96	7.93	0.73	**1.033 ± 0.090**	4.04
Ni-58(n,p)Co-58	117.5	1.30	114.6	0.95	0.60	0.74	0.975 ± 0.016	4.22
Zn-64(n,p)Cu-64	40.59	1.65	38.23	1.78	1.60	0.79	0.942 ± 0.023	4.35
Fe-54(n,p)Mn-54	86.84	1.34	89.22	1.25	0.97	0.79	1.027 ± 0.019	4.35
Al-27(n,p)Mg-27	4.880	2.14	5.163	1.37	0.73	1.16	1.058 ± 0.027	5.89
Ti-46(n,p)Sc-46	14.07	1.77	13.57	2.59	2.31	1.18	0.964 ± 0.030	5.99
Cu-63(n,α)Co-60	0.6887	1.96	0.7291	1.95	1.49	1.26	1.059 ± 0.029	7.00

TABLE 4.4. JENDL/D-99 (<σ> DATA IN A CALIFORNIUM-252 NEUTRON FIELD) (cont.)

Reaction	Experiment		Calculation		$\sigma(E)$ error (%)	$N(E)$ error (%)	C/E	E(50%) (MeV)
	<σ> (mb)	Error (%)	<σ> (mb)	Error (%)				
Ni-60(n,p)Co-60	[2.39]	5.44	2.281	18.75	18.70	1.45	**0.954 ± 0.186**	7.42
Fe-56(n,p)Mn-56	1.465	1.77	1.410	4.66	4.42	1.47	**0.962 ± 0.048**	7.68
Co-59(n,α)Mn-56	0.2218	1.88	0.2306	4.46	4.18	1.55	**1.040 ± 0.050**	8.23
Mg-24(n,p)Na-24	1.996	2.44	2.179	2.00	1.23	1.59	1.092 ± 0.034	8.25
Ti-48(n,p)Sc-48	0.4247	1.89	0.3954	2.39	1.82	1.56	0.931 ± 0.028	8.33
Al-27(n,α)Na-24	1.016	1.47	1.038	2.12	1.36	1.63	**1.022 ± 0.026**	8.66
Tm-169(n,2n)Tm-168	[6.69]	6.28	6.233	3.01	2.26	1.98	**0.932 ± 0.065**	10.34
Au-197(n,2n)Au-196	5.506	1.83	5.776	2.33	1.16	2.02	1.049 ± 0.031	10.60
Nb-93(n,2n)Nb-92m	[0.749]	5.07	0.7576	4.65	4.07	2.25	**1.011 ± 0.070**	11.47
I-127(n,2n)I-126	2.069	2.73	2.268	3.78	2.97	2.35	1.096 ± 0.051	11.69
Cu-65(n,2n)Cu-64	0.6582	2.22	0.6985	2.97	0.87	2.84	1.061 ± 0.039	12.55
Mn-55(n,2n)Mn-54	0.4075	2.33	0.5041	8.70	8.15	3.06	1.237 ± 0.111	12.82
Co-59(n,2n)Co-58	0.4051	2.51	0.4171	3.56	1.36	3.29	**1.030 ± 0.045**	13.09
Cu-63(n,2n)Cu-62	0.1844	3.98	0.2102	4.19	1.32	3.97	1.140 ± 0.066	13.70
Y-89(n,2n)Y-88	—	—	0.3440	4.47	1.40	4.25	—	13.90
F-19(n,2n)F-18	1.612E-2	3.37	1.855E-2	5.04	2.61	4.31	1.151 ± 0.070	13.94
Zr-90(n,2n)Zr-89	0.2210	2.89	0.2164	5.15	0.56	5.12	**0.979 ± 0.058**	14.44
Cr-52(n,2n)Cr-51	—	—	9.555E-2	5.75	1.29	5.60	—	14.69

TABLE 4.4. JENDL/D-99 (<σ> DATA IN A CALIFORNIUM-252 NEUTRON FIELD) (cont.)

Reaction	Experiment		Calculation		σ(*E*) error (%)	*N*(*E*) error (%)	*C*/*E*	*E*(50%) (MeV)
	<σ> (mb)	Error (%)	<σ> (mb)	Error (%)				
Ni-58(n,2n)Ni-57	8.952E-3	3.57	8.985E-3	6.24	0.85	6.19	**1.004 ± 0.072**	15.00
Ti-47(n,np)Sc-46	—	—	1.670E-2	6.90	2.58	6.40	—	15.19
Na-23(n,2n)Na-22	—	—	8.611E-3	8.16	3.90	7.17	—	15.40
Ti-48(n,np)Sc-47	—	—	4.175E-3	8.32	2.90	7.80	—	15.76
Ti-46(n,2n)Ti-45	—	—	1.308E-2	8.58	1.86	8.38	—	16.01
Ti-49(n,np)Sc-48	—	—	2.759E-3	13.49	10.45	8.52	—	16.15
Fe-57(n,np)Mn-56	—	—	2.112E-3	18.74	16.47	8.93	—	16.20

TABLE 4.5. UPDATED RRDF-98 (<σ> DATA IN A CALIFORNIUM-252 NEUTRON FIELD)

Reaction	Experiment		Calculation		σ(*E*) error (%)	*N*(*E*) error (%)	*C*/*E*	*E*(50%) (MeV)
	<σ> (mb)	Error (%)	<σ> (mb)	Error (%)				
Np-237(n,f)	1361	1.59	1359	1.74	1.72	0.21	**0.999 ± 0.024**	2.06
Rh-103(n,n′)Rh-103m	[809]	2.97	725.1	3.95	3.94	0.25	0.896 ± 0.044	2.38
In-115(n,n′)In-115m	197.4	1.37	191.8	1.70	1.66	0.37	0.972 ± 0.021	2.67
Nb-93(n,n′)Nb-93m	[146]	3.45	146.1	2.61	2.59	0.35	**1.001 ± 0.043**	2.69
Ni-58(n,p)Co-58	117.5	1.30	117.5	1.89	1.74	0.74	**1.000 ± 0.023**	4.20
Pb-204(n,n′)Pb-204m	[20.85]	4.41	20.39	4.67	4.57	0.98	**0.978 ± 0.063**	5.04
Al-27(n,p)Mg-27	4.880	2.14	4.912	2.37	2.06	1.17	**1.007 ± 0.032**	6.02
Ti-46(n,p)Sc-46	14.07	1.77	13.83	3.28	3.05	1.19	**0.983 ± 0.037**	6.08
Cu-63(n,α)Co-60	0.6887	1.96	0.6933	3.15	2.83	1.39	**1.007 ± 0.037**	7.27
Fe-54(n,α)Cr-51	—	—	1.113	3.48	3.18	1.42	—	7.43
Fe-56(n,p)Mn-56	1.465	1.77	1.475	2.99	2.61	1.46	**1.007 ± 0.035**	7.56
Mg-24(n,p)Na-24	1.996	2.44	2.142	1.96	1.14	1.59	1.073 ± 0.034	8.25
Ti-48(n,p)Sc-48	0.4247	1.89	0.4268	5.32	5.08	1.57	**1.005 ± 0.057**	8.35
Co-59(n,α)Mn-56	0.2218	1.88	0.2212	3.87	3.54	1.56	**0.997 ± 0.043**	8.37
V-51(n,α)Sc-48	3.900E-2	2.21	3.859E-2	3.56	3.02	1.89	**0.989 ± 0.041**	9.98
Nb-93(n,2n)Nb-92m	[0.749]	5.07	0.7717	2.46	1.03	2.24	**1.030 ± 0.058**	11.36
Pr-141(n,2n)Pr-140	—	—	1.990	11.37	11.03	2.45	—	11.85
As-75(n,2n)As-74	—	—	0.6209	6.55	5.76	3.14	—	12.91

TABLE 4.5. UPDATED RRDF-98 (<σ> DATA IN A CALIFORNIUM-252 NEUTRON FIELD) (cont.)

Reaction	Experiment		Calculation		$\sigma(E)$ error (%)	$N(E)$ error (%)	C/E	E(50%) (MeV)
	<σ> (mb)	Error (%)	<σ> (mb)	Error (%)				
F-19(n,2n)F-18	1.612E-2	3.37	1.627E-2	5.33	2.92	4.46	**1.009 ± 0.064**	14.04
Ti-47(n,np)Sc-46	—	—	1.941E-2	9.58	7.57	5.88	—	14.93
Ti-48(n,np)Sc-47	—	—	4.349E-3	11.62	8.20	8.24	—	15.88
Ti-49(n,np)Sc-48	—	—	2.644E-3	10.84	7.18	8.13	—	15.96
Ti-46(n,2n)Ti-45	—	—	1.218E-2	9.55	4.41	8.47	—	16.03
Fe-54(n,2n)Fe-53	—	—	3.498E-3	10.71	4.87	9.54	—	16.48

Notes: Data for the 93Nb(n,n′)93Nbm, 24Mg(n,p)24Na and 93Nb(n,2n)92Nbm reactions are based on the original version of RRDF-98. The calculated <σ> value of the 54Fe(n,2n)53Fe reaction is incomplete, with an upper limit to the neutron spectrum of 20 MeV.

TABLE 4.6. ENDF/B-VI AND JEFF-3.0 (<σ> DATA IN A CALIFORNIUM-252 NEUTRON FIELD)

Reaction	Experiment		Calculation		σ(*E*) error (%)	*N*(*E*) error (%)	*C*/*E*	*E*(50%) (MeV)
	<σ> (mb)	Error (%)	<σ> (mb)	Error (%)				
ENDF/B-VI								
Ni-58(n,p)Co-58	117.5	1.30	115.3	2.52	2.41	0.72	**0.981 ± 0.028**	4.13
Ni-60(n,p)Co-60	[2.39]	5.44	2.494	10.20	10.11	1.37	**1.044 ± 0.121**	7.10
Cu-65(n,2n)Cu-64	0.6582	2.22	0.6777	3.69	2.25	2.92	**1.030 ± 0.044**	12.65
Cu-63(n,2n)Cu-62	0.1844	3.98	0.2056	5.81	4.10	4.12	1.115 ± 0.078	13.79
Cr-52(n,2n)Cr-51	—	—	9.841E-2	9.83	8.11	5.56	—	14.69
Ni-58(n,n)Ni-57	8.952E-3	3.57	9.254E-3	6.58	2.48	6.10	**1.034 ± 0.077**	14.96
JEFF-3.0								
Ni-58(n,p)Co-58	117.5	1.30	117.1	3.46	3.38	0.72	**0.997 ± 0.037**	4.16
Ni-60(n,p)Co-60	[2.39]	5.44	2.796	8.37	8.26	1.36	1.170 ± 0.117	6.99
Fe-56(n,p)Mn-56	1.465	1.77	1.437	1.82	1.08	1.46	**0.981 ± 0.025**	7.57
Ni-58(n,2n)Ni-57	8.952E-3	3.57	9.256E-3	6.67	2.72	6.09	**1.034 ± 0.078**	14.96

REFERENCES TO SECTION 4

[4.1] KOCHEROV, N.P., McLAUGHLIN, P.K., The International Reactor Dosimetry File (IRDF-90 Version 2), Rep. IAEA-NDS-141, Rev. 3, IAEA, Vienna (1996).

[4.2] KOBAYASHI, K., et al., JENDL Dosimetry File (JENDL/D-99), Rep. JAERI 1344, Japan Atomic Energy Research Institute, Tokai-mura (2002).

[4.3] ZOLOTAREV, K.I., IGNATYUK, A.V., MAHOKHIN, V.N., PASHCHENKO, A.B., RRDF-98, Russian Reactor Dosimetry File, Rep. IAEA-NDS-193, Rev. 0, IAEA, Vienna (1999).

[4.4] ZOLOTAREV, K.I., "Revisions and new evaluations of cross sections for 19 dosimetry reactions", Summary Report of Technical Meeting on International Reactor Dosimetry File: IRDF-2002, Rep. IAEA(NDS)-435, IAEA, Vienna (2002) 39.

[4.5] MANNHART, W., "Evaluation of the Cf-252 fission neutron spectrum between 0 MeV and 20 MeV", Properties of Neutron Sources, IAEA-TECDOC-410, IAEA, Vienna (1987) 158.

[4.6] "Decay data library, MAT = 9861, MF = 5, MT = 18", ENDF/B-VI Summary Documentation (ROSE, P.F., Ed.), Rep. BNL-NCS-17541 (ENDF-201), Brookhaven Natl Lab., Upton, NY (1991); Data Library ENDF/B-VI Release 8, update 2001, by the US National Nuclear Data Center on behalf of the Cross-Section Evaluation Working Group.

[4.7] MANNHART, W., "Generation of covariance data while updating evaluated data using 'Bayesian' methods", Evaluation and Processing of Covariance Data (Specialists Mtg, Oak Ridge, TN, 1992), Rep. NEA/NSC/DOC(93)3, OECD, Paris (1993) 157.

[4.8] MANNHART, W., Physikalisch-Technische Bundesanstalt, Braunschweig, personal communication, 2001.

[4.9] MANNHART, W., "Californium-252 spectrum averaged neutron cross-sections", Handbook on Nuclear Activation Data, Technical Reports Series No. 273, IAEA, Vienna (1987) 413.

5. EVALUATION OF CROSS-SECTIONS AT 14 MeV FOR IRDF-2002

L.R. Greenwood

The selection of the evaluated neutron activation cross-sections for inclusion into IRDF-2002 depends in part on how well the various evaluations agree with the experimental data for thermal cross-sections, resonance integrals and near 14 MeV. Candidate evaluated neutron cross-section libraries included IRDF-90 [5.1], JENDL/D-99 [5.2], RRDF-98 [5.3], ENDF/B-VI and JEFF-3.0 [5.4], as listed in Table 5.1. Differences between these evaluations were assessed by plotting the evaluated cross-sections together with the available experimental data in the 14 MeV region. Appendix IV contains the plots for all of the reactions considered for IRDF-2002. These comparisons were then used to identify any significant differences between the various evaluations that would affect the selection for IRDF-2002. Differences between the various evaluations were negligible in most cases, and no clear preference could be made based solely on the fit to the experimental data near 14 MeV.

Detailed comments are provided for each of the reactions that were considered. It is important to note that this rapid and somewhat superficial evaluation of the experimental data and cross-section evaluations had the limited objective of aiding the selection of cross-section data for IRDF-2002. More detailed discussions of the data and cross-sections by the evaluators are readily available in the report section of each reaction in the cross-section libraries.

5.1. PLOTS OF EXPERIMENTAL DATA AND EVALUATED CROSS-SECTIONS

Most neutron activation reactions have been extensively studied near 14 MeV because of the widespread availability of deuterium + tritium 14 MeV neutron sources and other accelerator based neutrons. However, such data have normally been measured at a significant range of energies around 14 MeV, due to the characteristics of the various accelerators that have been used. Although the interaction of deuterium and tritium produces a neutron close to 14 MeV at low deuteron energies, many ‘14 MeV’ neutron sources accelerate the deuteron to several hundred kiloelectronvolts or more, and use a correspondingly thicker target containing the tritium in order to increase the

neutron yield substantially. Furthermore, the neutron energy distributions vary with the angle between the incoming deuteron beam and the location of the measurement. Consequently, these effects lead to a predictable distribution of neutron energies around 14 MeV for all of the experimental data. After an examination of the available experimental neutron data, these experimental data were plotted in the range of 13.5–15.0 MeV. The experimental data were taken from EXFOR, which is available on the IAEA web site as the Nuclear Reaction Database Retrieval System [5.5]. Cross-section evaluations were taken from 640 group representations processed by the IAEA Nuclear Data Section.

Available experimental data in the 13.5–15 MeV region exhibited excessive scatter, and therefore selection criteria were applied to the data to be plotted as outlined below:

(a) Experimental data were taken directly from EXFOR in many cases. However, while preparing the various cross-section evaluations, the original cross-section evaluators examined all the data in more detail, and then renormalized them on the basis of changes in the monitor reaction cross-sections made after the original measurements were performed and reported. While there was insufficient time to perform this task for all of the reactions in IRDF-2002, Zolotarev provided evaluated and renormalized data for a number of reactions, as indicated in the discussion given below. Comparisons of the raw data and their normalized data show significant reductions in the scatter of data for most cases, as would be expected.
(b) Data that vary from most of the other data by significantly more than the stated uncertainties were omitted for clarity in the plots. Where only a few data measurements were available, no data were omitted.
(c) Data with very large energy uncertainties or poor energy resolution were generally omitted. Such data can be difficult to interpret, especially for reactions in which the cross-section is rapidly changing in the 14 MeV energy region (such data are more integral than differential in nature).
(d) Data published prior to 1970 were frequently omitted because they were superseded by more recent measurements of much higher quality. Again, no data were omitted when only a few measurements were available.

Data omission is generally not the best practice, but the agreement between the data and cross-section evaluations implies that the earlier evaluations involved similar data selections. All available data can be plotted using the EXFOR software whenever rapid assessment is considered necessary. Most of the plots are presented on expanded linear scales with suppressed

zeros in order to show the relatively small differences between the various cross-section evaluations.

The list of reactions and cross-section evaluations is given in Table 5.1. Symbol X indicates that plots were prepared and/or cross-sections were evaluated from the various data libraries; N indicates that no experimental data were available at 14 MeV and consequently plots were not prepared; D denotes that some of the cross-section files were duplicates of the cross-sections found in IRDF-90.

5.2. DETAILED COMMENTS ON THE CANDIDATE CROSS-SECTION LIBRARIES NEAR 14 MeV

Detailed comments are provided below for each of the plots shown in Appendix IV. IRDF means IRDF-90, JENDL is JENDL/D-99, RRDF refers to either RRDF-98 or new evaluations, ENDF is ENDF/B-VI, and JEFF refers to JEFF-3.0.

- $^{6}Li(n,\alpha)^{3}H$ and $^{10}B(n,\alpha)^{7}Li$: No experimental data were available in EXFOR, and therefore no plots were prepared.
- $^{19}F(n,2n)^{18}F$: Experimental data were evaluated and renormalized by Zolotarev. Evaluated cross-section files were available in JENDL and the RRDF. The RRDF-98 file clearly gives the best fit to the data with the lowest uncertainties.
- $^{24}Mg(n,p)^{24}Na$: The IRDF and JENDL are very similar, and both agree well with the data.
- $^{27}Al(n,p)^{27}Mg$: Experimental data were evaluated and renormalized by Zolotarev. The IRDF, JENDL and new RRDF evaluations are very similar and appear to be slightly lower than most of the experimental data.
- $^{27}Al(n,\alpha)^{24}Na$: JENDL is a duplicate of the IRDF, which fits the data reasonably well.
- $^{31}P(n,p)^{31}Si$: The IRDF and JENDL are nearly identical and fit the data equally well, although there is one data point that appears to be discrepant and should probably be rejected.
- $^{32}S(n,p)^{32}P$: The IRDF was the only file available and the cross-section fits the data quite well, neglecting one apparently discrepant data point.
- $^{45}Sc(n,\gamma)^{46}Sc$: The IRDF was the only file available. Neglecting a data point with very high uncertainties, the evaluation fits the data reasonably well.

TABLE 5.1. CROSS-SECTION EVALUATIONS AT 14 MeV

Reaction	Plot	IRDF-90	JENDL/ D-99	RRDF-98 or new	ENDF/ B-VI	JEFF-3.0
$^{6}Li(n,\alpha)^{3}H$	N	X				
$^{10}B(n,\alpha)^{7}Li$	N	X				
$^{19}F(n,2n)^{18}F$	X		X	X		
$^{23}Na(n,\gamma)^{24}Na$ [a]					X	
$^{23}Na(n,2n)^{22}Na$ [a]			X			
$^{24}Mg(n,p)^{24}Na$	X	X	X	Q		
$^{27}Al(n,p)^{27}Mg$	X	X	X	X		
$^{27}Al(n,\alpha)^{24}Na$	X	X	D			
$^{31}P(n,p)^{31}Si$	X	X	X			
$^{32}S(n,p)^{32}P$	X	X				
$^{45}Sc(n,\gamma)^{46}Sc$	X	X				
$^{46}Ti(n,2n)^{45}Ti$	X		X	X		
$^{46}Ti(n,p)^{46}Sc$	X	X	X	X		
$Ti(n,x)^{46}Sc$	X		X			
$^{47}Ti(n,np+pn+d)^{46}Sc$	X	X		X		
$^{47}Ti(n,p)^{47}Sc$	X	X				
$^{48}Ti(n,np+pn+d)^{47}Sc$	X	X	X	X		
$Ti(n,x)^{48}Sc$	X		X			
$^{48}Ti(n,p)^{48}Sc$	X	X		X		
$^{49}Ti(n,np+pn+d)^{48}Ti$	X		X	X		
$^{51}V(n,\alpha)^{48}Sc$	X			X		
$^{55}Cr(n,2n)^{51}Cr$	X	X	X		X	
$^{55}Mn(n,\gamma)^{56}Mn$	X	X	D			
$^{54}Fe(n,2n)^{53}Fe$	X			X		
$^{54}Fe(n,\alpha)^{51}Cr$	X			X		
$^{54}Fe(n,p)^{54}Mn$	X	X	X			
$^{56}Fe(n,p)^{56}Mn$	X			X		X
$^{58}Fe(n,\gamma)^{59}Fe$	N	X	X			
$^{59}Co(n,2n)^{58}Co$	X	X				
$^{59}Co(n,\alpha)^{56}Mn$	X			X		
$^{59}Co(n,\gamma)^{60}Co$	X	X				

TABLE 5.1. CROSS-SECTION EVALUATIONS AT 14 MeV (cont.)

Reaction	Plot	IRDF-90	JENDL/ D-99	RRDF-98 or new	ENDF/ B-VI	JEFF-3.0
^{58}Ni(n,2n)^{57}Ni	X	X	X			X
^{58}Ni(n,p)^{58}Co	X	X	X	X	D	X
^{60}Ni(n,p)^{60}Co	X				X	X
^{63}Cu(n,2n)^{62}Cu	X		X		X	
^{63}Cu(n,γ)^{64}Cu	X	X			D	
^{63}Cu(n,α)^{60}Co	X	X	X	X		
^{65}Cu(n,2n)^{64}Cu	X	X			D	
^{64}Zn(n,p)^{64}Cu	X	X				
^{75}As(n,2n)^{74}As	X			X		
^{89}Y(n,2n)^{88}Y	X		X			
^{90}Zr(n,2n)^{89}Zr	X	X	X			
^{93}Nb(n,γ)^{94}Nb [a]		X				
^{93}Nb(n,2n)^{92}Nb^{m}	X	X		X		
^{93}Nb(n,n′)^{93}Nb^{m}	X	X		X		
^{103}Rh(n,n′)^{103}Rh^{m}	X	X		X		
^{109}Ag(n,γ)^{110}Ag^{m}	N	X				
^{115}In(n,2n)^{114}In^{m}	X	X				
^{115}In(n,γ)^{116}In^{m} [a]		X				
^{115}In(n,n′)^{115}In^{m}	X	X	D	X		
^{127}I(n,2n)^{126}I	X	X	X			
^{139}La(n,γ)^{140}La	X			X		
^{141}Pr(n,2n)^{140}Pr	X			X		
^{169}Tm(n,2n)^{168}Tm	X		X			
^{181}Ta(n,γ)^{182}Ta [a]			X			
^{186}W(n,γ)^{187}W	X			X		
^{197}Au(n,2n)^{196}Au	X	X	X			
^{197}Au(n,γ)^{198}Au	X	X				
^{199}Hg(n,n′)^{199}Hg^{m}	X		X			
^{204}Pb(n,n′)^{204}Pb^{m}	X			X		
^{232}Th(n,γ)^{233}Th [a]		X				
^{232}Th(n,f)	X	X				

TABLE 5.1. CROSS-SECTION EVALUATIONS AT 14 MeV (cont.)

Reaction	Plot	IRDF-90	JENDL/ D-99	RRDF-98 or new	ENDF/ B-VI	JEFF-3.0
^{235}U(n,f)	X	X				
^{238}U(n,f)	X	X	X			
^{238}U(n,γ)^{239}U	X	X				
^{237}Np(n,f)	X		X	Q		
^{239}Pu(n,f)	X	X	X			
^{241}Am(n,f)	X		X			

D: Files are duplicates of IRDF-90 files.
N: No cross-section data were available; plots were not prepared.
Q: New evaluation is nearly complete, but not yet available for consideration.
[a] Files did not meet the requirements specified for the covariance matrices, but were included due to their importance for reactor dosimetry.

— ^{46}Ti(n,2n)^{45}Ti: Experimental data were evaluated and renormalized by Zolotarev. Both the JENDL and RRDF evaluations are very similar and fit the data reasonably well, although the RRDF gives the best fit.
— ^{46}Ti(n,p)^{46}Sc: Evaluations were available in the IRDF, JENDL and RRDF, and all of them appear to be lower than the average of the experimental data. JENDL gives the best fit for all the data, although the IRDF and RRDF fit some of the data with the lowest uncertainties. Evaluator comments are very helpful and should be studied.
— Ti(n,x)^{46}Sc: JENDL is the only file available, and the evaluated cross-section is slightly higher than the available data from natural titanium.
— ^{47}Ti(n,np+pn+d)^{46}Sc: Experimental data were evaluated and renormalized by Zolotarev. Limited data include measurements of (n,np+d). The IRDF and RRDF are distinctly different, and the RRDF clearly gives the best fit to the data.
— ^{47}Ti(n,p)^{47}Sc: Experimental data were evaluated and renormalized by Zolotarev. The IRDF is the only available cross-section file. The evaluation appears to be somewhat lower than the available experimental data, although they exhibit considerable scatter.
— ^{48}Ti(n,np+pn+d)^{47}Sc: Experimental data were evaluated and renormalized by Zolotarev. Limited data include measurements of (n,np+d). Evaluations are available from the IRDF, RRDF and JENDL that all fit the data equally well.

— Ti(n,x)^{48}Sc: Only one data point was available from natural titanium, and the only evaluated file is from JENDL (which appears to be higher than the sole data point).
— ^{48}Ti(n,p)^{48}Sc: Experimental data were evaluated and renormalized by Zolotarev. The available files from the IRDF and RRDF are quite similar, and both fit the average of the available data (which exhibit considerable scatter).
— ^{49}Ti(n,np+pn+d)^{48}Ti: Experimental data were evaluated and renormalized by Zolotarev. Although JENDL and the RRDF are similar, the RRDF appears to fit the available data better.
— ^{51}V(n,α)^{48}Sc: Experimental data were evaluated and renormalized by Zolotarev. The RRDF is the only available file, and closely matches the available data.
— ^{55}Cr(n,2n)^{51}Cr: The IRDF, JENDL and ENDF files are almost identical. All of the recommended data in these files appear to be slightly higher than the average of the experimental measurements, although they are a good fit to the data with the lowest uncertainties.
— ^{55}Mn(n,γ)^{56}Mn: JENDL and the IRDF are essentially identical, and both fit the data with the lowest uncertainties reasonably well.
— ^{54}Fe(n,2n)^{53}Fe: Experimental data were evaluated and renormalized by Zolotarev. The only available file from the RRDF is a good fit to the experimental data, although there is some scatter.
— ^{54}Fe(n,α)^{51}Cr: Experimental data were evaluated and renormalized by Zolotarev. The only available file from the RRDF is a good fit to the experimental data.
— ^{54}Fe(n,p)^{54}Mn: Experimental data were evaluated and renormalized by Zolotarev. Evaluated files are available from the IRDF and JENDL: the IRDF gives a better fit over the entire energy range, although JENDL may be closer to the average of the data around 14.7 MeV.
— ^{56}Fe(n,p)^{56}Mn: Experimental data were evaluated and renormalized by Zolotarev. The RRDF and JEFF files are nearly identical, and both fit the data reasonably well.
— ^{58}Fe(n,γ)^{59}Fe: No experimental data are available near 14 MeV.
— ^{59}Co(n,γ)^{60}Co: The IRDF contains the only available file, and fits the data apart from one high data point.
— ^{59}Co(n,2n)^{58}Co: The IRDF contains the only available file, and fits the average of the data that have significant scatter.
— ^{59}Co(n,α)^{56}Mn: Experimental data were evaluated and renormalized by Zolotarev. The RRDF contains the only available file, and fits the data reasonably well.

— $^{58}Ni(n,2n)^{57}Ni$: The IRDF, JENDL and JEFF files are in good agreement, and fit the experimental data reasonably well.
— $^{58}Ni(n,p)^{58}Co$: Experimental data were evaluated and renormalized by Zolotarev. Evaluated cross-sections are available from the IRDF, JENDL, JEFF and a new evaluation in the RRDF (the IRDF and ENDF files are the same). All of these evaluations differ by about 10%; however, selection of one file has proved difficult because the differences are generally less than the scatter in experimental data. The JEFF evaluation appears to be too high, especially at the lower energies.
— $^{60}Ni(n,p)^{60}Co$: Experimental data were evaluated and renormalized by Zolotarev. Evaluated files in the ENDF and JEFF are nearly identical, and both fit the data with the lowest uncertainties (although there is considerable scatter).
— $^{63}Cu(n,\gamma)^{64}Cu$: The single experimental data point conforms with the IRDF evaluation (only file available).
— $^{63}Cu(n,2n)^{62}Cu$: Available from both the ENDF and JENDL, although the ENDF file gives a better fit to the data with the lowest uncertainties.
— $^{63}Cu(n,\alpha)^{60}Co$: Experimental data were evaluated and renormalized by Zolotarev. Data from the RRDF are about 5% higher than the equivalent data from the IRDF, and give a much better fit to those data with the lowest uncertainties.
— $^{65}Cu(n,2n)^{64}Cu$: The IRDF and JENDL are almost the same, and both fit the data equally well.
— $^{64}Zn(n,p)^{64}Cu$: The IRDF is the only file available. There is considerable scatter in the measured data, although the evaluation is reasonably close to the average of the data with the lowest uncertainties.
— $^{75}As(n,2n)^{74}As$: Experimental data were evaluated and renormalized by Zolotarev. The new RRDF evaluation fits the data reasonably well, although these data exhibit considerable scatter.
— $^{89}Y(n,2n)^{88}Y$: JENDL is the only available file, and fits the available data extremely well.
— $^{90}Zr(n,2n)^{89}Zr$: Data from the IRDF are somewhat higher than the equivalent data from JENDL, and give a slightly improved fit to the data.
— $^{93}Nb(n,2n)^{92}Nb^{m}$: Experimental data were evaluated and renormalized by Zolotarev. The IRDF and RRDF are essentially identical, and both fit the data reasonably well.
— $^{93}Nb(n,n')^{93}Nb^{m}$: Experimental data were evaluated and renormalized by Zolotarev. Unfortunately, there is only one credible data point near 14 MeV, and the data from the RRDF give the best fit. The RRDF data are slightly higher than the equivalent data from the IRDF.

— $^{103}Rh(n,n')^{103}Rh^{m}$: Experimental data were evaluated and renormalized by Zolotarev. Data from the RRDF are almost the same as from the IRDF, although slightly higher above 14.5 MeV; both data sets are slightly lower than experimental measurements.
— $^{109}Ag(n,\gamma)^{110}Ag^{m}$: No experimental data are available near 14 MeV.
— $^{115}In(n,2n)^{114}In^{m}$: The IRDF is the only available file, and fits the data with the lowest uncertainties.
— $^{115}In(n,n')^{115}In^{m}$: Experimental data were evaluated and renormalized by Zolotarev. JENDL is the same as the IRDF, while the RRDF data appear to give the best fit to the experimental data.
— $^{127}I(n,2n)^{126}I$: JENDL and the IRDF are essentially identical, and both give a reasonable fit to the experimental data (which have relatively large uncertainties).
— $^{139}La(n,\gamma)^{140}La$: Experimental data were evaluated and renormalized by Zolotarev. The RRDF evaluation gives a reasonable fit to the experimental data with the lowest uncertainties, although these data exhibit considerable scatter around 14 MeV.
— $^{141}Pr(n,2n)^{140}Pr$: Experimental data were evaluated and renormalized by Zolotarev. The RRDF evaluation gives a reasonable fit to the experimental data, which have relatively large scatter and uncertainties.
— $^{169}Tm(n,2n)^{168}Tm$: JENDL gives a good fit to the experimental data.
— $^{186}W(n,\gamma)^{187}W$: Experimental data were evaluated and renormalized by Zolotarev. The RRDF fits the experimental data, ignoring one high data point.
— $^{197}Au(n,\gamma)^{198}Au$: Sparse experimental data have considerable scatter around 14 MeV; the IRDF evaluation gives a reasonable fit.
— $^{197}Au(n,2n)^{196}Au$: Data from the IRDF are slightly higher than those from JENDL, although both give reasonably good fits to the available experimental data.
— $^{199}Hg(n,n')^{199}Hg^{m}$: JENDL gives a good fit to the sole data point for this reaction.
— $^{204}Pb(n,n')^{204}Pb^{m}$: The RRDF evaluated cross-section appears to be somewhat lower than suggested by the available experimental data, although there is considerable scatter in these data.
— $^{232}Th(n,f)$: The IRDF is the only available file, and gives a reasonable fit to the available data.
— $^{237}Np(n,f)$: Experimental data were evaluated and renormalized by Zolotarev. JENDL is the only available file, and gives a good fit to the available data with the lowest uncertainties.
— $^{235}U(n,f)$: The IRDF gives a good fit to the data with the lowest uncertainties.

— $^{238}U(n,\gamma)^{239}U(\beta^-)^{239}Np$: The IRDF provides the only evaluated data file, and fits the data reasonably well, apart from one high data point near 14.5 MeV.
— $^{238}U(n,f)$: JENDL and the IRDF are nearly identical, and both sets of data are slightly lower than the available experimental data.
— $^{239}Pu(n,f)$: JENDL gives a better fit to the data than the IRDF.
— $^{241}Am(n,f)$: JENDL is the only available file, and gives a good fit to the average of the available experimental data.

ACKNOWLEDGEMENT

K.I. Zolotarev of the Institute of Physics and Power Engineering, Obninsk, Russian Federation, kindly made available his evaluations and renormalizations of the experimental data for many of the reactions, as noted in the text. Such evaluations provide the best basis for assessment of the various cross-section files, and were usually adopted and taken into account during the review process.

REFERENCES TO SECTION 5

[5.1] KOCHEROV, N.P., McLAUGHLIN, P.K., The International Reactor Dosimetry File (IRDF-90), Rep. IAEA-NDS-141, Rev. 2, IAEA, Vienna (1993).
[5.2] KOBAYASHI, K., et al., JENDL Dosimetry File (JENDL/D-99), Rep. JAERI 1344, Japan Atomic Energy Research Institute, Tokai-mura (2002).
[5.3] ZOLOTAREV, K.I., IGNATYUK, A.V., MAHOKHIN, V.N., PASHCHENKO, A.B., RRDF-98, Russian Reactor Dosimetry File, Rep. IAEA-NDS-193, IAEA, Vienna (1999).
[5.4] Joint European Fusion File 3.0 (JEFF-3.0); JEFF-3 is available on CD-ROM on request from the IAEA, Nuclear Data Section, http://www.nea.fr/html/dbdata/projects/nds_jef.htm; JACQMIN, R., et al., Status of the JEFF project, J. Nucl. Sci. Technol, Suppl. 2 (2002) 54–55.
[5.5] ZERKIN, V.V., et al., "EXFOR-CINDA-ENDF: Migration of databases to give higher-quality nuclear data services", Nuclear Data for Science and Technology (Proc. Int. Conf. Santa Fé, NM, 2004), American Institute of Physics, NY (2005) 586–589.

6. FINAL SELECTION OF CROSS-SECTIONS FOR IRDF-2002, AND CHARACTERIZATION OF THE SELECTED DATA

E.M. Zsolnay, H.J. Nolthenius

The final selection of cross-section data for IRDF-2002 was made during a technical meeting held at the IAEA in Vienna from 1 to 3 October 2003 [6.1]. This selection procedure was based on the following considerations:

(a) Comparison of the integral values of the candidate cross-sections with the corresponding experimental results in the four standard neutron fields (thermal Maxwellian, 1/E slowing down, ^{252}Cf fission and 14 MeV neutron field) recommended for the purpose of cross-section selection [6.2].
(b) Quality of the uncertainty information.
(c) Consistency of the data (C/E values compared with the corresponding uncertainty information).

The cross-section and uncertainty data described in Sections 3, 4 and 5 were used. However, in addition, spectrum averaged cross-sections were calculated for the theoretical function of the Watt fission spectrum [6.3–6.6]. These data are presented in Table 6.1 for the candidate cross-sections of the fast neutron threshold reactions [6.6]. Such integral cross-section data are also published in standard neutron cross-section tables. The uncertainty information for the cross-sections is represented by the corresponding standard deviations above 1.05 MeV, weighted with a typical MTR spectrum [6.7]. The results in Table 6.1 show good agreement with those of Mannhart that were obtained in the ^{252}Cf fission spectrum (Section 4). The observed variations may be attributed to the differences between the two spectrum functions.

Based on the results outlined in Sections 3, 4 and 5, and following the recommendations of Ref. [6.6], the final selection procedure resulted in the data files being chosen as summarized in Table 6.2. This table lists the cross-sections included in IRDF-2002, together with their integral characteristics and the ratios of the corresponding calculated and experimental cross-section data (C/E). Uncertainties of the C/E values involve the standard deviations of both the calculated and experimental cross-sections. The following shortcomings occur in the chosen cross-section data:

(i) Only diagonal covariance matrices are available for the cross-sections of the following reactions: $^{23}Na(n,\gamma)^{24}Na$, $^{93}Nb(n,\gamma)^{94}Nb$, $^{115}In(n,\gamma)^{116}In^{m}$, $^{181}Ta(n,\gamma)^{182}Ta$ and $^{232}Th(n,\gamma)^{233}Th$ below 15 eV. New evaluations with complete covariance information are required.

(ii) Covariance information for the cross-sections of the $^{197}Au(n,\gamma)^{198}Au$ and $^{235}U(n,f)$ reactions are not reliable (corresponding data have been withdrawn from ENDF/B-VI); updating is required.

(iii) The resonance integral has a large deviation from the recommended experimental values for the following reactions: $^{55}Mn(n,\gamma)^{56}Mn$, $^{58}Fe(n,\gamma)^{59}Fe$ and $^{93}Nb(n,\gamma)^{94}Nb$. A revision of the resonance parameters in the corresponding evaluations is necessary.

(iv) Deviations of *C*/*E* values from unity by more than 5% are observed for the following reactions (in addition to those mentioned in (iii)): $^{24}Mg(n,p)^{24}Na$, $^{63}Cu(n,2n)^{64}Cu$, $^{103}Rh(n,n')^{103}Rh^{m}$, $^{127}I(n,2n)^{126}I$, $^{169}Tm(n,2n)^{168}Tm$, $^{199}Hg(n,n')^{199}Hg^{m}$ and $^{232}Th(n,f)$. Although the majority of these data can be interpreted by considering the related uncertainty information, revisions are merited. The large deviation of the *C*/*E* value from unity for the cross-section of the $^{103}Rh(n,n')^{103}Rh^{m}$ reaction is caused by a discrepancy in the experimental data for this reaction in the spontaneous neutron field of ^{252}Cf; new measurements of the cross-section of the $^{103}Rh(n,n')^{103}Rh^{m}$ reaction in this neutron spectrum are recommended [6.8].

(v) No experimental cross-section values are available in the ^{252}Cf (standard) spontaneous fission neutron field for the following fast neutron reactions: $^{23}Na(n,2n)^{24}Na$, $^{31}P(n,p)^{31}Si$, $^{46}Ti(n,2n)^{45}Ti$, $^{47}Ti(n,np)^{46}Sc$, $^{48}Ti(n,np)^{47}Sc$, $^{49}Ti(n,np)^{48}Sc$, $^{52}Cr(n,2n)^{51}Cr$, $^{54}Fe(n,2n)^{53}Fe$, $^{54}Fe(n,\alpha)^{51}Cr$, $^{75}As(n,2n)^{74}As$, $^{89}Y(n,2n)^{88}Y$, $^{115}In(n,2n)^{114}In$, $^{141}Pr(n,2n)^{140}Pr$ and $^{241}Am(n,f)$.

The most important problems listed above should be resolved before any further comprehensive revision of the library is made.

TABLE 6.1. INTEGRAL CHARACTERISTICS OF THE FAST NEUTRON CROSS-SECTIONS AS CANDIDATES FOR IRDF-2002 (CROSS-SECTIONS AVERAGED OVER THE WATT FISSION SPECTRUM)

Reaction	Library	Cross-section $\langle\sigma_f\rangle$ (m^2)	Relative standard deviation of $\langle\sigma_f\rangle$ [a] (%)
^{19}F(n,2n)	JENDL/D-99	6.773E-34	2.92
^{19}F(n,2n)	RRDF-98 (u)	5.855E-34	3.02
^{23}Na(n,2n)	JENDL/D-99 (u)	2.570E-34	1.21
^{24}Mg(n,p)	IRDF-90	1.473E-31	2.26
^{24}Mg(n,p)	JENDL/D-99	1.488E-31	1.24
^{27}Al(n,p)	IRDF-90	3.825E-31	3.31
^{27}Al(n,p)	JENDL/D-99	4.224E-31	0.72
^{27}Al(n,p)	RRDF-98 (n)	3.980E-31	2.06
^{27}Al(n,α)	IRDF-90	6.860E-32	1.37
^{27}Al(n,α)	JENDL/D-99	6.860E-32	1.37
^{31}P(n,p)	IRDF-90	2.783E-30	3.60
^{31}P(n,p)	JENDL/D-99	2.938E-30	1.34
^{32}S(n,p)	IRDF-90	6.345E-30	3.54
^{nat}Ti(n,x)^{46}Sc	JENDL/D-99	9.117E-32	2.28
^{nat}Ti(n,x)^{48}Sc	JENDL/D-99 (u)	1.971E-32	2.10
^{46}Ti(n,2n)	JENDL/D-99	3.621E-34	1.84
^{46}Ti(n,2n)	RRDF-98 (u)	3.359E-34	4.40
^{46}Ti(n,p)	IRDF-90	1.002E-30	2.43
^{46}Ti(n,p)	JENDL/D-99	1.105E-30	2.27
^{46}Ti(n,p)	RRDF-98 (u)	1.118E-30	3.13
^{47}Ti(n,np)	IRDF-90	7.958E-34	30.00
^{47}Ti(n,np)	RRDF-98 (u)	6.380E-34	8.53
^{47}Ti(n,p)	IRDF-90	1.760E-30	3.69
^{48}Ti(n,np)	IRDF-90	1.302E-34	30.00
^{48}Ti(n,np)	JENDL/D-99	1.235E-34	2.65
^{48}Ti(n,np)	RRDF-98 (u)	1.264E-34	8.59
^{48}Ti(n,p)	IRDF-90	2.596E-32	2.54
^{48}Ti(n,p)	JENDL/D-99	2.673E-32	1.85

TABLE 6.1. INTEGRAL CHARACTERISTICS OF THE FAST NEUTRON CROSS-SECTIONS AS CANDIDATES FOR IRDF-2002 (CROSS-SECTIONS AVERAGED OVER THE WATT FISSION SPECTRUM) (cont.)

Reaction	Library	Cross-section $\langle\sigma_f\rangle$ (m^2)	Relative standard deviation of $\langle\sigma_f\rangle$ [a] (%)
^{48}Ti(n,p)	RRDF-98 (u)	2.878E-32	5.17
^{49}Ti(n,np)	JENDL/D-99	7.668E-35	10.01
^{49}Ti(n,np)	RRDF-98 (u)	7.657E-35	7.31
^{51}V(n,α)	RRDF-98 (u)	2.231E-33	3.13
^{52}Cr(n,2n)	IRDF-90	3.194E-33	2.68
^{52}Cr(n,2n)	JENDL/D-99	3.149E-33	1.29
^{52}Cr(n,2n)	ENDF/B-VI	3.248E-33	8.09
^{54}Fe(n,2n)	RRDF-98 (u)	9.138E-35	4.96
^{54}Fe(n,α)	RRDF-98 (u)	8.122E-32	3.28
^{54}Fe(n,p)	IRDF-90	7.880E-30	2.13
^{54}Fe(n,p)	JENDL/D-99 (u)	7.955E-30	0.99
^{56}Fe(n,p)	RRDF-98 (u)	1.053E-31	2.62
^{59}Co(n,2n)	IRDF-90	1.719E-32	2.85
^{59}Co(n,α)	RRDF-98 (u)	1.498E-32	3.76
^{58}Ni(n,2n)	IRDF-90	2.947E-34	3.11
^{58}Ni(n,2n)	JENDL/D-99	2.850E-34	0.90
^{58}Ni(n,2n)	JEFF-3.0	2.946E-34	2.75
^{58}Ni(n,p)	IRDF-90	1.038E-29	2.20
^{58}Ni(n,p)	JENDL/D-99	1.029E-29	0.61
^{58}Ni(n,p)	RRDF-98 (n)	1.055E-29	1.73
^{58}Ni(n,p)	ENDF/B-VI	1.038E-29	2.45
^{58}Ni(n,p)	JEFF-3.0	1.054E-29	3.56
^{60}Ni(n,p)	ENDF/B-VI	1.867E-31	10.15
^{60}Ni(n,p)	JEFF-3.0	2.111E-31	8.83
^{63}Cu(n,2n)	IRDF-90	7.738E-33	1.75
^{63}Cu(n,2n)	JENDL/D-99 (u)	7.877E-33	1.36
^{63}Cu(n,2n)	ENDF/B-VI	7.608E-33	4.43
^{63}Cu(n,α)	IRDF-90	5.017E-32	2.34

TABLE 6.1. INTEGRAL CHARACTERISTICS OF THE FAST NEUTRON CROSS-SECTIONS AS CANDIDATES FOR IRDF-2002 (CROSS-SECTIONS AVERAGED OVER THE WATT FISSION SPECTRUM) (cont.)

Reaction	Library	Cross-section $\langle\sigma_f\rangle$ (m^2)	Relative standard deviation of $\langle\sigma_f\rangle$ [a] (%)
^{63}Cu(n,α)	RRDF-98 (u)	5.128E-32	2.84
^{65}Cu(n,2n)	IRDF-90	2.894E-32	1.84
^{65}Cu(n,2n)	JENDL/D-99 (u)	3.024E-32	0.92
^{65}Cu(n,2n)	ENDF/B-VI	2.894E-32	2.31
^{64}Zn(n,p)	IRDF-90	3.774E-30	4.80
^{75}As(n,2n)	RRDF-98 (u)	2.562E-32	6.12
^{89}Y(n,2n)	JENDL/D-99	1.255E-32	1.45
^{90}Zr(n,2n)	IRDF-90	7.536E-33	1.60
^{90}Zr(n,2n)	JENDL/D-99	7.355E-33	0.55
^{93}Nb(n,2n) [b]	IRDF-90	3.878E-32	2.80
^{93}Nb(n,2n) [b]	RRDF-98	3.839E-32	1.06
^{93}Nb(n,n′) [b]	IRDF-90	1.376E-29	3.01
^{93}Nb(n,n′) [b]	RRDF-98	1.410E-29	2.80
^{103}Rh(n,n′) [b]	IRDF-90	6.968E-29	3.01
^{103}Rh(n,n′) [b]	RRDF-98 (u)	7.061E-29	3.95
^{115}In(n,2n) [b]	IRDF-90	7.535E-32	1.14
^{115}In(n,n′) [b]	IRDF-90	1.828E-29	2.18
^{115}In(n,n′) [b]	JENDL/D-99	1.828E-29	2.18
^{115}In(n,n′) [b]	RRDF-98 (u)	1.848E-29	1.71
^{127}I(n,2n)	IRDF-90	1.045E-31	0.60
^{127}I(n,2n)	JENDL/D-99	1.090E-31	3.09
^{141}Pr(n,2n)	RRDF-98 (u)	9.328E-32	11.68
^{169}Tm(n,2n)	JENDL/D-99	3.458E-31	2.33
^{197}Au(n,2n)	IRDF-90	3.112E-31	4.28
^{197}Au(n,2n)	JENDL/D-99	3.140E-31	1.18
^{199}Hg(n,n′) [b]	JENDL/D-99 (u)	2.354E-29	8.08
^{204}Pb(n,n′) [b]	RRDF-98 (n)	1.744E-30	4.64
^{232}Th(n,f)	IRDF-90	7.372E-30	5.18

TABLE 6.1. INTEGRAL CHARACTERISTICS OF THE FAST NEUTRON CROSS-SECTIONS AS CANDIDATES FOR IRDF-2002 (CROSS-SECTIONS AVERAGED OVER THE WATT FISSION SPECTRUM) (cont.)

Reaction	Library	Cross-section $<\sigma_f>$ (m^2)	Relative standard deviation of $<\sigma_f>$ [a] (%)
^{238}U(n,f)	IRDF-90	2.997E-29	0.54
^{238}U(n,f)	JENDL/D-99	3.034E-29	2.09

$<\sigma_f>$ Cross-section averaged over the Watt fission spectrum.
[a] Weighted with a typical MTR spectrum from 1.05 MeV to 20 MeV.
[b] Metastable state of the product nuclide.
(u): Updated data.
(n): New data.

TABLE 6.2. CROSS-SECTIONS IN IRDF-2002 AND THEIR CHARACTERISTICS (TEMPERATURE OF 300 K)

Reaction	Selected evaluation	Calculated library cross-section (2200 m/s) σ_L (b)	Resonance integral from library data IR_L (b)	Uncertainty in library data		Calculated average library cross-section in ^{252}Cf spontaneous fission $\langle\sigma_C\rangle$ (mb) [a]	Uncertainty in $\langle\sigma_C\rangle$ (%) [a]	*C/E*
				Thermal (%)	Epithermal (%)			
^{6}Li(n,t)	IRDF-90	942	427	0.14	0.14	—	—	Thermal: 1.00 ± 0.01 [b] Epithermal: 1.00 ± 0.01 [b]
^{10}B(n,α)	IRDF-90	3840	1730	0.16	0.16	—	—	Thermal: 1.00 ± 0.01 [b] Epithermal: 0.99 ± 0.01 [b]
^{19}F(n,2n)	RRDF-98 (u)	—	—	—	—	1.627E-2	2.92 (5.33)	1.009 ± 0.064 [a]
^{23}Na(n,γ) [c]	IRDF-90	0.529	0.317	2.00	3.14	—	—	Thermal: 1.00 ± 0.02 [d] Epithermal: 0.97 ± 0.04 [d]
^{23}Na(n,2n)	JENDL/D-99 (u)	—	—	—	—	8.611E-3	3.90 (8.16)	No experimental data in ^{252}Cf fission field
^{24}Mg(n,p)	IRDF-90	—	—	—	—	2.160	2.24 (2.75)	1.082 ± 0.040 [a]
^{27}Al(n,p)	RRDF-98 (n)	—	—	—	—	4.912	2.06 (2.37)	1.007 ± 0.032 [a]
^{27}Al(n,α)	IRDF-90	—	—	—	—	1.038	1.36 (2.12)	1.022 ± 0.026 [a]
^{31}P(n,p)	IRDF-90	—	—	—	—	30.68	3.58 (3.65)	No experimental data in ^{252}Cf fission field
^{32}S(n,p)	IRDF-90	—	—	—	—	70.30	3.60 (3.67)	0.969 ± 0.049 [a]
^{45}Sc(n,γ)	IRDF-90	27.3	12.0	0.73	0.76	—	—	Thermal: 1.00 ± 0.01 [d] Epithermal: 1.00 ± 0.04 [d]

TABLE 6.2. CROSS-SECTIONS IN IRDF-2002 AND THEIR CHARACTERISTICS (TEMPERATURE OF 300 K) (cont.)

Reaction	Selected evaluation	Calculated library cross-section (2200 m/s) σ_L (b)	Resonance integral from library data IR_L (b)	Uncertainty in library data		Calculated average library cross-section in ^{252}Cf spontaneous fission $\langle\sigma_C\rangle$ (mb) [a]	Uncertainty in $\langle\sigma_C\rangle$ (%) [a]	*C/E*
				Thermal (%)	Epithermal (%)			
$^{46}Ti(n,2n)$	RRDF-98 (u)	—	—	—	—	1.218E-2	4.41 (9.55)	No experimental data in ^{252}Cf fission field
$^{46}Ti(n,p)$	RRDF-98 (u)	—	—	—	—	13.83	3.05 (3.28)	0.983 ± 0.037 [a]
$^{47}Ti(n,np)$ [e]	RRDF-98 (u)	—	—	—	—	1.941E-2	7.57 (9.58)	No experimental data in ^{252}Cf fission field
$^{47}Ti(n,p)$	IRDF-90	—	—	—	—	19.38	3.78 (3.83)	1.006 ± 0.042 [a]
$^{48}Ti(n,np)$ [e]	RRDF-98 (u)	—	—	—	—	4.349E-3	8.20 (11.62)	No experimental data in ^{252}Cf fission field
$^{48}Ti(n,p)$	RRDF-98 (u)	—	—	—	—	0.4268	5.08 (5.32)	1.005 ± 0.057 [a]
$^{49}Ti(n,np)$ [e]	RRDF-98 (u)	—	—	—	—	2.644E-3	7.18 (10.84)	No experimental data in ^{252}Cf fission field
$^{51}V(n,\alpha)$	RRDF-98 (u)	—	—	—	—	3.859E-2	3.02 (3.56)	0.989 ± 0.041 [a]
$^{52}Cr(n,2n)$	IRDF-90	—	—	—	—	9.703E-2	2.72 (6.23)	No experimental data in ^{252}Cf fission field
$^{55}Mn(n,\gamma)$	IRDF-90	13.4	11.8	4.18	3.84	—	—	Thermal: 1.00 ± 0.04, [d] 1.01 ± 0.04 [b] Epithermal: 0.84 ± 0.04, [d] 0.84 ± 0.04 [b]

TABLE 6.2. CROSS-SECTIONS IN IRDF-2002 AND THEIR CHARACTERISTICS (TEMPERATURE OF 300 K) (cont.)

Reaction	Selected evaluation	Calculated library cross-section (2200 m/s) σ_L (b)	Resonance integral from library data IR_L (b)	Uncertainty in library data		Calculated average library cross-section in ^{252}Cf spontaneous fission $\langle\sigma_C\rangle$ (mb) [a]	Uncertainty in $\langle\sigma_C\rangle$ (%) [a]	*C/E*
				Thermal (%)	Epithermal (%)			
^{54}Fe(n,2n)	RRDF-98 (u)	—	—	—	—	3.498E-3	4.87 (10.71)	No experimental data in ^{252}Cf fission field
^{54}Fe(n,α)	RRDF-98 (u)	—	—	—	—	1.113	3.18 (3.48)	No experimental data in ^{252}Cf fission field
^{54}Fe(n,p)	IRDF-90	—	—	—	—	88.16	2.09 (2.23)	1.015 ± 0.026 [a]
^{56}Fe(n,p)	RRDF-98 (u)	—	—	—	—	1.475	2.61 (2.99)	1.007 ± 0.035 [a]
^{58}Fe(n,γ)	JENDL/D-99 (u)	1.30	1.37	12.60	8.70	—	—	Thermal: 1.00 ± 0.13, [d] 1.00 ± 0.15 [b] Epithermal: 0.81 ± 0.08, [d] 1.05 ± 0.18 [b]
^{59}Co(n,2n)	IRDF-90	—	—	—	—	0.4228	2.67 (4.20)	1.044 ± 0.051 [a]
^{59}Co(n,α)	RRDF-98 (u)	—	—	—	—	0.2212	3.54 (3.87)	0.997 ± 0.043 [a]
^{59}Co(n,γ)	IRDF-90	37.2	76.0	0.66	0.77	—	—	Thermal: 1.00 ± 0.01 [d] Epithermal: 1.00 ± 0.01 [d]
^{58}Ni(n,2n)	JEFF-3.0	—	—	—	—	9.256E-3	2.72 (6.67)	1.034 ± 0.078 [a]
^{58}Ni(n,p)	RRDF-98 (n)	—	—	—	—	117.5	1.74 (1.89)	1.000 ± 0.023 [a]
^{60}Ni(n,p)	ENDF/B-VI	—	—	—	—	2.494	10.11 (10.20)	1.044 ± 0.121 [a]

TABLE 6.2. CROSS-SECTIONS IN IRDF-2002 AND THEIR CHARACTERISTICS (TEMPERATURE OF 300 K) (cont.)

Reaction	Selected evaluation	Calculated library cross-section (2200 m/s) σ_L (b)	Resonance integral from library data IR_L (b)	Uncertainty in library data		Calculated average library cross-section in ^{252}Cf spontaneous fission $\langle\sigma_C\rangle$ (mb) [a]	Uncertainty in $\langle\sigma_C\rangle$ (%) [a]	*C/E*
				Thermal (%)	Epithermal (%)			
^{63}Cu(n,2n)	ENDF/B-VI	—	—	—	—	0.2056	4.10 (5.81)	1.115 ± 0.078 [a]
^{63}Cu(n,γ)	IRDF-90	4.47	4.96	4.11	3.86	—	—	Thermal: 0.99 ± 0.04 [d] 0.99 ± 0.06 [b] Epithermal: 1.00 ± 0.04, [d] 0.99 ± 0.04 [b]
^{63}Cu(n,α)	RRDF-98 (u)	—	—	—	—	0.6933	2.83 (3.15)	1.007 ± 0.037 [a]
^{65}Cu(n,2n)	IRDF-90	—	—	—	—	0.6779	1.83 (3.44)	1.030 ± 0.042 [a]
^{64}Zn(n,p)	IRDF-90	—	—	—	—	42.10	4.87 (4.93)	1.037 ± 0.054 [a]
^{75}As(n,2n)	RRDF-98 (u)	—	—	—	—	0.6209	5.76 (6.55)	No experimental data in ^{252}Cf fission field
^{89}Y(n,2n)	JENDL/D-99	—	—	—	—	0.344	1.40 (4.47)	No experimental data in ^{252}Cf fission field
^{90}Zr(n,2n)	IRDF-90	—	—	—	—	0.2212	1.57 (5.31)	1.001 ± 0.061 [a]
^{93}Nb(n,2n) [f]	RRDF-98	—	—	—	—	0.7717	1.03 (2.46)	1.03 ± 0.058 [a]
^{93}Nb(n,n′) [f]	RRDF-98	—	—	—	—	146.1	2.59 (2.61)	1.001 ± 0.043 [a]
^{93}Nb(n,γ) [c]	IRDF-90	1.16	9.91	10.00	9.49	—	—	Thermal: 1.01 ± 0.11 [d] Epithermal: 1.17 ± 0.13 [d]

TABLE 6.2. CROSS-SECTIONS IN IRDF-2002 AND THEIR CHARACTERISTICS (TEMPERATURE OF 300 K) (cont.)

Reaction	Selected evaluation	Calculated library cross-section (2200 m/s) σ_L (b)	Resonance integral from library data IR_L (b)	Uncertainty in library data		Calculated average library cross-section in ^{252}Cf spontaneous fission $\langle\sigma_C\rangle$ (mb) [a]	Uncertainty in $\langle\sigma_C\rangle$ (%) [a]	*C/E*
				Thermal (%)	Epithermal (%)			
$^{103}Rh(n,n')$ [f]	RRDF-98 (u)	—	—	—	—	725.1	3.94 (3.95)	0.896 ± 0.044 [a]
$^{109}Ag(n,\gamma)$ [f]	IRDF-90	4.21	68.6	5.10	6.93	—	—	Thermal: 1.00 [b] Epithermal: 0.98 [b] No experimental uncertainty
$^{115}In(n,2n)$ [f]	IRDF-90	—	—	—	—	1.586	3.23 (4.02)	No experimental data in ^{252}Cf fission field
$^{115}In(n,n')$ [f]	RRDF-98 (u)	—	—	—	—	191.8	1.66 (1.70)	0.972 ± 0.021 [a]
$^{115}In(n,\gamma)$ [c, f]	IRDF-90	167	2590	6.00	5.98	—	—	Thermal: 1.04 ± 0.06 [d] Epithermal: 0.96 ± 0.07 [d]
$^{127}I(n,2n)$	IRDF-90	—	—	—	—	2.197	2.28 (3.30)	1.062 ± 0.045 [a]
$^{139}La(n,\gamma)$	RRDF-98 (n)	9.04	12.0	3.87	5.50	—	—	Thermal: 1.00 ± 0.04, [d] 0.98 ± 0.04 [b] Epithermal: 0.99 ± 0.07, [d] 1.00 ± 0.1 [b]
$^{141}Pr(n,2n)$	RRDF-98 (u)	—	—	—	—	1.990	11.03 (11.37)	No experimental data in ^{252}Cf fission field
$^{169}Tm(n,2n)$	JENDL/D-99	—	—	—	—	6.233	2.26 (3.01)	0.932 ± 0.065 [a]

TABLE 6.2. CROSS-SECTIONS IN IRDF-2002 AND THEIR CHARACTERISTICS (TEMPERATURE OF 300 K) (cont.)

Reaction	Selected evaluation	Calculated library cross-section (2200 m/s) σ_L (b)	Resonance integral from library data IR_L (b)	Uncertainty in library data		Calculated average library cross-section in ^{252}Cf spontaneous fission $\langle\sigma_C\rangle$ (mb) [a]	Uncertainty in $\langle\sigma_C\rangle$ (%) [a]	*C/E*
				Thermal (%)	Epithermal (%)			
$^{181}Ta(n,\gamma)$ [c]	JENDL/D-99	20.7	659	3.00	3.77	—	—	Thermal: 1.01 ± 0.04 [d] Epithermal: 1.00 ± 0.05 [d]
$^{186}W(n,\gamma)$	RRDF-98 (n)	38.5	480	2.31	3.32	—	—	Thermal: 1.00 ± 0.03, [d] 1.04 ± 0.06 [b] Epithermal: 0.99 ± 0.04, [d] 0.94 ± 0.10 [b]
$^{197}Au(n,2n)$	IRDF-90	—	—	—	—	5.747	4.19 (4.65)	1.044 ± 0.052 [a]
$^{197}Au(n,\gamma)$ [g]	IRDF-90	98.8	1570	0.14	0.17	—	—	Thermal: 1.00 ± 0.01, [d] 1.00 ± 0.01 [b] Epithermal: 1.01 ± 0.02, [d] 1.01 ± 0.02 [b]
$^{199}Hg(n,n')$ [f]	JENDL/D-99 (u)	—	—	—	—	248.6	7.82 (7.83)	0.833 ± 0.067 [a]
$^{204}Pb(n,n')$ [f]	RRDF-98 (n)	—	—	—	—	20.39	4.57 (4.67)	0.978 ± 0.063 [a]
$^{232}Th(n,\gamma)$ [c]	IRDF-90	7.41	85.6	4.33	10.92	—	—	Thermal: 1.01 ± 0.04, [d] 1.00 ± 0.04 [b] Epithermal: 1.01 ± 0.12, [d] 1.01 ± 0.12 [b]
$^{232}Th(n,f)$	IRDF-90	—	—	—	—	78.55	5.09 (5.11)	0.879 ± 0.052

TABLE 6.2. CROSS-SECTIONS IN IRDF-2002 AND THEIR CHARACTERISTICS (TEMPERATURE OF 300 K) (cont.)

Reaction	Selected evaluation	Calculated library cross-section (2200 m/s) σ_L (b)	Resonance integral from library data IR_L (b)	Uncertainty in library data		Calculated average library cross-section in ^{252}Cf spontaneous fission $\langle\sigma_C\rangle$ (mb) [a]	Uncertainty in $\langle\sigma_C\rangle$ (%) [a]	*C/E*
				Thermal (%)	Epithermal (%)			
$^{235}U(n,f)$ [g]	IRDF-90	586	272	0.19	0.26	1218	0.32 (0.32)	Thermal: 1.00 ± 0.004, [b] Epithermal: 0.99 ± 0.02, [b] 1.007 ± 0.0102 [a]
$^{238}U(n,f)$	JENDL/D-99	—	—	—	—	319.2	2.00 (2.04)	0.980 ± 0.026 [a]
$^{238}U(n,\gamma)$	IRDF-90	2.72	277	0.35	0.37	—	—	Thermal: 1.01 ± 0.01, [d] 1.00 ± 0.04 [b] Epithermal:1.00 ± 0.01, [d] 1.00 ± 0.01 [b]
$^{237}Np(n,f)$	RRDF-98 (n)	—	—	—	—	1359	1.72 (1.74)	0.999 ± 0.024 [a]
$^{239}Pu(n,f)$	JENDL/D-99	747	297	0.71	3.82	1804	2.04 (2.04)	Thermal: 0.99 ± 0.01 [b] Epithermal: 0.99 ± 0.05 [b], 0.996 ± 0.025 [a]

TABLE 6.2. CROSS-SECTIONS IN IRDF-2002 AND THEIR CHARACTERISTICS (TEMPERATURE OF 300 K) (cont.)

Reaction	Selected evaluation	Calculated library cross-section (2200 m/s) σ_L (b)	Resonance integral from library data IR_L (b)	Uncertainty in library data		Calculated average library cross-section in ^{252}Cf spontaneous fission $\langle\sigma_C\rangle$ (mb) [a]	Uncertainty in $\langle\sigma_C\rangle$ (%) [a]	*C/E*
				Thermal (%)	Epithermal (%)			
^{241}Am(n,f)	JENDL/D-99	3.03	7.84	2.00	1.56	1396	2.81 (2.90)	Thermal: 0.99 ± 0.004 [b] Epithermal: no experimental data No experimental data in ^{252}Cf fission field

[a] Calculated and experimental data for the response of the activation detectors in the neutron field of the ^{252}Cf spontaneous fission are from Mannhart (see Section 4).
[b] Evaluated experimental data from Ref. [6.9].
[c] Diagonal matrix.
[d] Evaluated experimental data from Ref. [6.10].
[e] Sum of cross-sections of (n,np)+(n,pn)+(n,d) reactions.
[f] Metastable state of the product nucleus.
[g] Unreliable uncertainty (corresponding data have been withdrawn from ENDF/B-VI).
(u): Updated data.
(n): New data.

Notes: Column 8 shows the contribution of the energy dependent library cross-section data to the uncertainty of $\langle\sigma_C\rangle$; values in brackets give the total standard deviation of $\langle\sigma_C\rangle$, including the contribution of the uncertainty of the ^{252}Cf spectrum function. Uncertainties given for the *C/E* values involve the standard deviations of both the calculated and experimental cross-section data. All uncertainty data in the table are expressed in terms of one standard deviation.

REFERENCES TO SECTION 6

[6.1] GRIFFIN, P.J., PAVIOTTI-CORCUERA, R. (Eds), Summary Report of the Final Technical Meeting on International Reactor Dosimetry File: IRDF-2002, Rep. INDC(NDS)-448, IAEA, Vienna (2003).

[6.2] "Benchmarks and intercomparisons, supplementary workshop on testing of the IRDF-2002 File, workshop session III", Reactor Dosimetry in the 21st Century (Proc. 11th Int. Symp. Brussels, 2002), World Scientific, Singapore (2003) 718–719.

[6.3] ZSOLNAY, E.M., NOLTHENIUS, H.J., SZONDI, E.J., Nuclear Data for Reactor Dosimetry Libraries: Analysis, Intercomparison and Selection of Data, Rep. BME-NTI-251/2001, Institute of Nuclear Techniques, Budapest University of Technology and Economics, Budapest (2001).

[6.4] ZSOLNAY, E.M., NOLTHENIUS, H.J., SZONDI, E.J., Analysis, Intercomparison and Selection of Data for the Preliminary Version of the International Reactor Dosimetry File IRDF-2002, Rep. BME-NTI-265/2002, Institute of Nuclear Techniques, Budapest University of Technology and Economics, Budapest (2002).

[6.5] ZSOLNAY, E.M., NOLTHENIUS, H.J., "Selection of cross sections in the thermal and epithermal neutron energy for the file IRDF-2002, and characterization of the selected data", Summary Report of the Final Technical Meeting on International Reactor Dosimetry File: IRDF-2002 (GRIFFIN, P.J., PAVIOTTI-CORCUERA, R., Eds), Rep. INDC(NDS)-448, IAEA, Vienna (2003) 73–83.

[6.6] ZSOLNAY, E.M., NOLTHENIUS, H.J., "Selection of fast neutron cross sections for the file IRDF-2002, and characterization of the selected data", ibid., pp. 85–93.

[6.7] BAARD, J.H., ZIJP, W.L., NOLTHENIUS, H.J., Nuclear Data Guide for Reactor Neutron Metrology, Kluwer, Dordrecht (1989).

[6.8] ZOLOTAREV, K.I., Institute of Physics and Power Engineering, Obninsk, personal communication, 2004.

[6.9] HOLDEN, N.E., "Neutron scattering and absorption properties (revised 2003)", CRC Handbook of Chemistry and Physics, 84th edn (LIDE, D.R., Ed.), CRC Press, Boca Raton, FL (2003) 198–213.

[6.10] MUGHABGHAB, S.F., Thermal Neutron Capture Cross Sections, Resonance Integrals and g-factors, Rep. INDC(NDS)-440, IAEA, Vienna (2003).

7. CONSISTENCY TEST OF THE CROSS-SECTION DATA IN REFERENCE NEUTRON FIELDS

P.J. Griffin

After selection of the recommended cross-section evaluations for inclusion in IRDF-2002, validation of the fidelity of the selected data files was required prior to the release of the library. There are well characterized neutron fields, called 'reference' neutron benchmark fields, that have been used to validate the selection of the dosimetry cross-sections. Test validation of the preferred IRDF-2002 data in selected reference neutron fields is described in this section.

'Reference' fields should not be confused with 'standard' benchmark fields. The 1976 IAEA consultants meeting [7.1] and the recent ISRD11 workshop [7.2] reflect a consensus that only standard benchmark fields can be used to differentiate between candidate evaluations. Standard neutron fields are those that are permanent and reproducible and which, in the energy range of their principal response, are described to the best accuracy possible by means of differential spectrometry and/or by fundamental physical laws. Only four benchmark standard fields are recognized by the dosimetry community:

(a) Spontaneous fission neutron field of ^{252}Cf;
(b) $1/E$ slowing down spectrum in a hydrogenous moderator;
(c) Maxwellian thermal spectrum at a specified neutron temperature;
(d) Monoenergetic 14 MeV neutron field from a deuterium–tritium source.

Note that the ^{235}U thermal fission benchmark field is not included in this list of standard neutron fields. This field has been designated as a 'reference' rather than a 'standard' benchmark field because only one standard is permitted in a given energy region and the ^{252}Cf spontaneous fission field is a much better characterized neutron field. The data of interest in a standard field are typically the spectrum averaged cross-sections. For the thermal Maxwellian spectrum at a temperature of 293.6°C, the spectrum averaged cross-section is uniquely related to the 2200 m/s cross-section. The measured data are corrected for the thermal contribution of the spectrum in the case of the $1/E$ field and are used to deduce the resonance integrals, typically corrected to represent the integral between the energy bounds from 0.5 eV to 100 keV.

When comparing a measurement with a calculated quantity, the uncertainty on both the measurement and the calculation must be determined, and all sources of uncertainty should be taken into account. The evaluation

covariance file is folded with the neutron spectrum to obtain the cross-section contribution to the uncertainty. All acceptable measurement data must include a measurement uncertainty. Great care must be taken in combining the experimental data in a statistically valid manner while addressing the issue of discrepant data [7.3]. Criteria for identifying and rejecting discrepant data must be established prior to establishing the recommended experimental value.

The uncertainty in the representation of the neutron spectrum within the standard and reference fields must be taken into account when comparing measurements with calculated quantities, in which the comparison quantity of interest is the calculated to experimental ratio (C/E). Sources of uncertainty in both the calculated and the measured quantities should be combined to provide an uncertainty in the C/E ratio, and the result should always be reported as the C/E ratio together with the number of standard deviations.

Note that the validation procedure for library selection using reference neutron fields did not result in any changes in the selected cross-sections. However, this process did serve to identify those values where either the cross-section or the reference field characterization should be further examined. Even if not required to have only one standard field in a given energy region, the reference neutron fields have neutron spectrum characterizations that were derived from activation foils in conjunction with spectrum unfold or adjustment methods. Since this spectrum characterization process introduces correlations between the spectrum and the cross-section evaluations that are not taken into account in the least squares spectrum adjustment, these data cannot be used in the cross-section selection process, only in the validation process.

7.1. DESCRIPTION OF SELECTED REFERENCE NEUTRON FIELDS

IRDF-2002 consistency tests were performed over as many reference neutron fields as possible in order to obtain the most extensive validation. The reference neutron fields that are considered are those for which there exist published activation foil measurement data for a large set of the important dosimetry reactions, supported by published and peer reviewed neutron spectrum characterizations. Fields considered include those listed in Table 7.1.

Unfortunately, due to time constraints and difficulties in obtaining details on the neutron spectrum characterization for the reference neutron fields, only two fields were included in this initial validation for IRDF-2002. The problem with many potential fields that had reported activation data was that the field neutron spectrum uncertainty and covariance matrix were not available to the authors of this report. Hopefully, as more detail is acquired on other reference

TABLE 7.1. REFERENCE NEUTRON FIELDS CONSIDERED FOR THE VALIDATION OF IRDF-2002

Neutron field	Ref.
ACRR central cavity	[7.4]
SPR-III central cavity	[7.5]
MDRF	[7.6]
JOYO	[7.7, 7.8]
JMTR	[7.8, 7.9]
YAYOI	[7.8]
CFRMF	[7.8]
ISNF	[7.8]
Sigma–sigma (Σ–Σ)	[7.8]

Note: ACRR: Annular Core Research Reactor; SPR-III: Sandia Pulsed Reactor-III; MDRF: Materials Dosimetry Reference Facility; JOYO: experimental fast reactor; JMTR: Japan Materials Testing Reactor; YAYOI: fast neutron source reactor; CFRMF: Coupled Fast Reactivity Measurement Facility; ISNF: Intermediate Energy Standard Neutron Field; sigma–sigma: coupled thermal/fast uranium and boron carbide spherical assembly.

neutron fields, the set of reference neutron fields used for this validation will expand in future releases of the IRDF-2002 dosimetry library. The following sections provide reference citations available in the literature and baseline characterization details for the fast neutron field and the water moderated neutron field used for this validation procedure.

7.1.1. ACRR reference neutron field

The ACRR is a water moderated test reactor with a dry central cavity and a fuelled external cavity. A total of 236 cylindrical fuel elements contain a unique BeO–UO_2 fuel with 35% enriched ^{235}U that allows operation at fuel temperatures of up to 1400°C in pulse and steady state modes. This reactor is capable of steady state operation at 2 MW, intermittent operation at 4 MW, and pulsed operation with a maximum pulse of 300 MJ, a peak power of 30 000 MW, and a pulse width of 6.5 ms. The reactor core is located in a 3.1 m diameter and 8.5 m deep pool, with a 22.5 cm (9 in) diameter dry central cavity that supports

large test fixtures and provides good uniformity. Figure 7.1 shows the ACRR reactor and the dry experimental cavity. A more comprehensive description of this reference field appears in Ref. [7.4]. Details of the radiation transport models and 640 group representation of the neutron spectrum in the ACRR central cavity appear in Ref. [7.10].

Figure 7.2 shows the calculated spectrum in a typical logarithmic number fluence plot (written as $\Phi(E)$ or dn/dE). The calculated spectrum in a linear lethargy plot is shown in Fig. 7.3 (notated as $E\Phi(E)$, but often notated as $\Phi(\mu)$ or dE/dE). Equal areas under the curve in the lethargy plot (with linear y axis and logarithmic energy x axis or lethargy) correspond to equal neutron content. Figure 7.3 shows some prominent resonance absorption structure in the 0.5–2 MeV neutron energy region. Excellent sampling statistics in the Monte Carlo radiation transport calculation (<1%) indicated that this structure related to some aspect of the nuclear data used in the transport model. The high energy structure seen in the calculated neutron spectrum is due to the presence of high energy resonances in the ^{16}O elastic cross-section.

Oxygen is present in the oxide fuel form and in the ACRR water moderator. This source of the structures comes from a high energy elastic

FIG. 7.1. ACRR reactor with dry central cavity (left) and external fuelled cavity (right).

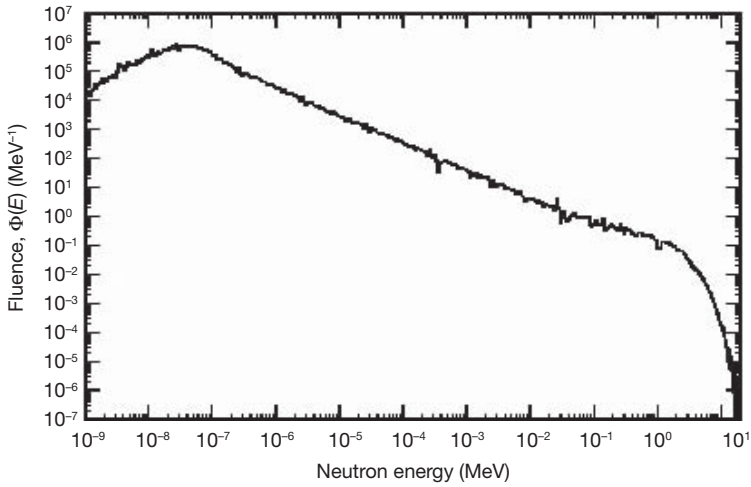

FIG. 7.2. Φ(E) representation of calculated spectrum (MCNP).

rather than an absorption event. The presence of this structure as a meaningful feature poses problems for iterative spectrum unfolding codes that depend upon local smoothness criteria in the spectrum for their convergence methodology [7.11]. Accordingly, a least squares spectrum adjustment with the least squares logarithmic (LSL) code was used to determine the final neutron

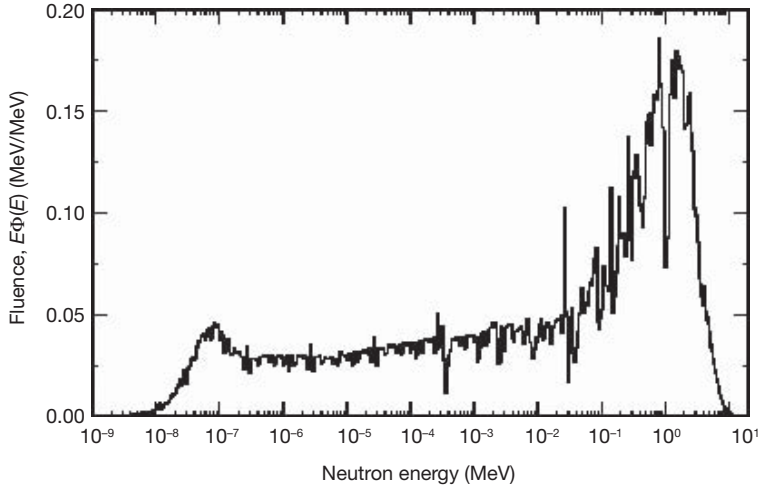

FIG. 7.3. EΦ(E) representation of calculated spectrum (MCNP).

spectrum for this field [7.12]. A high fidelity treatment is applied to the fluence by the dosimetry itself in order to provide the highest quality neutron field characterization. Responses from a 640 group Monte Carlo calculation are used to account for the detailed response of the dosimetry covers and the self-shielding in resonance regions of the activation foil [7.13]. A version of the LSL code was used in the analysis, and has been modified to use foil covers. This spectrum adjustment was performed using 366 energy groups selected to include the energy break points from all of the representations of the reaction cross-section covariance matrices. Figure 7.4 shows the relative covariance matrix that resulted from the baseline neutron field characterization.

The baseline activation data for this neutron field have been detailed in Ref. [7.13] and are summarized in Table 7.2. Cadmium and ^{10}B covers were used to alter the region of energy response for some of the activation foils. The ^{10}B cover was a 5 cm diameter 91% ^{10}B enriched B_4C ball that was large enough to alter the neutron field in the surrounding region; therefore, each boron covered activation foil was exposed on a separate reactor operation. Fission foils were not stacked in the boron ball because previous testing had shown that the neutron scattering between adjacent 1 g fission foils thermalized enough neutrons to alter the dosimeter response of ^{235}U and ^{239}Pu foils. The $^{58}Ni(n,p)$ reaction was used to normalize the separate reactor operations to a uniform neutron fluence. When a boron ball was used, internal as well as external nickel foils were introduced for normalization. Table 7.2 details the 44

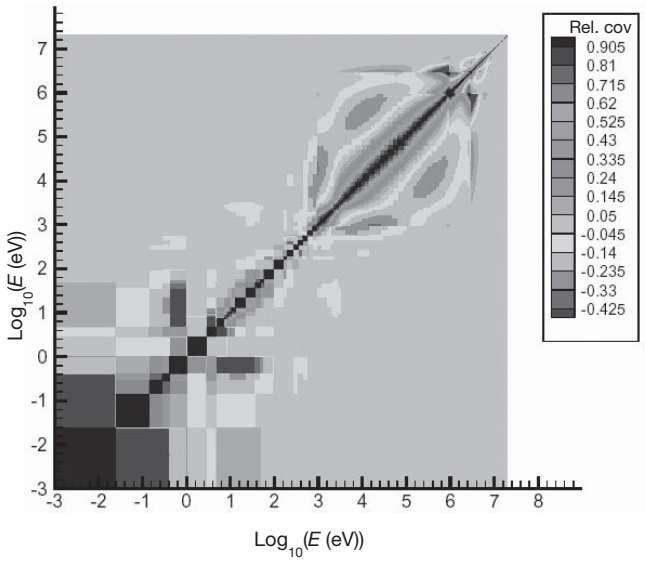

FIG. 7.4. ACRR spectrum relative covariance matrix.

TABLE 7.2. SPECTRUM AVERAGED DOSIMETRY CROSS-SECTIONS FOR THE ANNULAR CORE RESEARCH REACTOR CENTRAL CAVITY

Reaction/ cover [a]	Median energy response, $E(50\%)$ (eV)	Cross-section (mb)			Uncertainty (%)		
		Experiment	Calculation	C/E	Experiment	Cross-section	Neutron spectrum
Nb93g[Cd]	852.3	2.054E-12	2.517E-12	1.225	7.83	9.5	21.12
Ni58p	3.765E6	1.572E-13	1.557E-13	0.990	5.43	2.48	12.06
Ni58p[Cd]	3.765E6	1.552E-13	1.557E-13	1.003	5.44	2.48	12.06
S32p	3.856E6	9.040E-14	9.279E-14	1.026	5.94	3.52	12.91
Na23g	7.138E-2	2.599E-13	3.052E-13	1.174	5.45	2.17	163.2
Na23g[Cd]	8.180	5.527E-14	6.813E-14	1.233	5.45	5.40	37.62
Na23g[Fi]	2717	5.091E-15	7.197E-15	1.414	5.90	15.3	19.63
Mg24p[Cd]	8.026E6	1.754E-15	1.952E-15	1.113	6.33	2.36	20.67
Al27a[Cd]	8.346E6	8.717E-16	8.891E-16	1.13	6.28	2.18	20.60
Sc45g[Cd]	1.673	2.290E-12	2.628E-12	1.148	6.09	1.13	59.84
Sc45g	6.729E-2	1.437E-11	1.460E-11	1.016	6.09	0.98	175.4
Ti46p[Cd]	5.623E6	1.498E-14	1.347E-14	0.899	5.43	2.46	16.05
Ti48p[Cd]	8.01E6	3.699E-16	3.415E-16	1.083	5.95	2.54	19.34
Ti47p[Cd]	3.290E6	2.691E-14	2.777E-14	1.032	7.06	3.64	11.24
Mn55g[Cd]	236.9	2.093E-12	2.779E-12	1.329	5.38	4.48	39.97
Fe54p[Cd]	4.011E6	1.157E-13	1.144E-13	0.989	6.30	2.14	12.78
Fe56p[Cd]	7.155E6	1.326E-15	1.302E-15	0.982	5.39	2.29	18.80
Fe56p[Fi]	7.1598E6	1.195E-15	1.255E-15	1.050	5.42	2.29	18.80
Fe58g[Cd]	229.5	2.593E-13	2.796E-13	1.078	5.76	5.88	38.84
Co59p[Cd]	5.454E6	1.828E-15	1.863E-15	1.019	6.33	4.10	15.43
Co59g[Cd]	113	8.225E-12	1.807E-11	2.197	5.53	0.77	53.78
Co59g	0.6426	2.529E-11	3.473E-11	1.373	6.09	0.73	105.1
Co592[Cd]	1.326E7	2.799E-16	2.909E-16	1.039	9.78	2.54	33.02
Ni582[Cd]	1.631E7	5.010E-18	8.740E-18	1.745	6.50	2.74	35.69
Ni60p[Cd]	6.739E6	2.847E-15	2.484E-15	0.872	5.68	10.49	17.6
Cu63g[Cd]	528.2	8.655E-13	1.249E-12	1.44	6.42	4.17	35.52
Cu63g	8.589E-2	2.998E-12	3.220E-12	1.074	5.57	4.00	131.3
Zn64p[Cd]	3.919E6	5.146E-14	5.432E-14	1.056	5.37	4.79	12.95
Zr902[Cd]	1.536E7	2.039E-16	1.798E-16	0.882	9.41	1.56	34.97

TABLE 7.2. SPECTRUM AVERAGED DOSIMETRY CROSS-SECTIONS FOR THE ANNULAR CORE RESEARCH REACTOR CENTRAL CAVITY (cont.)

Reaction/ cover [a]	Median energy response, $E(50\%)$ (eV)	Cross-section (mb)			Uncertainty (%)		
		Experiment	Calculation	C/E	Experiment	Cross-section	Neutron spectrum
Nb932[Cd]	1.137E7	5.744E-16	5.072E-16	0.883	6.24	2.60	30.33
In115g	1.497	3.969E-10	5.853E-10	1.475	5.91	5.98	71.38
In115g[Cd]	1.586	2.820E-10	4.966E-10	1.761	6.30	5.98	73.91
In115n[Cd]	2.269E6	1.924E-13	2.731E-13	1.420	7.04	2.18	10.55
Au197g	3.099	3.243E-10	3.421E-10	1.055	6.70	0.16	63.90
Au197g[Cd]	3.292	2.702E-10	2.971E-10	1.099	6.31	0.17	66.03
Au197g[Fi]	6318	1.491E-12	1.432E-12	0.960	6.71	0.49	7.66
Np237f[Fi]	1.497E6	2.480E-12	2.910E-12	1.173	5.66	9.58	8.59
U235f[Fi]	2.463E5	5.733E-12	5.874E-12	1.025	5.64	0.29	4.90
U238f[Fi]	2.336E6	5.300E-13	5.212E-13	0.983	5.66	0.53	11.26
Pu239f[Fi]	5.961E5	6.986E-12	6.635E-12	0.950	5.42	0.39	5.35
Mo98g[Cd] [b]	—	2.453E-16	—	—	7.12	—	—
Ag109g [b]	—	8.828E-18	—	—	2.46	—	—
Ag109g[Cd] [b]	—	5.816E-18	—	—	3.33	—	—
W186g2	—	1.464E-14	—	—	6.54	—	—

[a] Cross-section identifier is the target isotope with a reaction symbol followed by a cover in square brackets. Reaction symbols include: g = (n,γ), p = (n,p), 2 = (n,2n), a = (n,α), f = (n,f), n = (n,n′). Covers include [Cd] = cadmium, and [Fi] = ^{10}B enriched boron ball.

[b] These data were not used in the spectrum adjustment due to the lack of cross-section covariance matrices; experimental data quoted for these reactions are activities in Bq/atom.

dosimetry reactions and cover combinations that were used in the spectrum characterization, and also shows the least squares uncertainty contributions from the experimental activation measurements, a priori neutron spectrum and dosimetry cross-sections. The χ^2 per degree of freedom (dof) for the spectrum adjustment was a highly acceptable value of 1.68.

7.1.2. SPR-III reference neutron field

SPR-III is an advanced fast burst Godiva type reactor with a large 16.5 cm central cavity, and is positioned in the centre of an air filled shield building called a kiva (Fig. 7.5). Commissioned in 1975 and developed primarily for the radiation

testing of electronic components and systems, this reactor has been used in a wide variety of research activities. Experiments are conducted not only in the cavity but also outside the core at distances between 0.3 and 3.0 m from the core axis. There are also ports in the shield wall in order to support experiments that require collimated beam geometries. The reactor can be operated in steady state (up to 10 kW power) or pulsed mode (10 MJ in an 80 μs FWHM (full width at half maximum) pulse that yields approximately 5×10^{14} n/cm^2 in the cavity). This fast burst ^{235}U metal assembly has a very similar neutron spectrum to the ^{235}U thermal fission reference benchmark field, but has a larger thermal component

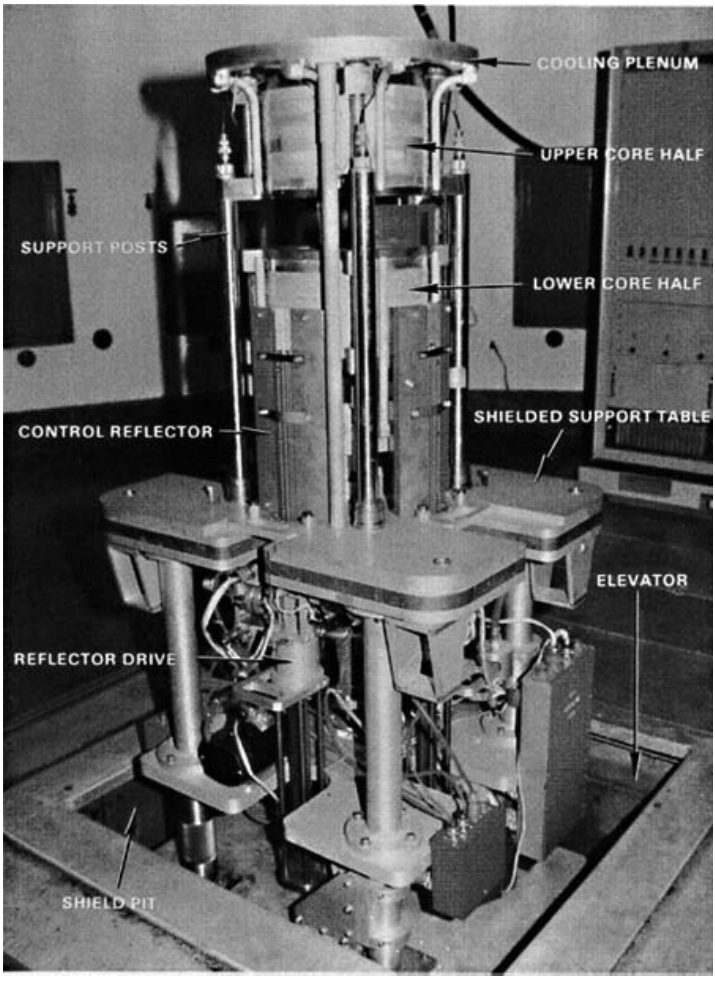

FIG. 7.5. The SPR-III reactor.

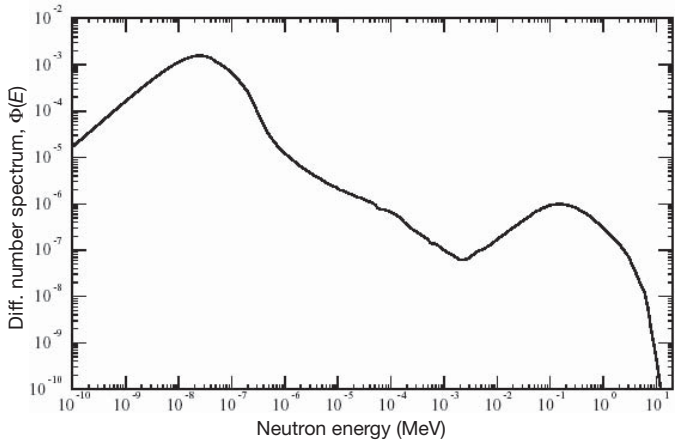

FIG. 7.6. Φ(E)E representation of calculated spectrum.

due to neutron backscattering from the walls of the kiva into the reactor experiment cavity (centre of the core). A more extensive description of this reference field appeared in Ref. [7.5], while details of the radiation transport models and 640 group representation of the neutron spectrum in the central cavity can be found in Ref. [7.10].

Figure 7.6 shows the SAND-II unfolded neutron spectrum in a typical logarithmic fluence plot (written as $\Phi(E)$ or dn/dE). The calculated spectrum in a linear lethargy plot (written as $E\Phi(E)$, but often written as $\Phi(\mu)$ or dE/dE) is shown in Fig. 7.7; equal areas under the curve correspond to equal neutron content in the lethargy plot (with linear y axis and logarithmic energy x axis or lethargy).

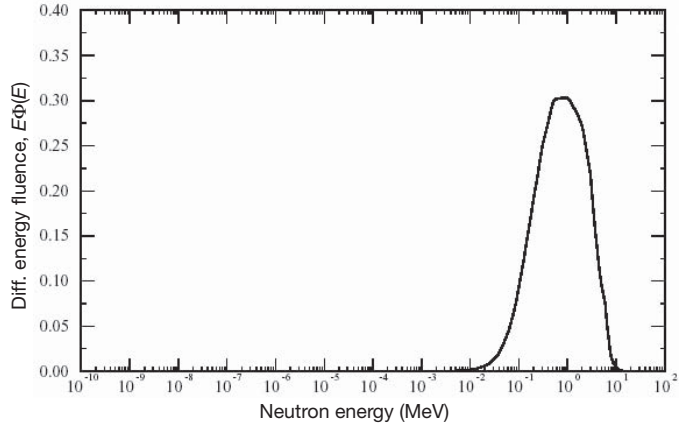

FIG. 7.7. EΦ(E) representation of calculated spectrum.

Table 7.3 details the 34 dosimetry reactions and their cover combinations that were measured in support of the SPR-III spectrum characterization. MCNP calculations were undertaken to determine an a priori neutron spectrum to be used in the spectrum adjustment [7.14]. Models used in these calculations were validated by a series of reactor worth measurements reported in Ref. [7.5]. The SAND-II [7.15] iterative spectrum unfold code was used to produce the baseline spectrum [7.10]. A Monte Carlo based iterative application of the SAND methodology was used to produce a neutron spectrum uncertainty and covariance matrix. The Monte Carlo simulations sampled from a statistically valid representation of the foil activities and the input trial spectrum. An LSL spectrum adjustment was also performed for this spectrum.

TABLE 7.3. SPECTRUM AVERAGED DOSIMETRY CROSS-SECTIONS FOR THE SPR-III CENTRAL CAVITY

			Measured		MCNP calculated		SAND-II unfold	
Reaction number	Sensor reaction	Foil cover [a]	Activity (Bq/nucleus)	$\Delta\sigma_{cnt}$ (%)	*C*/*E* ratio	$\Delta\sigma_{score}$ (%)	*C*/*E* ratio	Measured to calculated deviation (%)
1	$^{197}Au(n,\gamma)^{198}Au$	Cd	6.574E-18	4.5	0.7428	1.16	1.0269	–2.621
2	$^{197}Au(n,\gamma)^{198}Au$		7.414E-18	4.5	0.6931	1.12	0.9766	2.410
3	$^{59}Co(n,\gamma)^{60}Co$	Cd	6.923E-22	2.9	0.5928	1.69	0.9747	2.568
4	$^{63}Cu(n,\gamma)^{64}Cu$	Cd	3.302E-18	2.2	0.8776	0.13	1.0266	–2.585
5	$^{115}In(n,n')^{115}In^{m}$		6.204E-17	4.7	1.1280	0.14	0.9766	2.350
6	$^{nat}Ti(n,x)^{46}Sc$	Cd	7.325E-21	3.4	0.9416	0.62	0.9524	5.009
7	$^{nat}Ti(n,p)^{47}Sc$	Cd	2.882E-19	2.7	1.1590	0.27	1.0673	–6.314
8	$^{48}Ti(n,p)^{48}Sc$	Cd	8.684E-21	1.2	0.9456	1.43	0.9443	5.869
9	$^{32}S(n,p)^{32}P$		2.508E-19	3.0	1.0746	0.31	1.0050	–0.486
10	$^{58}Ni(n,p)^{58}Co$	Cd	8.752E-20	3.1	1.0311	0.26	0.9662	3.462
11	$^{54}Fe(n,p)^{54}Mn$	Cd	1.400E-20	3.2	1.0893	0.33	1.0331	–3.197
12	$^{56}Fe(n,p)^{56}Mn$	Cd	5.408E-19	2.4	0.9791	1.10	1.0097	–0.956
13	$^{64}Zn(n,p)^{64}Cu$	Cd	3.882E-18	2.2	1.1090	0.27	1.0452	–4.323
14	$^{24}Mg(n,p)^{24}Na$	Cd	1.242E-19	3.0	1.1055	1.48	1.0648	–6.086
15	$^{27}Al(n,\alpha)^{24}Na$	Cd	6.135E-20	1.9	1.0386	1.63	0.9940	0.561

TABLE 7.3. SPECTRUM AVERAGED DOSIMETRY CROSS-SECTIONS FOR THE SPR-III CENTRAL CAVITY (cont.)

Reaction number	Sensor reaction	Foil cover [a]	Measured		MCNP calculated		SAND-II unfold	
			Activity (Bq/nucleus)	$\Delta\sigma_{cnt}$ (%)	C/E ratio	$\Delta\sigma_{score}$ (%)	C/E ratio	Measured to calculated deviation (%)
16	$^{90}Zr(n,2n)^{89}Zr$	Cd	1.616E-21	3.4	0.8843	10.38	1.0016	–0.161
17	$^{235}U(n,f)^{140}La$	Cd	1.755E-11	3.0	0.9595	0.08	0.9872	1.280
18	EU:$^{235}U(n,f)^{140}La$	B_4C, Cd	1.500E-11	—	tbd	tbd	0.9872	1.266
19	$^{238}U(n,f)^{140}La$	Cd	2.317E-12	3.2	1.1104	0.15	0.9747	2.624
20	DU:$^{238}U(n,f)^{140}La$	B_4C, Cd	2.223E-12	—	tbd	tbd	0.9833	1.718
21	$^{239}Pu(n,f)^{140}La$	Cd	2.233E-11	2.7	1.0518	0.08	1.0377	–3.633
22	PU:$^{239}Pu(n,f)^{140}La$	B_4C, Cd	1.912E-11	—	tbd	0.08	1.0524	–4.979
23	$^{237}Np(n,f)^{140}La$	Cd	1.234E-11	2.8	1.1336	0.01	0.9709	3.039
24	$^{237}Np(n,f)^{140}La$	B_4C, Cd	1.182E-11	—	1.1336	0.01	0.9690	3.183
25	$^{45}Sc(n,\gamma)^{46}Sc$	B_4C, Cd	1.192E-20	3.5	0.8163	0.14	—	—
26	$^{45}Sc(n,\gamma)^{46}Sc$	Cd	1.372E-20	3.3	0.8149	0.16	—	—
27	$^{23}Na(n,\gamma)^{24}Na$	B_4C, Cd	5.963E-20	2.1	0.9551	0.18	—	—
28	$^{23}Na(n,\gamma)^{24}Na$	Cd	7.170E-20	2.1	0.8944	2.65	—	—
29	$^{55}Mn(n,\gamma)^{56}Mn$	B_4C, Cd	4.557E-18	2.7	0.7950	0.13	—	—
30	$^{55}Mn(n,\gamma)^{56}Mn$	Cd	6.618E-18	2.6	0.6383	0.4	—	—
31	$^{58}Fe(n,\gamma)^{59}Fe$	Cd	7.974E-21	2.8	tbd	tbd	—	—
32	$^{27}Al(n,p)^{27}Mg$	Cd	2.872E-17	3.0	tbd	tbd	—	—
33	$^{115}In(n,\gamma)^{115}In^{m}$	Cd	4.916E-16	1.3	tbd	tbd	—	—
34	$^{23}Na(n,\gamma)^{24}Na$		7.087E-20	2.1	tbd	tbd	—	—

[a] Cover composition: 91.6% ^{10}B enriched B_4C = 0.1481 atoms/b; cadmium = 2.587E-3 atoms/b.

tbd: To be determined.

7.2. RESULTS OF CONSISTENCY TESTING

Since neither of the reference neutron spectra used in the consistency testing (ACRR and SPR-III) included time of flight spectrum measurements, an absolute calculated to experimental ratio (C/E) could not be formed. The activity produced by the ^{58}Ni(n,p) reaction in a nickel foil is typically used as an irradiation monitor.[1] This reaction is a high quality dosimetry reaction and has a threshold close to 3 MeV. The nickel activity was also used in the ACRR and SPR-III reactor exposures in order to normalize the dosimetry activities that were obtained from different reactor exposures. Multiple reactor exposures were required to obtain all of the activation data, while at the same time maintaining a small uniform region for spectrum characterization. In the absence of an absolute fluence measurement, ratios were formed of the individual dosimetry reaction activities to the ^{58}Ni(n,p) reference/monitor, and then the C/E ratio of this dosimetry reaction activity to nickel activity was examined. Table 7.4 contains the results of the C/E consistency checks for the various reactions in the IRDF-2002 library.

The acceptable agreement for the C/E ratio in Table 7.4 was two standard deviations. No selected dosimetry cross-section had to be removed from the IRDF-2002 library as a result of this validation check. However, an inspection of Table 7.4 shows clearly that many IRDF-2002 cross-sections were not covered by this checking process. Hopefully, additional reference fields will be added in order to check the reactions not addressed in Table 7.4.

The bare foil reaction activity values appeared to be acceptable in several cases, but a problem occurred when a cadmium cover was used on the sensor that appears to be related to the ^{nat}Cd(n,abs) cross-section for the dosimetry cover. There are no uncertainty or covariance data for the cadmium absorption cross-section. An analysis of the experimental data on cadmium indicated a lack of measurements in the resonance region above the thermal cut-off energy. The uncertainty in the ^{nat}Cd(n,abs) cross-section just above the large cadmium cut-off absorption energy was considered as a potential source of the disagreements between the calculated and measured activities for cadmium covered dosimeters during the original ACRR spectrum adjustment [7.4]. A problem with some cadmium covered C/E ratios can be observed in both the ACRR and SPR-III analyses. For those cases where the C/E ratio deviated by more than two standard deviations from unity for the cadmium covered reaction but acceptable agreement was obtained for the uncovered and boron

[1] Cobalt-58 activity produced through the ^{58}Ni(n,p) reaction in the nickel monitor is used to quantify the response of the monitor foil.

TABLE 7.4. RATIO OF SPECTRUM AVERAGED CROSS-SECTIONS TO MONITOR THE Ni58p REACTION

Reaction number	IRDF-2002 reaction	Cover [a]	*C*/*E* ratio [b]		Comments
			ACRR	SPR-III	
1	Li6t		—	—	No activation product — signature is alpha recoil. Reference dosimetry cross-section. No experimental data available in reference neutron fields.
2	B10a		—	—	No true activation product — signature is decay of $^{7}Li^{m}$ or alpha recoil. Reference dosimetry cross-section. No experimental data available in reference neutron fields.
3	F192		—	—	Product is beta emitter. No reference field data available.
4	Na23g	Bare	1.05 ± 6.7%	1.297 ± 10.2%	Good consistency in moderated spectrum, poor in fast spectrum. Cadmium cover issue in ACRR.
		[Cd]	1.23 ± 5.8%	1.147 ± 10.9%	
		[Fi]	0.999 ± 13.2%	1.230 ± 11.2%	
5	Na232		—	—	Need data in reference fields.
6	Mg24p	[Cd]	1.12 ± 5.77%	1.10 ± 5.4%	Adequate consistency.
7	Al27p		—	NA	Product has short half-life (10 min); SPR-III result slightly outside 2σ.
8	Al27a	[Cd]	1.063 ± 5.4%	1.03 ± 4.54%	Good consistency.
9	P31p		—	—	Product is beta emitter. No reference field data available.

TABLE 7.4. RATIO OF SPECTRUM AVERAGED CROSS-SECTIONS TO MONITOR THE Ni58p REACTION (cont.)

Reaction number	IRDF-2002 reaction	Cover [a]	*C/E* ratio [b]		Comments
			ACRR	SPR-III	
10	S32p	Bare	1.02 ± 8.0%	1.038 ± 8.0%	Product is beta emitter. Transfer calibration to ^{252}Cf field typically used.
11	Sc45g	Bare	1.01 ± 8.86%	—	Good consistency. Cadmium cover issue in ACRR.
		[Cd]	1.25 ± 6.9%	1.08 ± 6.3%	
		[Fi]	—	1.1 ± 6.4%	
12	Ti462		—	—	Need data in reference fields.
13	Ti46p		—	—	Data only for composite ^{46}Sc production.
	natTi(n,x)Sc46	[Cd]	1.05 ± 5.26%	1.09 ± 6.8%	Good consistency. No composite covariance file — used dominant reaction.
14	Ti47p		—	—	Data only for composite ^{47}Sc production.
15	Ti47np		—	—	Data only for composite ^{46}Sc production.
	natTi(n,x)Sc47	[Cd]	0.996 ± 6.9%	1.09 ± 5.9%	Good consistency. No composite covariance — used dominant reaction.
16	Ti48p		—	—	Data only for composite ^{48}Sc production.
17	Ti48np		—	—	Data only for composite ^{47}Sc production.
	natTi(n,x)Sc48		1.056 ± 6.8%	1.07 ± 6.8%	Good consistency. No composite covariance — used dominant reaction.
18	Ti49np		—	—	Data only for composite ^{48}Sc production.
19	V51a		—	—	Need data in reference fields.

TABLE 7.4. RATIO OF SPECTRUM AVERAGED CROSS-SECTIONS TO MONITOR THE Ni58p REACTION (cont.)

Reaction number	IRDF-2002 reaction	Cover [a]	*C*/*E* ratio [b]		Comments
			ACRR	SPR-III	
20	Cr532		—	—	Need data in reference fields.
21	Mn55g	Bare	—	1.05 ± 11%	Good consistency.
		[Cd]	1.006 ± 7.4%	0.894 ± 12.2%	
		[Fi]	—	1.11 ± 11.2%	
22	Fe542		—	—	Need data in reference fields.
23	Fe54p	[Cd]	0.983 ± 5.5%	1.05 ± 5.4%	Good consistency.
24	Fe54a		—	—	Need data in reference fields.
25	Fe56p	[Cd]	1.10 ± 4.5%	1.12 ± 5.9%	Adequate consistency.
		[Fi]	1.10 ± 4.5%	—	
26	Fe58g	[Cd]	0.89 ± 12.6%	0.93 ± 6.3%	Good consistency.
27	Co592	[Cd]	0.997 ± 11.8%	—	Good consistency.
28	Co59a		—	—	Need data in reference fields.
29	Co59g	Bare	1.017 ± 7.5%	—	Good consistency. Cadmium cover issue in ACRR.
		[Cd]	1.20 ± 5.4%	0.912 ± 6.8%	
30	Ni582	[Cd]	1.03 ± 7.2%	—	Good consistency.
31	Ni58p	Bare	1.0 ± 6.2%	1.0 ± 5%	Baseline for ratio.
		[Cd]	0.994 ± 3.7%	1.0 ± 5%	
32	Ni60p	[Cd]	0.936 ± 11.3%	—	Good consistency.
33	Cu63g	Bare	1.04 ± 9.01%	—	Good consistency.
		[Cd]	1.36 ± 9.7%	1.07 ± 11.8%	Good consistency. Cadmium cross-section problem with ACRR data.
34	Cu632		—	—	Need data in reference fields. Problems with interference reactions.

TABLE 7.4. RATIO OF SPECTRUM AVERAGED CROSS-SECTIONS TO MONITOR THE Ni58p REACTION (cont.)

Reaction number	IRDF-2002 reaction	Cover [a]	*C*/*E* ratio [b]		Comments
			ACRR	SPR-III	
35	Cu63a		—	—	Need data in reference fields. Problems with interference reactions.
36	Cu652		—	—	Need data in reference fields. Problems with interference reactions.
37	Zn64p	[Cd]	1.05 ± 5.8%	1.07 ± 6.6%	Good consistency.
38	As752		—	—	Need data in reference fields.
39	Y892		—	—	Need data in reference fields.
40	Zr902	[Cd]	NA	1.03 ± 7.1%	Good consistency. Interference thermal neutron reactions suspected in ACRR data.
41	Nb932	[Cd]	1.05 ± 7.0%	—	Good consistency.
42	Nb93n		—	—	Soft low probability photon makes test data difficult to acquire. Transfer calibration of beta may be used. Need data in reference field.
43	Nb93g	[Cd]	1.08 ± 12.7%	—	Good consistency.
44	Rh103n		—	—	Need data in reference fields.
45	Ag109g		NA	—	Self-shielding correction must be applied to ACRR data.
46	In1152		—	—	Need data in reference fields.
47	In115n	Bare	—	1.04 ± 3.4%	Good consistency.
		[Cd]	1.04 ± 7.5%	—	

TABLE 7.4. RATIO OF SPECTRUM AVERAGED CROSS-SECTIONS TO MONITOR THE Ni58p REACTION (cont.)

Reaction number	IRDF-2002 reaction	Cover [a]	*C/E* ratio [b]		Comments
			ACRR	SPR-III	
48	In115g	Bare	1.100 ± 9.3%	—	Adequate agreement. Cadmium cross-section problem.
		[Cd]	1.188 ± 10.3%	1.26 ± 7.6%	
49	I1272		—	—	Need data in reference fields.
50	La139g		—	—	Need data in reference fields.
51	Pr1412		—	—	Need data in reference fields.
52	Tm1692		—	—	Need data in reference fields.
53	Ta181		—	—	Need data in reference fields.
54	W186g	Bare	NA	—	Self-shielding corrections must be applied to ACRR data.
55	Au1972		—	—	Need data in reference fields.
56	Au197g	Bare	0.9887 ± 7.5%	1.02 ± 7.6%	Good consistency.
		[Cd]	1.016 ± 7.7%	1.07 ± 7.0%	
		[Fi]	0.894 ± 6.3%	—	
57	Ho199n		—	—	Need data in reference fields.
58	Pb204n		—	—	Need data in reference fields.
59	Th232g		—	—	Need data in reference fields.
60	Th232f		—	—	Need data in reference fields.
61	U235f	[Cdna]	—	1.04 ± 4.6%	Good consistency.
		[Fi]	1.03 ± 3.97%	1.08 ± 4.6%	

TABLE 7.4. RATIO OF SPECTRUM AVERAGED CROSS-SECTIONS TO MONITOR THE Ni58p REACTION (cont.)

Reaction number	IRDF-2002 reaction	Cover [a]	*C/E* ratio [b]		Comments
			ACRR	SPR-III	
62	U238f	[Cdna]	—	1.02 ± 4.7%	Good consistency.
		[Fi]	0.982 ± 4.96%	0.989 ± 4.7%	
63	U238g		—	—	Need data in reference fields.
64	Np237f	[Cdna]	—	1.06 ± 4.6%	Good consistency.
		[Fi]	1.08 ± 5.5%	1.02 ± 4.6%	
65	Pu239f	[Cdna]	—	1.09 ± 4.8%	Good consistency.
		[Fi]	0.960 ± 4.3%	1.09 ± 4.7%	Adequate agreement.
66	Am241f		—	—	Need data in reference fields.

[a] Cover nomenclature: [Cd] = cadmium, [Cdna] = thick cadmium, [Fi] = ^{10}B enriched boron carbide ball.

[b] Uncertainty only includes that of the main reaction cross-section; the Ni58p cross-section is treated as a reference with zero uncertainty.

NA: There was reason to suspect a problem with the foil measurement in the facility characterization (e.g. presence of interferents in the foil that result in a similar activation product (e.g. an interferent would be the presence of manganese in an iron foil; ^{56}Fe(n,p)^{56}Mn dosimetry activity would have interference from ^{56}Mn produced by the ^{55}Mn(n,γ)^{55}Mn reaction), or failure to adequately document the abundance of the target isotope in the sample foil), or the use of a cadmium cover over the dosimetry foil may have interfered with the comparison due to problems with the cover cross-section.

—: No experimental data exist.

covered reactions, the problem was attributed to the cadmium cross-section. Requests have been made to the experimental nuclear data community to gather additional data for the cadmium absorption cross-section in the resonance region in order to assist in resolving this measurement conflict with some cadmium covered dosimeters.

The ^{23}Na(n,γ) reaction showed good agreement between the calculated and measured activities in a moderated neutron spectrum, but poor agreement in a fast neutron spectrum. This problem is well known to the user community, and more work must be done to resolve the high energy part of this cross-section. Thus the ^{23}Na(n,γ) reaction should not be used for spectrum adjustments in fast neutron fields until this problem has been resolved.

7.3. SUMMARY OF THE VALIDATION

IRDF-2002 testing in reference neutron fields has validated 29 of the 66 reactions included in the library. Data were not available for the reference neutron fields for 32 reactions. Six of the reactions are partial reactions that are addressed in composite form in three other validation entries. The two remaining reactions are affected either by the short half-lives or by self-shielding considerations, and additional data should be obtained.

No reactions had to be removed from the IRDF-2002 library as a result of these consistency tests. Two of the reactions (Mg24p and Fe56p) were found to be only 'adequately' validated due to a C/E deviation of about two standard deviations, and for one of these reactions (Mg24p) this marginal level of agreement is also seen in the C/E ratios for the ^{252}Cf standard field (Section 4).

Users of IRDF-2002 are requested to provide data for the reference neutron fields when studying reactions not found in this analysis. These data may then be included in future revisions of this dosimetry library.

REFERENCES TO SECTION 7

[7.1] Neutron Cross Sections for Reactor Dosimetry (Proc. Mtg Vienna, 1976), Vol. 1, IAEA-TECDOC-208, IAEA, Vienna (1978).

[7.2] "Benchmarks and intercomparisons, supplementary workshop on testing of the IRDF-2002 File, workshop session III", Reactor Dosimetry in the 21st Century (Proc. Int. Symp. Brussels, 2002), World Scientific, Singapore (2003) 718–719.

[7.3] RAJPUT, M.U., MacMAHON, T.D., Techniques for evaluating discrepant data, Nucl. Instrum. Meth. Phys. Res. **A312** (1992) 289.

[7.4] GRIFFIN, P.J., et al., "Characterization of the ACRR reference benchmark field", Reactor Dosimetry in the 21st Century (Proc. Int. Symp. Brussels, 2002) (WAGEMANS, J., ABDERRAHIM, H.A., D'HONDT, P., DE RAEDT, C., Eds), World Scientific, Singapore (2003) 323–331.

[7.5] KELLY, J.G., GRIFFIN, P.J., FAN, W.C., Benchmarking the Sandia Pulsed Reactor III cavity neutron spectrum for electronic parts calibration and testing, IEEE Trans. Nucl. Sci. **40** (1993) 1418.

[7.6] HAWARI, A.I., et al., The Materials Dosimetry Reference Facility, Proc. 8th Symp. on Reactor Dosimetry (FARRAR, H., LIPPINCOTT, E., WILLIAMS, J., VEHAR, D., Eds), American Society for Testing and Materials, Philadelphia, PA (1994) 401–410.

[7.7] SEKINE, T., MAEDA, S., AOYAMA, T., "Characterization of neutron field in the experimental fast reactor JOYO", Reactor Dosimetry in the 21st Century (Proc. Int. Symp. Brussels, 2002) (WAGEMANS, J., ABDERRAHIM, H.A., D'HONDT, P., DE RAEDT, C., Eds), World Scientific, Singapore (2003) 381–388.

[7.8] SHIBATA, K., "Average cross sections calculated in various neutron fields", Summary Report of the Technical Meeting on International Reactor Dosimetry File: IRDF-2002, Rep. INDC(NDS)-435, IAEA, Vienna (2002) 49–58.

[7.9] SHIMAKAWA, S., et al., "Neutron dosimetry for material irradiation tests in JMTR", Reactor Dosimetry (Proc. Int. Symp. Prague, 1996) (ABDERRAHIM, H.A., D'HONDT, P., OSMERA, B., Eds), World Scientific, Singapore (1998) 857–864.

[7.10] GRIFFIN, P.J., KELLY, J.G., VEHAR, D.W., Updated Neutron Spectrum Characterization of SNL Baseline Reactor Environments, Vol. 1: Characterization, Rep. SAND93-2554, Sandia Natl Lab. (1994).

[7.11] KELLY, J.G., "Neutron spectrum adjustment with SAND-II using arbitrary trial functions", Reactor Dosimetry: Methods, Applications, and Standardization, Rep. ASTM STP 1001, American Society for Testing and Materials, Philadelphia, PA (1989) 460–468.

[7.12] STALLMAN, W., LSL-M2: A computer program for least-squares logarithmic adjustment of neutron spectra, Rep. NUREG/CR-4349, ORNL/TM-9933, Oak Ridge Natl Lab., TN (1986).

[7.13] GRIFFIN, P.J., A rigorous treatment of self-shielding and covers in neutron spectra determination, IEEE Trans. Nucl. Sci. **42** (1995) 1878.

[7.14] BRIESMEISTER, J., MCNP — A General Monte Carlo N-particle Transport Code, Version 4A, Rep. LA-12625-M, US 705 and US 706, Los Alamos Natl Lab., NM (1993).

[7.15] McELROY, W.N., BERG, S., CROCKETT, T., HAWKINS, R., A Computer-automated Iterative Method for Neutron Flux Spectral Determination by Foil Activation, Rep. AFWL-TR-67-41, Vol. 1, Air Force Weapons Lab., Kirtland, NM (1967).

8. RADIATION DAMAGE FILES AND COMPUTER CODES

P.J. Griffin, L.R. Greenwood

Commonly used response functions can be usefully formatted so that they may be readily interfaced with neutron spectra. Therefore, the IRDF-2002 library has included response functions for neutron displacement damage per atom (dpa) for iron, silicon and GaAs to support this application. The following sections detail the response functions and provide attribution for the derivation of the response.

8.1. IRON dpa (LIGHT WATER REACTOR PRESSURE VESSEL DAMAGE)

The ASTM standard E693 is the source for the iron dpa response [8.1]. Iron dpa (Fig. 8.1) is used in applications supporting pressure vessel surveillance calculations, which are performed in compliance with the US Nuclear Regulatory Commission requirements. The standard incorporates the ENDF/B-VI cross-sections in the iron dpa exposure function and recommends the use of the Norgett–Robinson–Torrens (NRT) displacement formalism. This 'damage energy to displacement' conversion procedure is consistent with the

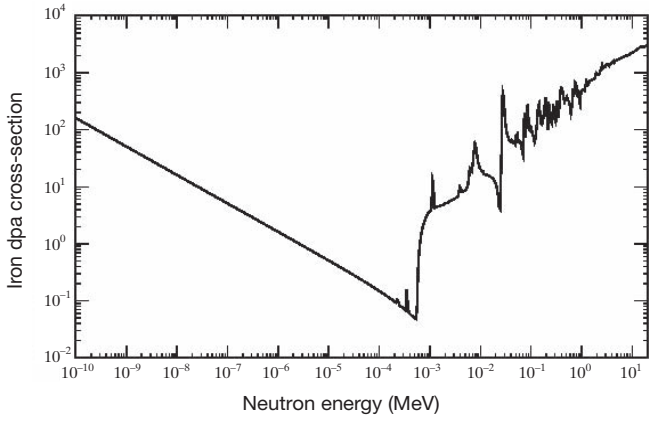

FIG. 8.1. ENDF/B-VI based iron displacement cross-section.

recommendations found in ASTM practices E521 and E821 for the treatment of radiation damage caused by charged particles. Values of the displacement cross-section are based on ENDF/B-VI Release 5, cross-sections as processed into dpa cross-sections with the NJOY-97 code [8.2], using the Robinson analytic representation [8.3] of the Lindhard model of energy partition between atoms and electrons [8.4] and NRT recommended conversion of damage energy to displacements [8.5] with an effective displacement threshold energy of E_d = 40 eV and an atomic scattering correction factor of β = 0.8. The NRT displacement equation defines the number of displacements (N_d) corresponding to a given damage energy (T_d) through the following equation:

$$N_d(T_d) = \begin{bmatrix} 0 & T_d < E_d \\ 1 & E_d \le T_d < 2E_d/\beta \\ \dfrac{\beta T_d}{2E_d} & 2E_d/\beta \le T_d < \infty \end{bmatrix} \tag{8.1}$$

The iron dpa cross-section combines dpa from the individual ENDF/B-VI iron isotopic evaluations using the natural iron isotopic abundance values from Ref. [8.6]. Isotopic cross-sections and relative abundances were adopted:

26-Fe-54, Mat = 2625, Rev. 5, tape 140; relative abundance = 5.9%
26-Fe-56, Mat = 2631, Rev. 1, tape 123; relative abundance = 91.72%
26-Fe-57, Mat = 2634, Rev. 1, tape 123; relative abundance = 2.1%
26-Fe-58, Mat = 2637, Rev. 5, tape 140; relative abundance = 0.28%

Version 97.45 of the NJOY-97 code used in this analysis was modified to implement the NRT displacement threshold model.

8.2. SILICON dpa (ELECTRONICS DAMAGE)

The basis of the currently accepted protocol for the correlation of radiation damage effects in a semiconductor device with a neutron irradiation is through the displacement kerma produced in bulk silicon. This correlation assumes that volume rather than surface effects is the dominant radiation damage mechanism. Experimental evidence indicates that displacement kerma is a valid measure of device performance degradation (e.g. reduction in current gain) in bipolar transistors whose operation depends basically on volume mechanisms. This correlation is clearly not valid for device types governed by surface phenomena (such as MOSFET devices). Surface effect devices are

more sensitive than volume effect devices to ionization radiation effects produced by either a neutron field or a mixed neutron–gamma field.

The accepted methodology is to relate the damage caused by a specific fluence of a given neutron spectrum to an equivalent fluence from a monoenergetic spectrum at a reference energy that would produce the same level of damage. 1 MeV is the reference energy used by the semiconductor radiation effects community, and the ratio of the fluence from a specific neutron with energy E to the fluence of a reference 1 MeV neutron required to cause the same level of damage is referred to as the 1 MeV(Si) damage response function. IRDF-2002 response functions include the results of the calculation of silicon displacement kerma factors (displacement kerma per unit neutron fluence) as a function of neutron energy over the range 10^{-10}–20 MeV. The unit of the displacement kerma factor is megaelectronvolts times millibarns (MeV·mb). Each factor can be multiplied by 3.435×10^{-13} to convert to rad(Si)·cm^2, or by 3.435×10^{-19} to convert to J·m^2/kg or Gy(Si)·m^2.

An average value of the neutron displacement kerma factor near 1 MeV is difficult to determine because of sharp neutron cross-section resonances in that energy region. To avoid these difficulties, the semiconductor radiation effects community has defined the displacement kerma of a reference 1 MeV neutron to be exactly a reference displacement kerma level of 95 MeV·mb. Values for the silicon displacement kerma are determined by calculating the total kerma and then partitioning the data into ionization and displacement fractions [8.7]. The correlation of the displacement kerma with the measured damage in many neutron fields has been confirmed with integral uncertainties no larger than 10% [8.8]. Figure 8.2 shows the neutron energy dependent silicon displacement kerma.

For any given neutron spectrum, a 1 MeV(Si) equivalent fluence is derived by convoluting the displacement kerma with the neutron spectrum and dividing by 95 MeV·mb. The uncertainty in the specification of the neutron spectrum should be propagated through this convolution and used to determine the uncertainty in the resulting 1 MeV(Si) equivalent fluence. Note that the displacement kerma is considered to be a radiation effects community specified exposure metric and has no uncertainty (i.e. it represents a specified response).

8.3. GALLIUM ARSENIDE dpa (ELECTRONICS DAMAGE)

The basis of the currently accepted protocol for the correlation of neutron damage effects to a neutron fluence in a GaAs semiconductor device is through the displacement kerma produced in bulk GaAs. However, this

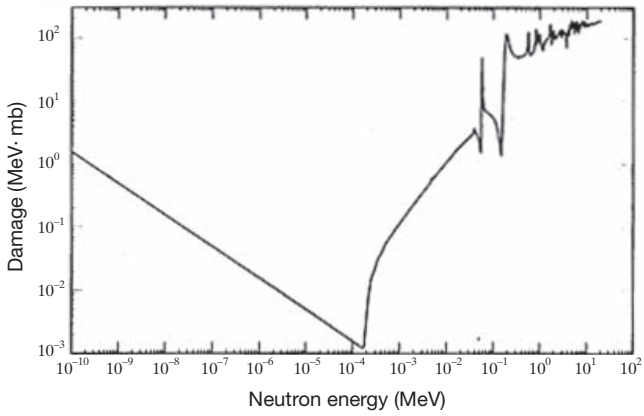

FIG. 8.2. Energy dependence of silicon displacement damage response function.

correlation depends on the assumption that displacement effects are the dominant radiation damage mechanism and that equal numbers of initially displaced atoms produce equal changes in device performance. Experimental evidence indicates that displacement kerma is not a valid measure of changes in the fundamental properties (carrier concentration, mobility and carrier lifetime) that determine device performance [8.9, 8.10]. The reason that the displacement kerma does not correlate with the property changes in GaAs over the entire range of neutron energies of interest is attributed to variations in the defect production efficiency for different sizes of displacement cascades. This effect is also known to occur in other types of material, including structural metals [8.11]. Despite these deficiencies (a lack of a strict proportionality between the observed GaAs semiconductor damage and the calculated displacement kerma), displacement kerma is still useful as an exposure parameter, and is analogous to the use of dpa for exposures of iron.

Empirical efficiency factors that depend on the energies of the primary knock-on atoms (PKA) have been proposed in order to remove the discrepancies described above [8.9]. Figure 8.3 shows the shape of the empirical damage efficiency factor for GaAs, and can be described by an empirical function. As in Ref. [8.11], this PKA energy damage efficiency factor is used in conjunction with a normalization factor of 2.2 to preserve the equivalence of the GaAs damage function and the displacement kerma for 1 MeV neutrons.

The results of the calculation of GaAs displacement kerma factors (displacement kerma per unit neutron fluence) are shown in Fig. 8.4 as a function of neutron energy. Figure 8.5 shows the complete energy dependence of the GaAs damage function. The unit of the kerma factor is megaelectronvolts times millibarns (MeV·mb). The kerma factor can be multiplied by

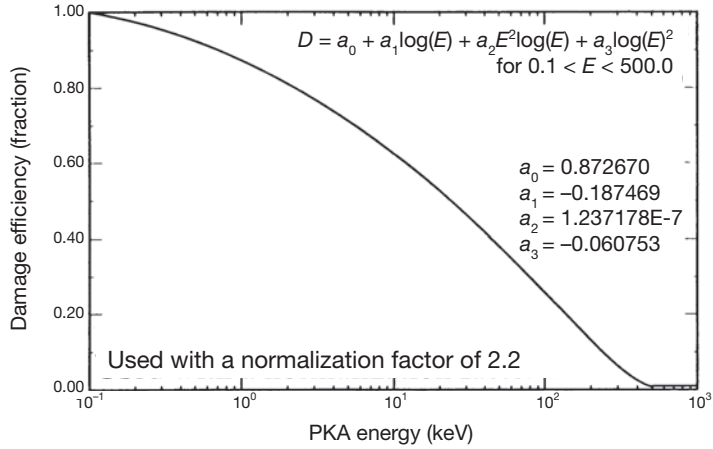

FIG. 8.3. GaAs damage efficiency curve.

1.334×10^{-13} to convert from units of MeV·mb to rad(GaAs)·cm^2, and can be multiplied by 1.334×10^{-19} to convert from MeV·mb to J·m^2/kg or Gy(GaAs)·m^2. An average value of the neutron displacement kerma factor near 1 MeV is 70 MeV·mb. As is the case for silicon [8.12], the actual value chosen for the designated 1 MeV reference damage is arbitrary. What is important is that the whole radiation hardness community uses the same value in setting hardness specifications and when testing electronic parts.

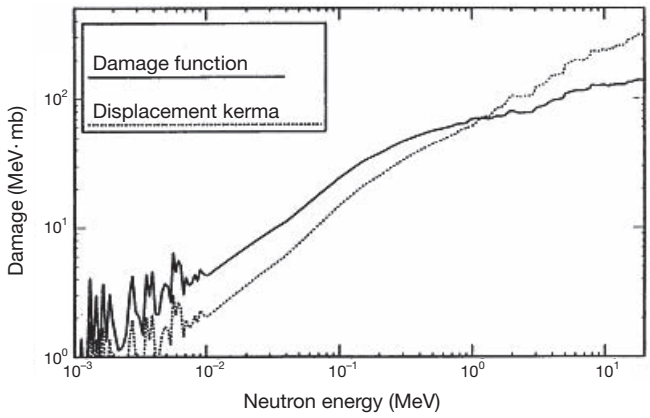

FIG. 8.4. Energy dependence of the GaAs displacement and damage response functions.

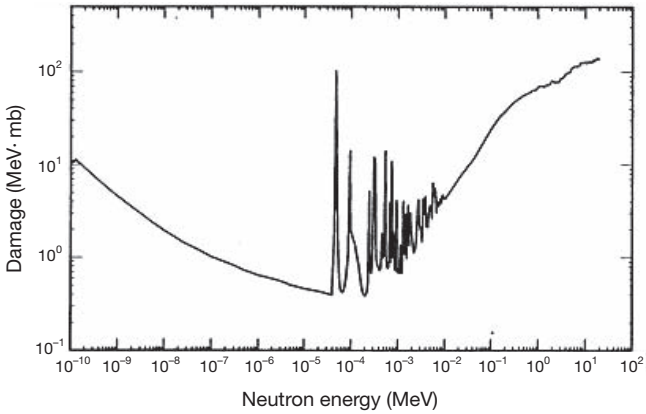

FIG. 8.5. Energy dependence of the GaAs damage function.

REFERENCES TO SECTION 8

[8.1] 1997 Annual Book of ASTM Standards, Vol. 12.02: Nuclear (II), Solar, and Geothermal Energy, American Society for Testing and Materials, Philadelphia, PA (1997).

[8.2] MacFARLANE, R.E., MUIR, D.W., The NJOY nuclear data processing system, Version 91, Los Alamos Natl Lab., LA-12740-M, October 1994; code updated to Version 97.0 in a "Readme0" memorandum by R.E. MacFarlane dated 31 October 1997 — this version of the code is distributed by the Radiation Safety Information Computational Center at Oak Ridge Natl Lab. as code package PSR-368; Version 97.45 is further updated, and is available using an update file from the web address http://t2.lanl.gov/codes/njoy97/

[8.3] ROBINSON, M.T., "The energy dependence of neutron radiation damage in solids", Nuclear Fusion Reactor (Proc. Int. Conf. Culham, UK, 1969), British Nuclear Energy Society, London (1970) 364–377.

[8.4] LINDHARD, J., SCHARFF, M., SCHIØTT, H.E., Range concepts and heavy ion ranges (notes on atomic collisions, II), K. Dan. Vidensk. Selsk., Mat.-Fys. Medd. **33** 14 (1963).

[8.5] NORGETT, M.J., ROBINSON, M.T., TORRENS, I.M., A proposed method of calculating displacement dose rates, Nucl. Eng. Des. **33** (1975) 50.

[8.6] TULI, J.K., Nuclear Wallet Cards, Brookhaven Natl Lab., Upton, NY (1990).

[8.7] ROGERS, V.C., HARRIS, L., Jr., STEINMAN, D.K., BRYAN, D.E., Silicon ionization and displacement kerma for neutrons from thermal to 20 MeV, IEEE Trans. Nucl. Sci. **NS-22** (1975) 2326; Erratum, **NS-23** (1976) 875.

[8.8] SPARKS, M.H., et al., Energy dependence of neutron damage in silicon bipolar transistors, IEEE Trans. Nucl. Sci. **NS-36** (1989) 1904.

[8.9] GRIFFIN, P.J., KELLY, J.G., LUERA, T.F., BARRY, A.L., LAZO, M.S., Neutron damage equivalence in GaAs, IEEE Trans. Nucl. Sci. **NS-38** (1991) 1937.
[8.10] LUERA, T.F., et al., Neutron damage equivalence for silicon, silicon dioxide and gallium arsenide, IEEE Trans. Nucl. Sci. **NS-34** (1987) 1557.
[8.11] AVERBACK, R., BENEDEK, R., MERKLE, K.L., Ion-irradiation studies of the damage function of copper and silver, Phys. Rev. B **18** (1978) 4156.
[8.12] CONRAD, E.E., Considerations in establishing a standard for neutron displacement effects in semiconductors, IEEE Trans. Nucl. Sci. **NS-18** (1971) 200.

9. DECAY DATA AND ISOTOPIC ABUNDANCES FOR DOSIMETRY APPLICATIONS

O. Bersillon

A major objective of dosimetry is to determine the neutron fluence (also described as the neutron flux) by the use of activation measurements made at various points in a nuclear reactor. Other possible areas of application of dosimetry include the determination of activation and transmutation products, and of radiation damage and gas production. Nuclear data libraries such as IRDF-90 are dedicated to such applications, and consist only of neutron induced cross-sections. The main experimental method uses the measurement of selected radiations emitted by the radionuclides, which are produced by the neutron irradiation process. A new IRDF-2002 library has been prepared that contains a section dedicated to evaluated decay data, containing all such data necessary to reduce and process the experimental results.

The successive steps described in this section start with the basic data given in the Evaluated Nuclear Structure Data File (ENSDF) library [9.1] and progress to the final database in ENDF-6 format [9.2]. Recommendations are also made concerning the use of a recent determination of isotopic abundances.

9.1. DECAY DATA

9.1.1. Selection of radionuclides

A selection of the target elements has been made (Section 6), together with the associated nuclear reactions with those nuclear reactions for which cross-sections are given in the IRDF-2002 library. This procedure was used to establish an initial list of radionuclides to be considered for inclusion in the decay data section of the library. Furthermore, the fission channel is characterized by the following selected fission products [9.3]: ^{95}Zr + ^{95}Nb; ^{97}Zr + ^{97}Nb; ^{103}Ru; ^{106}Ru + ^{106}Rh; ^{131}I; ^{132}Te + ^{132}I; ^{137}Cs + ^{137}Ba^{m}; ^{140}Ba + ^{140}La; ^{141}Ce; ^{143}Ce + ^{143}Pr; and ^{144}Ce + ^{144}Pr.

The list of nuclides is completed by the inclusion of the intermediate radionuclides that are required to reach the stability valley. Thus the decay data included in the IRDF-2002 library contain a total of 85 radionuclides: 58 ground states (of which seven have two decay modes), 25 first isomeric states (of which eight have two decay modes) and two second isomeric states (^{116}In^{n} and ^{196}Au^{n}).

9.1.2. Type of data

In addition to the basic decay data (half-life, decay modes and intensities, branching to isomeric levels), the experimental data reduction must also be supported with knowledge of such decay characteristics as the energy and intensity of some specific radiations (e.g. gamma rays, X rays) emitted during the decay process. Knowledge of the complete decay processes is not essential, but could help to increase confidence in the partial decay data required for a specific application.

9.1.3. Origin of the data

Many of the required decay data have been determined experimentally and published in the literature. Within the International Network of Nuclear Structure and Decay Data Evaluators, these data are collected, evaluated when necessary, and included in the ENSDF library. The format of this library has the advantage that the data closely follow the layout of a decay scheme, and there is also suitable space for detailed comments; however, a major limitation is the resulting complexity of these card images. An example is given in Fig. 9.1, which describes the β^- decay of ^{60}Co.

```
60NI    60CO B- DECAY (1925.3 D)                                          200009
60NI  H TYP=UPD$AUT=R. Helmer$CIT=ENSDF$CUT=01-SEP-1996$DAT=12-SEP-2000$
60NI  N 1.0         1.0       1.0       1.0
60CO  P 0.0          5+               1925.3 D  3               2823.9   5
60NI  L 0            0+               STABLE
60NI  L 1332.508  4  2+               0.9 PS    3
60NI  B 1492      20 0.12   3             14.70 11                          2U
60NIS B EAV=625.87 21
60NI  G 1332.492  4 99.9826 6  E2                     1.28E-4 5           <===
60NI2 G EKC=1.15E-4 5
60NI  L 2158.61   3  2+
60NI  B 670       20 0.000  2             14.0  GE                          2U
60NIS B EAV=274.93 21
60NI  G 826.10    3  0.0076  8 D+Q      +0.9     3    3.3E-4 4
60NI2 G KC=3.1E-4 4 $ LC=2.94E-5 17
60NI  G 2158.57   3 0.0012  2                        4.91E-5
60NI2 G KC=4.48E-5 14 $ LC=4.3E-6 2
60NI  L 2505.748  5  4+               0.30 PS    9
60NI  B 317.88    10 99.88  3            7.512  2
60NIS B EAV=95.77 15
60NI  G 347.14    7  0.0075 4                      5.54E-317
60NI2 G KC=5.03E-3 15 $ LC=5.08E-4 15
60NI  G 1173.228  3  99.85  3  E2(+M3)  -0.0025  22   1.68E-4 4           <===
60NI2 G EKC=1.51E-4 7
60NI  G 2505.692  5  2.0E-6 4  E4                     8.6E-5 3
60NI2 G KC=7.8E-5 3 $ LC=7.6E-6 3
```

FIG. 9.1. ENSDF format (^{60}Co β^- decay). This set of data illustrates the close connection between the physical quantities and the data structure (L denotes level description, B for branching, G for gamma ray, etc.); for clarity the comments are not included. The arrows at the right hand side of the data listing denote two well known gamma rays (i.e. these arrows are not part of the ENSDF format).

9.1.4. Data processing

The required decay data must be extracted from the ENSDF library and converted to the ENDF-6 format that is now included in the library. This conversion is achieved by means of the SDF2NDF code [9.4], which was derived from RADLST Version 5.5 [9.5] through extensive recoding and translation into double precision and was enhanced with several new features. Radiations emitted from the electron cloud (X rays, Auger electrons, etc.) are also calculated. Several auxiliary output files were added in order to make data checking easier. The ENDF file for ^{60}Co β^- decay is partly listed in Fig. 9.2

9.1.5. Data control

SDF2NDF also performs a number of physical checks to verify the consistency of the data; for example:

```
header section
2.70600+04  5.94190+01           0           0           0           4
1.66346+08  2.59200+04           0           0           6           0
9.67355+04  2.42148+02  2.50384+06  3.52186+02  0.00000+00  0.00000+00
5.00000+00  1.00000+00           0           0           6           1
1.00000+00  0.00000+00  2.82390+06  5.00000+02  1.00000+00  0.00000+00
gamma section
0.00000+00  0.00000+00           0           0           6           6
1.00000-02  0.00000+00  2.50384+06  3.52186+02  0.00000+00  0.00000+00
3.47140+05  7.00000+01           0           0          12           0
1.00000+00  0.00000+00  7.50000-03  4.00000-04  0.00000+00  0.00000+00
5.54000-03  1.70000-04  5.03000-03  2.12769-04  5.08000-04  2.13836-05
8.26100+05  3.00000+01           0           0          12           0
1.00000+00  0.00000+00  7.60000-03  8.00000-04  0.00000+00  0.00000+00
3.30000-04  4.00000-05  3.10000-04  4.10669-05  2.94000-05  1.91518-06
1.17323+06  3.00000+00           0           0          12           0
1.00000+00  0.00000+00  9.98500+01  3.00000-02  0.00000+00  0.00000+00
1.68000-04  4.00000-06  1.51000-04  7.00000-06  0.00000+00  0.00000+00
1.33249+06  4.00000+00           0           0          12           0
1.00000+00  0.00000+00  9.99826+01  6.00000-04  0.00000+00  0.00000+00
1.28000-04  5.00000-06  1.15000-04  5.00000-06  0.00000+00  0.00000+00
2.15857+06  3.00000+01           0           0          12           0
1.00000+00  0.00000+00  1.20000-03  2.00000-04  0.00000+00  0.00000+00
4.91000-05  0.00000+00  4.48000-05  1.94071-06  4.30000-06  2.37994-07
2.50569+06  5.00000+00           0           0          12           0
1.00000+00  0.00000+00  2.00000-06  4.00000-07  0.00000+00  0.00000+00
8.60000-05  3.00000-06  7.80000-05  3.80468-06  7.60000-06  3.76808-07
```

FIG. 9.2. ENDF-6 format (^{60}Co β^- decay) as converted from ENSDF format; only two sections are given for clarity. The two underlined numbers are the energies (in eV) of the two well known gamma rays denoted in Fig. 9.1.

(a) The overall energy balance between the decay Q value and the sum of the energies of all emitted particles (including recoils);
(b) The sum of the transition intensities depopulating an excited level must be equal to the feeding of this level;
(c) The transition intensity between two excited levels has to be equal to the sum of the gamma intensity and the converted electron intensities;
(d) The total conversion coefficient must be close to the sum of the partial coefficients for the different electron shells.

9.1.6. Results

The most intense radiations are presented and some explanations are given in the header of the table on the CD-ROM (this information has the same title as this section, and the data in the ENDF-B6 format are included on the CD-ROM of IRDF-2002.

Nine radionuclides (^{95}Zr, ^{97}Zr, ^{103}Ru, ^{106}Ru, ^{116}In^{m}, ^{131}I, ^{132}Te, ^{137}Cs and ^{144}Ce) have a decay branch leading to a daughter isomeric state. The total decay intensity in this particular mode is given together with the fractions of the decay that feed the ground and isomeric states.

For approximately 25% of the radionuclides considered, the main gamma rays received special attention during the course of an IAEA coordinated research project (CRP) [9.6]. Those readers who require a more extensive evaluation of the nuclear decay data for radionuclides used as detector efficiency calibration standards should consult the final document of this CRP: Update of X-ray and Gamma-ray Decay Data Standards for Detector Calibration and Other Applications.

9.2. ISOTOPIC ABUNDANCES

The proportion of nuclides affected by the neutron flux is directly related to the isotopic composition of the elements. Thus these isotopic abundances are very important quantities. Three major evaluations of isotopic composition have been published over the previous ten years [9.7–9.9]. These three data references give very similar values for the isotopic abundances of the 287 stable isotopes, except for the following four isotopes, for which the deviations exceed 1%:

(a) Hydrogen-2 (3.04%);
(b) Xenon-124 (1.11%);
(c) Osmium-187 (–1.84%);
(d) Platinum-190 (–2.86%).

Protactinium-231 is stated to have 100% abundance [9.9], which is incorrect: this nuclide has a finite half-life ($t_{1/2}$ = 32 760 years), and the generally accepted value for the isotopic abundance of this isotope is 0%.

9.3. RECOMMENDATIONS

Recently evaluated decay data are proposed for many radionuclides that are of importance in reactor dosimetry applications. These decay data originate from the ENSDF library and have been extracted, transferred, checked and converted to the ENDF format. These data, together with the isotopic abundances given in Ref. [9.9], are recommended for reactor dosimetry applications.

REFERENCES TO SECTION 9

[9.1] McLANE, V., et al., Data Formats and Procedures for the Evaluated Nuclear Data File, Rep. BNL-NCS-44945 (ENDF-102), Brookhaven Natl Lab., Upton, NY (1995).

[9.2] BHAT, M.R., "Evaluated nuclear structure data file", Nuclear Data for Science and Technology (QAIM, S.M., Ed.), Springer-Verlag, Berlin (1992) 817.

[9.3] ZSOLNAY, E.M., Institute of Nuclear Techniques, Budapest University of Technology and Economics, personal communication, 2003.

[9.4] BERSILLON, O., The SDF2NDF Code, Commissariat à l'énergie atomique, Bruyères-le-Châtel.

[9.5] BURROWS, T.W., The Program RADLST, Rep. BNL-NCS-52142, Brookhaven Natl Lab., Upton, NY (1988).

[9.6] INTERNATIONAL ATOMIC ENERGY AGENCY, IAEA Coordinated Research Project: Update of X-ray and Gamma-ray Decay Data Standards for Detector Calibration and Other Applications (in preparation).

[9.7] DE BIÉVRE, P., TAYLOR, D.P., Table of the isotopic compositions of the elements, Int. J. Mass Spectrom. Ion Process. **123** (1993) 149–166.

[9.8] HOLDEN, N.E., Table of Isotopes, Rep. BNL-61460, Brookhaven Natl Lab., Upton, NY (1995).

[9.9] ROSMAN, K.J.R., TAYLOR, P.D.P., Isotopic Compositions of the Elements 1997; International Union of Pure and Applied Chemistry, Inorganic Chemistry Division, Commission on Atomic Weights and Isotopic Abundances, Subcommittee for Isotopic Abundance Measurements, Pure Appl. Chem. **70** (1998) 217, and tabulated data from http://physics.nist.gov/PhysRefData/Compositions

Appendix I

CONTENTS AND MAT (MATERIAL NUMBER), MF (FILE NUMBER) AND MT (FILE SUBDIVISION) NUMBERS OF IRDF-2002

TABLE I.1. METROLOGY REACTIONS (ACTIVATION AND FISSION)

No.	Group library			Reaction code	Reaction	Point library		
	Mat	MF	MT			Mat	MF	MT
1	325	3	105	Li6T	6Li(N,T)4He	325	3	105
2	525	3	107	B10A	10B(N,A)7Li	525	3	107
3	925	3	016	F192	19F(N,2N)18F	925	3	016
4	1125	3	016	Na232	23Na(N,2N)22Na	1125	3	016
5	1125	3	102	Na23G	23Na(N,G)24Na	1125	3	102
6	1225	3	103	Mg24P	24Mg(N,P)24Na	1225	3	103
7	1325	3	103	Al27P	27Al(N,P)27Mg	1325	3	103
8	1325	3	107	Al27A	27Al(N,A)24Na	1325	3	107
9	1525	3	103	P31P	31P(N,P)31Si	1525	3	103
10	1625	3	103	S32P	32S(N,P)32P	1625	3	103
11	2126	3	102	Sc45G	45Sc(N,G)46Sc	2126	3	102
12	2225	3	016	Ti462	46Ti(N,2N)45Ti	2225	3	016
13	2225	3	103	Ti46P	46Ti(N,P)46Sc	2225	3	103
14	2228	3	231	Ti47Np	47Ti(N,NP)46Sc	2228	10	005
15	2228	3	103	Ti47P	47Ti(N,P)47Sc	2228	3	103
16	2231	3	231	Ti48Np	48Ti(N,NP)47Sc	2231	10	005
17	2231	3	103	Ti48P	48Ti(N,P)48Sc	2231	3	103
18	2234	3	231	Ti49Np	49Ti(N,NP)48Sc	2234	10	005
19	2328	3	107	V51A	51V(N,A)48Sc	2328	3	107
20	2431	3	016	Cr522	52Cr(N,2N)51Cr	2431	3	016
21	2525	3	102	Mn55G	55Mn(N,G)56Mn	2525	3	102
22	2625	3	016	Fe542	54Fe(N,2N)53Fe	2625	3	016
23	2625	3	103	Fe54P	54Fe(N,P)54Mn	2625	3	103
24	2625	3	107	Fe54A	54Fe(N,A)51Cr	2625	3	107
25	2631	3	103	Fe56P	56Fe(N,P)56Mn	2631	3	103
26	2637	3	102	Fe58G	58Fe(N,G)59Fe	2637	3	102

TABLE I.1. METROLOGY REACTIONS (ACTIVATION AND FISSION) (cont.)

No.	Group library			Reaction code	Reaction	Point library		
	Mat	MF	MT			Mat	MF	MT
27	2725	3	016	Co592	59Co(N,2N)58Co	2725	3	016
28	2725	3	102	Co59G	59Co(N,G)60Co	2725	3	102
29	2725	3	107	Co59A	59Co(N,A)56Mn	2725	3	107
30	2825	3	016	Ni582	58Ni(N,2N)57Ni	2825	3	016
31	2825	3	103	Ni58P	58Ni(N,P)58Co	2825	3	103
32	2831	3	103	Ni60P	60Ni(N,P)60Co	2831	3	103
33	2925	3	016	Cu632	63Cu(N,2N)62Cu	2925	3	016
34	2925	3	102	Cu63G	63Cu(N,G)64Cu	2925	3	102
35	2925	3	107	Cu63A	63Cu(N,A)60Co	2925	3	107
36	2931	3	016	Cu652	65Cu(N,2N)64Cu	2931	3	016
37	3025	3	103	Zn64P	64Zn(N,P)64Cu	3025	3	103
38	3325	3	016	As752	75As(N,2N)74As	3325	3	016
39	3925	3	016	Y892	89Y(N,2N)88Y	3925	3	016
40	4025	3	016	Zr902	90Zr(N,2N)89Zr	4025	3	016
41	4125	3	292	Nb932	93Nb(N,2N)92Nb^{m}	4125	10	016
42	4125	3	291	Nb93N	93Nb(N,N′)93Nb^{m}	4125	10	004
43	4125	3	102	Nb93G	93Nb(N,G)94Nb	4125	3	102
44	4525	3	291	RH103N	103RH(N,N′)103RHM	4525	10	004
45	4731	3	293	AG109G	109AG(N,G)110AGM	4731	10	102
46	4931	3	292	IN1152	115IN(N,2N)114INM	4931	10	016
47	4931	3	291	IN115N	115IN(N,N′)115INM	4931	10	004
48	4931	3	293	IN115G	115IN(N,G)116INM	4931	10	102
49	5325	3	016	I1272	127I(N,2N)126I	5325	3	016
50	5728	3	102	LA139G	139LA(N,G)140LA	5728	3	102
51	5925	3	016	PR1412	141PR(N,2N)140PR	5925	3	016
52	6925	3	016	TM1692	169TM(N,2N)168TM	6925	3	016
53	7328	3	102	TA181G	181TA(N,G)182TA	7328	3	102
54	7443	3	102	W186G	186W(N,G)187W	7443	3	102
55	7925	3	016	AU1972	197AU(N,2N)196AU	7925	3	016
56	7925	3	102	AU197G	197AU(N,G)198AU	7925	3	102
57	8034	3	291	HG199N	199HG(N,N′)199HGM	8034	10	004

TABLE I.1. METROLOGY REACTIONS (ACTIVATION AND FISSION) (cont.)

No.	Group library			Reaction code	Reaction	Point library		
	Mat	MF	MT			Mat	MF	MT
58	8225	3	291	PB204N	204PB(N,N′)204PBM	8225	10	004
59	9040	3	018	TH232F	232TH(N,F)FP	9040	3	018
60	9040	3	102	TH232G	232TH(N,G)233TH	9040	3	102
61	9228	3	018	U235F	235U(N,F)FP	9228	3	018
62	9237	3	018	U238F	238U(N,F)FP	9237	3	018
63	9237	3	102	U238G	238U(N,G)239U	9237	3	102
64	9346	3	018	NP237F	237NP(N,F)FP	9346	3	018
65	9437	3	018	PU239F	239PU(N,F)FP	9437	3	018
66	9543	3	018	AM241F	241AM(N,F)FP	9543	3	018

TABLE I.2. COVER REACTIONS

No.	Group library			Reaction code	Reaction	Point library		
	Mat	MF	MT			Mat	MF	MT
1	500	3	001	B	B-COVER	500	3	001
2	4800	3	001	CD	CD-COVER	4800	3	001
3	6400	3	001	GD	GD-COVER	6400	3	001

TABLE I.3. DAMAGE CHARACTERIZATION REACTIONS

No.	Group library			Reaction code	Reaction	Point library
	Mat	MF	MT			
1	1400	3	900	SI0DM	SI-DMA_ASTM	Not available
2	2400	3	900	CR0DP	CR-DPA	Not available
3	2600	3	900	FE0ASDP	FE-DPA_ASTM	Not available
4	2600	3	901	FE0EWDP	ST-DPA_EWGRD	Not available
5	2800	3	900	NI0DP	NI-DPA	Not available
6	3100	3	900	GA_ASDM	GA_AS-DMA	Not available

For the convenience of the metrology community, the group form of IRDF-2002 is also available in the simplified ENDF-like format, in addition to the pointwise and group files in strict ENDF-6 format. The simplified format means that all relevant metrology information is available in file MF = 3. Reaction data that produce a metastable state are normally given in file MF = 10. Conversion of MF = 10 information to MF = 3 data in the metrology file is accompanied by introducing special MT numbers to prevent confusion.

These special MT numbers for metastable nuclides in file MF = 10 are as follows:

MT = 292 for (n,2n) reaction products with metastable state in MF = 10;
MT = 291 for (n,n') reaction products with metastable state in MF = 10;
MT = 293 for (n,γ) reaction products with metastable state in MF = 10;
MT = 294 for (n,p) reaction products with metastable state in MF = 10;
MT = 295 for (n,α) reaction products with metastable state in MF = 10.

Another contribution from file MF = 10 is MT = 231 for (n,np) reactions stored in MF = 10 of the ENDF-6 file.

The pointwise cross-section data were converted to the extended SAND-II group structure using a flat weighting spectrum. Neutron temperature is 300 K.

Uncertainties are given in the form of covariance matrices for all metrology reactions. This information is included in the group version as NI subsection(s) in the file MF = 33.

Originally, the uncertainties were given in the 'point data' library for the Sc-45(n,γ)Sc-46 reaction as a combination of file MF = 32 and MF = 33 data. File MF = 32 was converted to file MF = 33 format, and this information was inserted as an extra NI subsection in file MF = 33 of the group version.

Appendix II

NEUTRON SELF-SHIELDING, COVER REACTIONS AND BURNUP CORRECTIONS FOR REACTOR DOSIMETRY APPLICATIONS

L.R. Greenwood

Neutron spectrum adjustments for reactor dosimetry applications can be made using a least squares computer code such as STAY'SL, in conjunction with the measured reaction rates, neutron cross-sections, and their uncertainties and covariances, as contained in IRDF-2002. However, prior to the spectral adjustment, corrections to the neutron cross-sections must be applied for neutron self-shielding or cover reactions. Such corrections are critical and may produce significant changes in the calculated reaction rate, especially for reactions that have large thermal or resonance cross-sections. If reactor measurements are made with highly dilute monitors, neutron self-shielding corrections may not be required. However, non-dilute monitors will always show significantly reduced reaction rates compared with dilute monitors, since thermal and resonance neutrons may be absorbed in the outer layers of a foil or wire, thereby reducing the activation rate in the interior of the material. Cover materials such as boron, cadmium or gadolinium are frequently used to suppress thermal neutrons, and cadmium ratios are used as an indicator of the ratio of thermal to epithermal or fast neutrons.

Ideally, neutron transport computer codes should be used to determine the neutron self-shielding and cover corrections that are to be applied to a given material. The reason for this requirement is that neutron scattering will result in higher than expected neutron fluxes in those energy groups that correspond to large thermal or resonance neutron cross-sections. Failure to include such neutron scattering effects will result in an overestimation of the neutron self-shielding corrections. Such neutron transport calculations require the use of neutron scattering cross-sections, usually taken as the total neutron cross-sections, in addition to the neutron activation cross-sections. The total neutron cross-sections are included in IRDF-2002 for target materials that have a dosimetry quality (n,γ) reaction.

Fortunately, lengthy neutron transport calculations may not be required for relatively thin samples or simple covers, where the neutron mean free paths for neutron scattering tend to be larger than the dimensions of the sample. Approximations have been developed that may allow sufficiently accurate neutron self-shielding and cover calculations. Some of the approximation formulas are described below.

Such approximate calculations are not necessarily applicable to all material types used for a specific reactor dosimetry application. The adequacy of the approximation may also be tested by using samples of different thickness, or comparing the results from dilute and non-dilute types of material. There are also a number of other effects that can have a significant impact on the calculation of activation rates, such as flux depression or the partial shielding of one sample by an adjacent sample. Such effects may not add linearly, especially when neutron scattering effects are significant.

II.1. USEFUL APPROXIMATIONS FOR COVER FOILS

The attenuation of neutrons in a neutron beam is given simply by the equation:

$$F = \exp(-x)$$

where $x = N\sigma t$, σ is the total neutron absorption cross-section and t is the thickness of the cover foil. This equation can be integrated over all angles for an isotropic neutron flux:

$$F = E_2(x)$$

where E_2 is the second exponential integral. Such a correction can then be applied to the neutron cross-section for any given activation reaction in each neutron energy group.

II.2. NEUTRON GROUP STRUCTURES FOR COVER OR SELF-SHIELDING CORRECTIONS

Since many neutron resonances are very narrow in width, a computer code such as LINEAR is required to process the point cross-sections so that the narrow neutron resonances will be adequately represented. Using a fixed group structure (such as the 640 groups in IRDF-2002) may not be adequate for reactions with narrow resonance structures. The cover and self-shielding calculations should be performed for each neutron energy group in the fine structure that results from the LINEAR processing code. Doppler broadening must also be taken into account at the temperature of the reactor experiments, using computer codes in the PREPRO2002 library available on the IAEA web site [II.1]. After the neutron self-shielding corrections have been applied to the

cross-sections in this manner, the very fine group cross-sections can then be collapsed to coarser group structures, which may be used in the neutron adjustment codes. Alternatively, computer codes have been developed to perform calculations of the neutron self-shielding corrections using the neutron resonance parameters directly. Although this process may be time consuming, the set of shielded activation cross-sections can be used routinely as long as the same geometry foils or wires are used, regardless of the application.

II.3. TABLES OF NEUTRON SELF-SHIELDING CORRECTIONS

Neutron self-shielding correction factors have been experimentally determined by irradiating foils or wires of varying thickness, with and without cadmium covers. The relevant tables can be found in the literature, for example in ASTM Standard Test Method E262 for Determining Thermal Neutron Reaction and Fluence Rates by Radioactivation Techniques. However, these tables list the neutron self-shielding corrections separately for the thermal and resonance integrals of only a few types of material, including cobalt, gold and indium. While such data can be used to determine corrections to very simple reactor dosimetry experiments involving only these types of material or for estimating the magnitude of such corrections, they are not generally applicable to reactor dosimetry applications. Furthermore, this approach is not appropriate to neutron spectral adjustment procedures, since the tabulated data can only be used to correct reaction rates prior to spectral adjustment. The neutron cross-sections are preferably shielded rather than the reaction rates. Spectral adjustments will then not depend on any prior assumptions concerning the thermal or epithermal neutron flux.

II.4. APPROXIMATION FORMULAS COMMONLY USED FOR NEUTRON SELF-SHIELDING

Reactor dosimetry measurements are frequently performed with relatively small foils or wires of such a size that the mean free path for neutron scattering tends to be larger than the sample dimensions. Therefore, the neutron self-shielding factor can be approximated by neglecting the neutron scattering effects. Formulas can then be derived to determine the neutron self-shielding for any given geometry, assuming an isotropic neutron flux. Such an assumption is generally acceptable for the thermal and epithermal neutron flux, and the derivation of such formulas is given in Refs [II.2, II.3]. Neutron self-shielding calculations should be performed for each neutron cross-section

of each neutron energy group. These shielded cross-sections can then be used in spectral adjustment codes so that neutron self-shielding can be properly calculated independent of the neutron energy spectrum. If cover materials such as boron, cadmium or gadolinium are also used, these corrections should also be applied to the neutron cross-sections prior to spectral adjustment.

Consider an isotropic neutron flux on a small foil for which the neutron self-shielding factor is given by:

$$G = \frac{(1 - 2E_3)}{2x} \tag{I.1}$$

where

G is the self-shielding factor;
E_3 is the third exponential integral of x;
x is $N\sigma_t a$;
σ_t is the total neutron absorption cross-section;
a is the mean chord defined as $2V/S$, where V is the volume and S is the surface area (as the size of the foil increases, a approaches the thickness of the foil).

The self-shielding factor for an isotropic neutron flux on wires is given by:

$$G = 2x/3\ \{2x[K_1I_1 + K_0I_0] - 2 + K_1I_1/x - K_0I_1 + K_1I_0\} \tag{II.2}$$

where K_n and I_n are Bessel functions of the parameter x, as defined above. If the parameter x is less than 0.5, G can be closely approximated by:

$$G = 2E_3\ (-8x/3\pi) \tag{II.3}$$

The total absorption cross-section is nearly equal to the neutron activation cross-section in many cases of interest. However, under certain circumstances, other neutron reactions may need to be included if the thermal cross-sections or resonance integrals for these reactions are significant relative to the total absorption cross-sections and resonance integral.

II.5. BURNUP CORRECTIONS

Nuclear burnup corrections may be required for reactions that have relatively high reaction rates involving either the target or product isotope.

Burnup is defined as the nuclear transmutation of a given isotope, and the correction for the nuclear burnup of a stable target isotope is given by:

$$B = [1 - \exp(-\sigma\varphi t)] \tag{II.4}$$

where:

B is the burnup correction factor (i.e. the ratio of the measured reaction rate to the true reaction rate);
φt is the neutron fluence for the irradiation;
σ is the spectral averaged cross-section;
t is the irradiation time;
φ is the total neutron flux.

$\sigma\varphi$ can be defined as the product of the activation cross-section and the neutron flux spectrum integrated over the entire neutron energy spectrum, and is also equal to the total activation rate in product atoms per target atoms per second that can be calculated from reactor dosimetry activation measurements. Prior to neutron spectral adjustment, measured activation data are converted to these saturated activation rates. Equation (II.4) may be applied in order to determine if a burnup correction may be required for a specific reaction. However, if the burnup is significant, the measured reaction rate will be much lower than the true reaction rate as implied in Eq. (II.4). Furthermore, the possibility of burnup of the product atoms has to be considered, which may well be at a higher rate than that of the target atoms. The more general form of the burnup equation (which also takes into account the decay of the product atom) is given by:

$$B = \lambda[\exp(-\sigma_a\varphi t) - \exp(-\sigma_b\varphi t)]/[(\lambda + \sigma_b\varphi - \sigma_a\varphi)(1 - \exp(-\lambda t))] \tag{II.5}$$

where:

B is the ratio of the measured reaction rate to the true reaction rate;
σ_a and σ_b are the spectral averaged cross-sections for the target and product atom, respectively;
λ is the decay constant for the product isotope.

As noted above, this equation requires that the true reaction rates be known, whereas only a measured reaction rate for the target reaction may be known. This problem can be easily solved by applying an iterative procedure. Given a measured and uncorrected reaction rate for the target isotope, the

activation rate for the product isotope can be estimated from the σ_b/σ_a ratio, using the thermal neutron cross-sections and resonance integrals for both the target and product isotopes. The burnup correction can then be calculated, applied to the target and product reaction rates, and then successively recalculated until convergence is attained. Unless the burnup corrections are very large, this process generally converges to a stable value after only a few iterations.

REFERENCES TO APPENDIX II

[II.1] INTERNATIONAL ATOMIC ENERGY AGENCY, PREPRO2002, IAEA, Vienna (2002); the computer code is available on the IAEA web site at http://www-nds.iaea.at or http://www-nds.iaea.at/pub/endf/prepro/

[II.2] CASE, K.M., DE HOFFMAN, F., PLACZEK, G., Introduction to the Theory of Neutron Diffusion, Los Alamos Scientific Lab., NM (1953).

[II.3] INTERNATIONAL ATOMIC ENERGY AGENCY, Neutron Fluence Measurements, Technical Reports Series No. 107, IAEA, Vienna (1970).

Appendix III

COMPARISON OF THERMAL CROSS-SECTIONS AND RESONANCE INTEGRALS FOR DOSIMETRY REACTIONS

A. Trkov

IRDF-2002 contains cross-sections for 66 reactions, of which 17 represent radiative capture. Verification and validation of the cross-section data from various sources are important steps in the selection of the source data and for validation of the final dosimetry library. Therefore, a comparison of the evaluated data from different sources was made using the following:

(a) Mughabghab evaluation of the thermal cross-sections and resonance integrals [III.1];
(b) Q_0 values, which are the ratios of the resonance integral to thermal cross-section from the k_0 database for neutron activation analysis (NAA) [III.2].

The Mughabghab compilation, commonly known as BNL-325, is the most comprehensive compilation of thermal cross-sections and resonance integrals and has been recently revised by the author.

Activation analysis is in some sense 'reverse dosimetry'. Well tested and applied in practice, the nuclear data for activation analysis are highly relevant to a dosimetry database. The k_0 standardization method is a variant of activation analysis, and requires the Q_0 value for each nuclide. The Q_0 values for several nuclides have been measured, usually by the cadmium ratio method, which is insensitive to the detector efficiency and the abundance of the nuclide in a natural mixture of an element.

The following evaluated nuclear data libraries were considered in the present study:

(i) The old IRDF-90.2 dosimetry library [III.3];
(ii) The JENDL-D/99 dosimetry library [III.4];
(iii) The latest Japanese JENDL-3.3 evaluated nuclear data library [III.5];
(iv) US library ENDF/B-VI Release 8 [III.6];
(v) European Activation File EAF-99 [III.7];
(vi) The new evaluations for ^{139}La and ^{186}W by Zolotarev [III.8].

III.1. THERMAL CROSS-SECTIONS

Generally, there is reasonably good agreement between the cross-section values in evaluated nuclear data files at the thermal energy of 0.253 eV, but there are a number of exceptions, which are listed below (see also Table III.1):

— ^{58}Fe: The adopted thermal cross-section is the value re-evaluated by Moxon [III.9], and differs marginally from the latest Mughabghab recommendation (1.30(2) b). JENDL-3.3 data are consistent with the Mughabghab recommendation, while all other evaluations are lower by more than 12% and lower still compared with the old value by Mughabghab of 1.28(5) b [III.10].
— ^{63}Cu: The uncertainty assigned to the Mughabghab value is very low; JENDL-3.3 data are consistent with the Mughabghab recommendation.
— ^{109}Ag: The observed differences arise because the dosimetry cross-sections represent excitation of the metastable state, while Mughabghab gives the total capture cross-section. No corrective action is needed at present.
— ^{115}In: The same argument applies as for ^{109}Ag.
— ^{139}La: The uncertainty assigned to the thermal capture cross-section by Mughabghab is very small. The value from ENDF/B-VI Release 8 agrees with the latest Mughabghab recommendation, while other evaluated data files adopted the older and lower Mughabghab value.
— ^{181}Ta: The thermal capture cross-section from JENDL-3.3 agrees with the Mughabghab recommendation.
— ^{186}W: The new Mughabghab recommendation for the thermal cross-section of 38.5 b is slightly higher than the old value of 37.9 b. JENDL-D/99 and the Zolotarev evaluation follow the old recommendation. The JENDL-3.3 value is higher than the new Mughabghab recommendation. The value from the new Zolotarev evaluation is closest to the new Mughabghab recommendation.
— ^{232}Th: The data from the evaluated libraries agree, but are slightly higher than the Mughabghab recommendation.
— ^{238}U: The Mughabghab recommendation is slightly lower than the value recommended for the ENDF/B-VI standards. A more detailed investigation indicates that the ENDF/B-VI value is strongly influenced by the measurement of Bigham, which may be incorrect [III.11]. Other recent measurements are consistent (after corrections) with the Mughabghab value.

TABLE III.1. COMPARISON OF THERMAL CAPTURE CROSS-SECTIONS FROM VARIOUS SOURCES

Target	Product	Mughabghab 2002		Note	IRDF-90.2		JENDL-D/99		JENDL-3.3		ENDF/B-VI Release 8		EAF-99		Zolotarev	
		σ_0 (b)	$\Delta\sigma_0$ (%)		σ_0 (b)	Diff. (%)	σ_0 (b)	Diff. (%)	σ_0 (b)	Diff. (%)	σ_0 (b)	Diff. (%)	σ_0 (b)	Diff. (%)	σ_0 (b)	Diff. (%)
Na-23	Na-24	0.53	0.9		5.28E-01	–0.3	5.32E-01	0.3	5.32E-01	0.3	5.28E-01	–0.3	5.32E-01	0.3		
Sc-45	Sc-46	27.2	0.7		2.72E+01	0.1	2.72E+01	–0.1	2.72E+01	–0.1	2.72E+01	–0.1				
Cr-50	Cr-51	15.9	1.3				1.59E+01	0.3	1.60E+01	0.9	1.59E+01	0.3	1.60E+01	0.4		
Mn-55	Mn-56	13.36	0.4		1.34E+01	0.4	1.34E+01	0.4	1.34E+01	0.4	1.34E+01	0.4				
Fe-58	Fe-59	1.316	1.9	a1	1.15E+00	–12.6	1.30E+00	–1.1	1.301E+00	–1.1	1.151E+00	–12.5	1.15E+00	–12.5		
Co-59	Co-60	37.18	0.2		3.72E+01	0.2	3.72E+01	0.0	3.72E+01	0.1	3.72E+01	0.1	3.72E+01	0.1		
Cu-63	Cu-64	4.52	0.4	a2	4.47E+00	–1.0	4.51E+00	–0.3	4.509E+00	–0.2	4.472E+00	–1.1				
Nb-93	Nb-94m	1.15	4.3		1.156E=00	0.5			1.15E+00	0.0	1.156E+00	0.5				
Ag-109	Ag-110m	91	1.1	a3	4.69E+00		4.17E+00		9.06E+01		4.46E+00					
In-115	In-116m	202	1.0	a4	2.11E+02		1.62E+02		2.01E+02		1.67E+02		7.21E+01			
La-139	La-140	9.04	0.4	a5					8.94E+00	–1.1	9.00E+00	–0.4			8.90E+00	–1.6
Eu-151	Eu-152	9200	1.1				9.21E+03	0.1	9.18E+03	–0.3	9.18E+03	–0.2				
Ta-181	Ta-182	20.5	2.4	a6			2.07E+01	0.9	2.07E+01	0.9	2.11E+01	3.1				
W-186	W-187	38.5	1.3	a7			3.79E+01	–1.6	3.95E+01	2.6	3.75E+01	–2.6			3.79E+01	–1.5
Au-197	Au-198	98.65	0.1		9.88E+01	0.1	9.87E+01	0.1			9.88E+01	0.2	9.87E+01	0.1		
Th-232	Th-233	7.35	0.4	a8	7.40E+00	0.7	7.41E+00	0.8	7.41E+00	0.8	7.41E+00	0.8	7.41E+00	0.8		

TABLE III.1. COMPARISON OF THERMAL CAPTURE CROSS-SECTIONS FROM VARIOUS SOURCES (cont.)

Target	Product	Mughabghab 2002		Note	IRDF-90.2		JENDL-D/99		JENDL-3.3		ENDF/B-VI Release 8		EAF-99		Zolotarev	
		σ_0 (b)	$\Delta\sigma_0$ (%)		σ_0 (b)	Diff. (%)	σ_0 (b)	Diff. (%)	σ_0 (b)	Diff. (%)	σ_0 (b)	Diff. (%)	σ_0 (b)	Diff. (%)	σ_0 (b)	Diff. (%)
U-238	U-239	2.68	0.7	a9	2.71E+00	1.1	2.72E+00	1.5	2.72E+00	1.5	2.72E+00	1.5	2.72E+00	1.5		

Notes:

Diff.: Difference relative to Mughabghab.

Fe-58 (a1): Re-evaluation by Moxon (JEF/DOC-831), differing marginally from the Mughabghab value (1.3 ± 2%).

Cu-63 (a2): JENDL-3.3 agrees with the Mughabghab evaluation within the uncertainty interval, which is very small.

Ag-109 (a3): Mughabghab does not give the cross-section for the excitation of the metastable state.

In-115 (a4): Mughabghab does not give the cross-section for the excitation of the metastable state.

La-139 (a5): ENDF/B-VI Release 8 agrees with the Mughabghab recommendation.

Ta-181 (a6): JENDL-3.3 agrees with the Mughabghab recommendation.

W-186 (a7): The new evaluation by Zolotarev is closer to the Mughabghab evaluation.

Th-232 (a8): All evaluated data libraries agree, but are slightly higher than the Mughabghab recommendation.

U-238 (a9): The Mughabghab recommendation is slightly lower than the value recommended for the ENDF/B-VI standards.

III.2. Q_0 VALUES

Only the values that are marked as 'reliable' in the k_0 database are included in the intercomparison (see also Table III.2). As specified in Refs [III.2, III.12], most of the measured data originate from two laboratories: the WWWR-SM reactor at the Central Research Institute for Physics, Budapest (labelled KFKI) and the THETIS reactor at the Institute for Nuclear Sciences, Gent (labelled INW). The Mughabghab recommendation is defined as the ratio of the resonance integral to the thermal cross-section, and the uncertainty is the sum of relative uncertainties. Comparison of the ratio for metastable products is valid if the assumption can be made that the branching ratio is independent of energy. Evaluated data files that give explicitly the excitation functions for metastable states support this assumption. The ratio values derived from evaluated data files are calculated as the ratio of the resonance integral (see below) and the thermal cross-section in the same file. The following nuclides exhibit discrepancies:

— ^{55}Mn: The capture reaction is considered standard in the k_0 NAA, and the resonance integral and thermal cross-section by Mughabghab were adopted for the k_0 database. The Q_0 value is reduced by 0.5% if the most recent Mughabghab recommendation for the thermal capture cross-section is used. Direct measurements show good consistency [III.2] (KFKI: 1.035 ± 4.5%, INW: 1.097 ± 3.9%, 1.077 ± 3.3%, 1.041 ± 3.9%), with a mean value of 1.062 ± 2.8%, where the uncertainty is the standard deviation. The maximum spread of any measurement from the mean does not exceed 3.3%. Since there is reasonably good agreement in the thermal cross-sections and Q_0 values from different sources, the resonance parameters in evaluated data files are suspect.
— ^{58}Fe: There is an extremely large discrepancy of more than 30% between the Q_0 value from the k_0 database and the Mughabghab recommendation. Resonance integrals in old publications might be susceptible to the natural abundance of ^{58}Fe, which was not known accurately for a long time. Direct measurements of Q_0 by the cadmium ratio method are not sensitive to the detector efficiency or the abundance. Direct measurements at several facilities show good consistency [III.2] (KFKI: 0.979 ± 2.1%, INW: 0.981 ± 1.9%, 0.975 ± 1.6%, 0.954 ± 2.9%), therefore they may be considered reliable. The Q_0 value derived from the JENDL-3.3 file shows less than 5% discrepancy from the value in the k_0 database.
— ^{59}Co: The value in the k_0 database was adopted from the literature and is in agreement with the Mughabghab recommendation. Direct measurements support a somewhat lower value [III.2].

TABLE III.2. COMPARISON OF CAPTURE RESONANCE INTEGRALS FROM VARIOUS SOURCES

Target	Product	Mughabghab 2002		Ref.	IRDF-90.2		JENDL-D/99		JENDL-3.3		ENDF/B-VI Release 8		EAF-99		Zolotarev	
		RI (b)	ΔRI (%)	$Q_0 \times \sigma_0$ (b)	RI	Diff. (%)	RI	Diff. (%)	RI	Diff. (%)	RI	Diff. (%)	RI	Diff. (%)	RI	Diff. (%)
Na-23	Na-24	0.311	3.2	0.3	3.05E-01	–2.4	3.01E-01	–3.8	3.01E-01	–3.9	3.05E-01	–2.4	3.00E-01	–4.0		
Sc-45	Sc-46	12	4.2	11.7	1.13E+01	–3.3	1.13E+01	–3.4	1.13E+01	–3.6	1.15E+01	–1.8				
Cr-50	Cr-51	7.8	5.1	8.4			7.07E+00	–16.1	7.17E+00	–14.9	7.15E+00	–15.1	7.09E+00	–15.9		
Mn-55	Mn-56	14	2.1	14.1	1.15E+01	–18.2	1.15E+01	–18.2	1.15E+01	–18.3	1.15E+01	–18.3				
Fe-58	Fe-59	1.7	5.9	1.3	1.487E+00	15.9	1.343E+00	4.7	1.33E+00	3.7	1.469E+00	14.5	1.47E+00	14.6		
Co-59	Co-60	75.9	2.6	74.1	7.37E+01	–0.5	7.48E+01	0.9	7.51E+01	1.3	7.50E+01	1.3	7.47E+01	0.8		
Cu-63	Cu-64	4.97	1.6	5.2	4.87E+00	–5.4	4.888E+00	–5.1	4.914E+00	–4.6	4.891E+00	–5.1				
Nb-93	Nb-94m	8.5	5.9	8.5	9.912E+00	17.3			9.403E+00	11.2	9.897E+00	17.1				
Ag-109	Ag-110m	1400	3.4		6.55E+01		6.78E+01		1.47E+03		1.48E+03					
In-115	In-116m	3300	3.0		3.27E+03		2.57E+03		3.20E+03		2.58E+03		3.21E+03			
La-139	La-140	12.1	5.0	11.2					1.16E+01	3.0	1.18E+01	5.5			1.19E+01	5.9
Eu-151	Eu-152	3300	9.1	6256.0			2.30E+03	–63.3	2.31E+03	–63.1	2.54E+03	–59.3				
Ta-181	Ta-182	660	3.5	682.7			6.58E+02	–3.6	6.60E+02	–3.4	7.39E+02	8.3				
W-186	W-187	485	3.1	527.5			4.78E+02	–9.4	5.28E+02	0.1	5.18E+02	–1.8			4.76E+02	–9.8
Au-197	Au-198	1550	1.8	1548.8	1.56E+03	1.0	1.56E+03	0.8			1.56E+03	0.8	1.56E+03	0.7		
Th-232	Th-233	85	3.5	84.7	8.57E+01	1.1	8.41E+01	–0.8	8.48E+01	0.0	8.58E+01	1.3	8.54E+01	0.7		
U-238	U-239	277	1.1	277.1	2.78E+02	0.1	2.78E+02	0.2	2.78E+02	0.3	2.78E+02	0.3	2.78E+02	0.3		

Notes:
Reference values (Ref.) are the product of the Q_0 value from the k_0 database and the σ_0 value of Mughabghab; differences (Diff.) refer and are relative to these reference values.
RI: Resonance integral.

— ^{93}Nb: There is good agreement between direct measurements for the k_0 database and published values from the literature [III.2]. Values derived from evaluated data files are significantly higher, and JENDL-3.3 data seem to be least discrepant.
— ^{115}In: Direct measurements for the k_0 database suggest a slightly higher value [III.2] compared with the Mughabghab recommendation. The values derived from evaluated data files are generally lower, and JENDL-D/99 and JENDL-3.3 show the smallest discrepancy. There might be a problem with the adopted cadmium factor due to overlapping resonances $F_{cd} = 0.93$ in direct measurements; cross-section data give a value of 0.973. A rough assessment of the impact of the change would give a Q_0 value of about 16.0, which is in good agreement with JENDL-3.3 data but slightly lower than the Mughabghab recommendation.
— ^{186}W: Measurements of the Q_0 value imply that the estimated cadmium factor of 0.908 due to overlapping resonances is incorrect [III.12]. Direct calculation using cross-sections to simulate the transmission of neutrons through a 1 mm cadmium layer results in a cadmium factor of about 1%, indicating that the Mughabghab recommendation is probably correct (the new Zolotarev evaluation and JENDL-D/99 are also consistent with this value).
— ^{197}Au: Gold is considered to be the 'ultimate' standard in k_0 NAA, and the literature value was adopted for the database.
— ^{232}Th: The literature value was adopted for the k_0 database, and is within the experimental uncertainty of a set of measurements that are slightly higher on average.
— ^{238}U: The literature value was adopted for the k_0 database, and is within the experimental uncertainty of a set of measurements that are slightly lower on average.

III.3. RESONANCE INTEGRALS

Resonance integrals were calculated by integrating the cross-sections from the evaluated data files over energy E with a $1/E$ weighting function between 0.55 eV and 2 MeV. The reference value for the comparison is the product of the Mughabghab thermal cross-section and the Q_0 value from the k_0 database. More discrepancies are observed in the resonance integrals, some of which are quite large (see also Table III.3):

— ^{23}Na: The resonance integrals from all libraries lie within (or very close to) the uncertainty of the Mughabghab recommendation; the value from ENDF/B-VI Release 8 is marginally better.

TABLE III.3. COMPARISON OF THE Q_0 RATIO INTEGRAL TO THERMAL CAPTURE CROSS-SECTIONS FROM VARIOUS SOURCES

Target	Product	Mughabghab			Note	Kayzero-96		IRDF-90.2		JENDL-D/99		JENDL-3.3		ENDF/B-VI Release 8		EAF-99		Zolotarev	
		Q_0	ΔQ_0 (%)	Diff. (%)		Q_0 (Ref.)	ΔQ_0 (%)	Q_0	Diff. (%)	Q_0	Diff. (%)	Q_0	Diff. (%)	Q_0	Diff. (%)	Q_0	Diff. (%)	Q_0	Diff. (%)
Na-23	Na-24	0.587	4.2	–0.5		0.59	4.7	5.78E-01	–2.1	5.66E-01	–4.2	5.65E-01	–4.2	5.78E-01	–2.1	5.65E-01	–4.3		
Sc-45	Sc-46	0.441	4.9	2.6		0.43		4.16E-01	–3.3	4.16E-01	–3.3	4.15E-01	–3.4	4.23E-01	–1.7				
Cr-50	Cr-51	0.491	6.4	–7.4		0.53	2.4			4.44E-01	–16.3	4.47E-01	–15.7	4.49E-01	–15.3	4.44E-01	–16.2		
Mn-55	Mn-56	1.048	2.5	–0.5	a1	**1.053**	**2.6**	8.57E-01	–18.6	8.57E-01	–18.6	8.56E-01	–18.7	8.56E-01	–18.7				
Fe-58	Fe-59	1.292	7.8	32.5	a2	**0.975**	**1.0**	1.293E+00	32.6	1.032E+00	5.8	1.022E+00	4.8	1.277E+00	31.0	1.28E+00	31.0		
Co-59	Co-60	2.041	2.8	2.4	a3	**1.993**	**2.7**	1.98E+00	–0.7	2.01E+00	0.9	2.02E+00	1.2	2.02E+00	1.2	2.01E+00	0.7		
Cu-63	Cu-64	1.100	2.1	–3.5		1.14		1.089E+00	–4.5	1.084E+00	–4.9	1.09E+00	–4.4	1.094E+00	–4.0				
Nb-93	Nb-94m	7.391	10.2	0.6	a4	**7.35**	**2.7**	8.574E+00	16.7			8.177E+00	11.3	8.559E+00	16.4				
Ag-109	Ag-110m	15.385	4.5			16.7		1.40E+01	–16.4	1.62E+01	–2.8	1.62E+01	–2.9	1.61E+01	–3.7				
In-115	In-116m	16.337	4.0		a5	**16.8**	**1.9**	1.55E+01	–7.7	1.59E+01	–5.3	1.59E+01	–5.4	1.55E+01	–7.7	1.59E+01	–5.5		
La-139	La-140	1.338	5.4	7.9		1.24	2.4					1.29E+00	4.2	1.31E+00	6.0			1.34E+00	7.7
Eu-151	Eu-152	0.359	10.2	–47.3		0.68				2.50E-01	–63.3	2.51E-01	–63.0	2.77E-01	–59.3				
Ta-181	Ta-182	32.195	5.9	–3.3		33.3				3.18E+01	–4.5	3.19E+01	–4.3	3.50E+01	5.0				
W-186	W-187	12.597	4.4	–8.0	a6	**13.7**	**1.8**			1.26E+01	–7.9	1.34E+01	–2.4	1.38E+01	0.9			1.26E+01	–8.4
Au-197	Au-198	15.712	1.9	0.1	a7	**15.7**	**1.8**	1.58E+01	0.8	1.58E+01	0.7			1.58E+01	0.6	1.58E+01	0.6		
Th-232	Th-233	11.565	3.9	0.3	a8	**11.53**	**3.6**	1.16E+01	0.4	1.14E+01	–1.6	1.15E+01	–0.7	1.16E+01	0.5	1.15E+01	0.0		

TABLE III.3. COMPARISON OF THE Q_0 RATIO INTEGRAL TO THERMAL CAPTURE CROSS-SECTIONS FROM VARIOUS SOURCES (cont.)

Target	Product	Mughabghab			Note	Kayzero-96		IRDF-90.2		JENDL-D/99		JENDL-3.3		ENDF/B-VI Release 8		EAF-99		Zolotarev	
		Q_0	ΔQ_0 (%)	Diff. (%)		Q_0 (Ref.)	ΔQ_0 (%)	Q_0	Diff. (%)	Q_0	Diff. (%)	Q_0	Diff. (%)	Q_0	Diff. (%)	Q_0	Diff. (%)	Q_0	Diff. (%)
U-238	U-239	103.358	1.8	0.0	a9	**103.4**	**1.3**	1.02E+02	–1.0	1.02E+02	–1.3	1.02E+02	–1.2	1.02E+02	–1.2	1.02E+02	–1.2		

Notes: Values in bold are marked highly reliable in the database calculated by means of the Kayzero software package ([III.2], released in 1996).
Reference (Ref.) values are from the Kayzero-96 k_0 database; all differences (Diff.) refer to this reference.
Mn-55 (a1): Literature value adopted (direct measurements average 1.063 ± 2.8%, maximum spread 1.097–1.035).
Fe-58 (a2): Average of direct measurements adopted.
Co-59 (a3): Literature value adopted (two direct measurements: 1.921 ± 2.8%, 1.912 ± 3%, average 1.916).
Nb-93 (a4): Direct measurements are consistent with values found in the literature.
In-115 (a5): The average of three direct measurements (each with uncertainty of about 3%) is adopted for Kayzero.
W-186 (a6): There seems to be a systematic error in the assumed cadmium factor in the k_0 database.
Au-197 (a7): 'Ultimate standard' — literature value adopted.
Th-232 (a8): Literature value adopted (three direct measurements average 11.77 ± 1.8%, maximum spread 12.0–11.6 with uncertainty ~2.5% each).
U-238 (a9): Literature value adopted (three direct measurements average 101.6 ± 2.0%, maximum spread 99.7–103.7 with uncertainty ~5% each).

— ^{50}Cr: Compared with the Mughabghab recommendation, all evaluated data libraries underpredict the resonance integral by approximately 15%. The Q_0 value from the k_0 database is not considered reliable enough to improve the estimate of the resonance integral.
— ^{55}Mn: Compared with the Mughabghab recommendation, all evaluated data libraries underpredict the resonance integral by the same amount, because they are probably based on the same resonance parameter set. Re-evaluation of the resonance parameters is required.
— ^{58}Fe: As discussed in the section on Q_0 values (see above), the recommended resonance integral may be incorrect and should be revisited. The resonance integral from JENDL-3.3 is reasonably consistent with the Q_0 value from the k_0 database.
— ^{63}Cu: The resonance integrals calculated from the evaluated data files agree reasonably well with the Mughabghab recommendation; the value derived from the Q_0 value in the k_0 database is not reliable enough to improve the estimate of the resonance integral.
— ^{93}Nb: The resonance integrals calculated from the evaluated data files are 11–17% higher than the Mughabghab recommendation.
— ^{109}Ag: The observed differences arise because the dosimetry cross-sections represent excitation of the metastable state, while Mughabghab gives the total capture cross-section. No corrective action is needed at present.
— ^{115}In: The same argument applies as for ^{109}Ag.
— ^{151}Eu: An extremely large discrepancy exists in the resonance integrals between the Mughabghab recommendation, the value derived from the k_0 database and those calculated from the evaluated data files. It is recommended that the resonance integral and the evaluation of the resonance parameters be reassessed.
— ^{181}Ta: The resonance integrals calculated from the evaluated data files agree reasonably well with the Mughabghab recommendation. The value derived from the Q_0 value in the k_0 database is not reliable enough to improve the estimate of the resonance integral.
— ^{186}W: The resonance integrals calculated from the cross-sections of the Zolotarev evaluation agree well with the Mughabghab recommendation. The value derived from the Q_0 value in the k_0 database is probably incorrect.

III.4. CONCLUSIONS

Table III.4 summarizes acceptable candidate evaluations for inclusion in the new IRDF-2002 dosimetry library, based solely on comparisons of the

TABLE III.4. CANDIDATE EVALUATED DATA FILES FOR THE IRDF-2002 DOSIMETRY LIBRARY

Nuclide	Candidate data files
^{23}Na	ENDF/B-VI Release 8
^{45}Sc	ENDF/B-VI Release 8; IRDF-90.2; JENDL-3.3
^{50}Cr	None (resonance integral inconsistency)
^{55}Mn	None
^{58}Fe	JENDL-3.3; JENDL-D/99
^{59}Co	All
^{63}Cu	All
^{93}Nb	JENDL-3.3
^{109}Ag	Metastable product: no comparison
^{115}In	JENDL-D/99; JENDL-3.3
^{139}La	ENDF/B-VI Release 8; JENDL-3.3; Zolotarev
^{151}Eu	None (resonance integral inconsistency)
^{181}Ta	JENDL-3.3
^{186}W	Zolotarev
^{197}Au	JENDL-D/99; ENDF/B-VI Release 8
^{232}Th	All
^{238}U	All

thermal cross-sections and the resonance integrals with the Mughabghab recommendations and the k_0 database. This analysis is intended to complement other selection criteria such as format correctness, completeness, internal consistency of other parameters and availability of covariance information.

Problem areas exist that need to be resolved:

— ^{50}Cr: The discrepancy between the Mughabghab recommendation and resonance parameter data in the files needs to be resolved.
— ^{55}Mn: The discrepancy between the Mughabghab recommendation and resonance parameter data in the files needs to be resolved.
— ^{58}Fe: The Q_0 value from the k_0 database suggests preference for JENDL-3.3 as the source data; the resonance integral should be reassessed.
— ^{151}Eu: The thermal capture cross-section is practically the same in all data sources. Although the resonance integral is less important, differences of almost a factor of three between measurements deserve further attention.

REFERENCES TO APPENDIX III

[III.1] MUGHABGHAB, S.F., Thermal Neutron Capture Cross Sections, Resonance Integrals and g-factors, Rep. INDC(NDS)-440, IAEA, Vienna (2003).

[III.2] DE CORTE, F., The k_0 Standardization Method, PhD Thesis, Rijksuniversiteit, Gent (1987).

[III.3] IRDF-90 Version 2 — The International Reactor Dosimetry File (KOCHEROV, N.P., McLAUGHLIN, P.K., Eds), Rep. IAEA-NDS-141, Rev. 2, IAEA, Vienna (1993).

[III.4] KOBAYASHI, K., et al., JENDL Dosimetry File 99, Rep. JAERI 1344, Japan Atomic Energy Research Institute, Tokai-mura (2002).

[III.5] SHIBATA, K., et al., Japanese Evaluated Nuclear Data Library, Version 3, Revision 3, JENDL-3.3, J. Nucl. Sci. Technol. **39** (2002) 1125.

[III.6] ROSE, P.F. (Ed.), ENDF/B-VI Summary Documentation, Rep. BNL-NCS-17541 (ENDF-201), Brookhaven Natl Lab., NY (1991); Data Library ENDF/B-VI Release 8, update 2001, by the US National Nuclear Data Center on behalf of the Cross-section Evaluation Working Group.

[III.7] SUBLET, J.-C., et al., The European Activation File: EAF-99 Cross Section Library, Rep. FUS 408, UKAEA, Culham, UK (1998).

[III.8] ZOLOTAREV, K.I., Institute of Physics and Power Engineering, Obninsk, personal communication.

[III.9] MOXON, M.C., The Thermal Activation Cross Section of Fe, Rep. JEF/DOC-831, NEA Data Bank, Issy-les-Moulinaux, France (2000).

[III.10] MUGHABGHAB, S.F., DIVADEENAM, M., HOLDEN, N.E., Neutron Cross Sections, Vol. 1, Neutron Resonance Parameters and Thermal Cross Sections, Parts A and B, Academic Press, New York (1981).

[III.11] TRKOV, A., et al., Revisiting the U-238 thermal capture cross section and gamma-ray emission probabilities from Np-239 decay, Nucl. Sci. Eng. **150** (2005) 336.

[III.12] SIMONITS, A., DE CORTE, F., EL NIMR, T., MOENS, L., HOSTE, J., Comparative study of measured and critically evaluated resonance integral to thermal cross-section ratios, Part II, J. Radioanal. Nucl. Chem. **81** (1984) 397.

Appendix IV

PLOTS OF CANDIDATE CROSS-SECTIONS FOR IRDF-2002

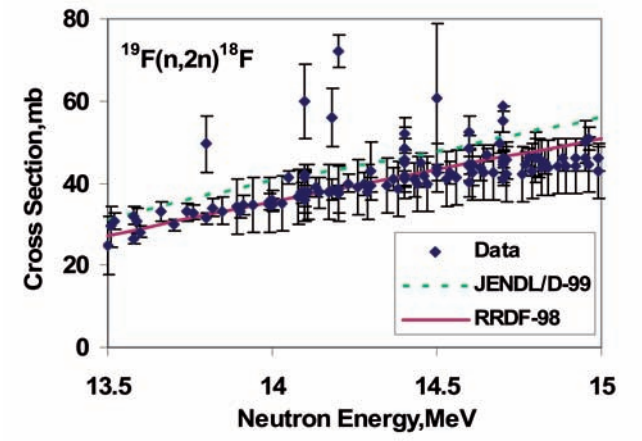

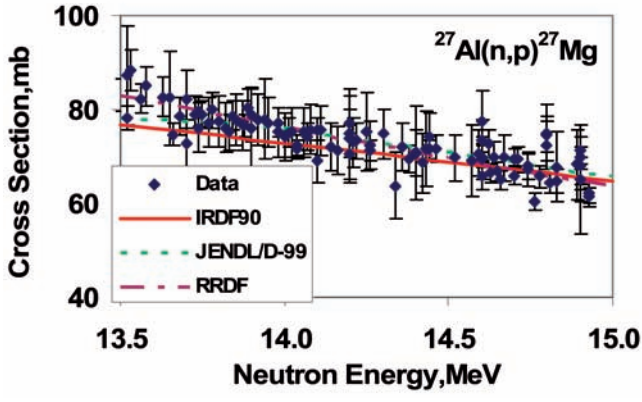

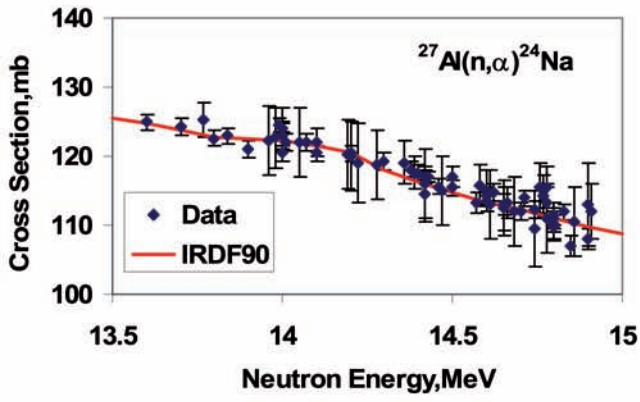
^{27}Al(n,α)^{24}Na
Cross Section,mb
Neutron Energy,MeV
Data
IRDF90
140
130
120
110
100
13.5
14
14.5
15

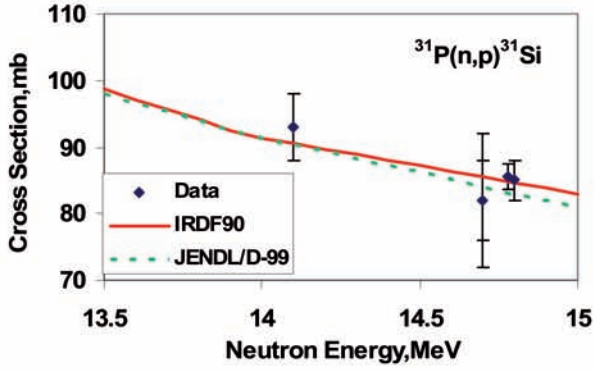
^{31}P(n,p)^{31}Si
Cross Section,mb
Neutron Energy,MeV
Data
IRDF90
JENDL/D-99
110
100
90
80
70
13.5
14
14.5
15

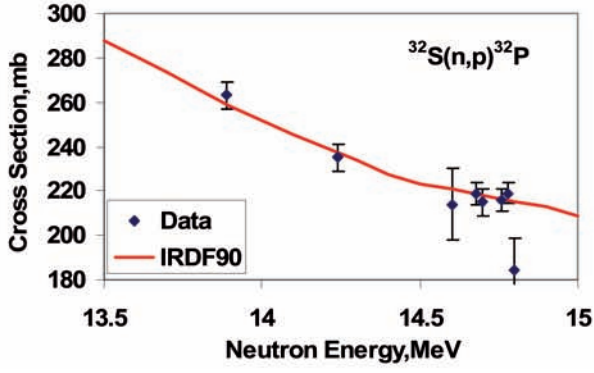
^{32}S(n,p)^{32}P
Cross Section,mb
Neutron Energy,MeV
Data
IRDF90
300
280
260
240
220
200
180
13.5
14
14.5
15

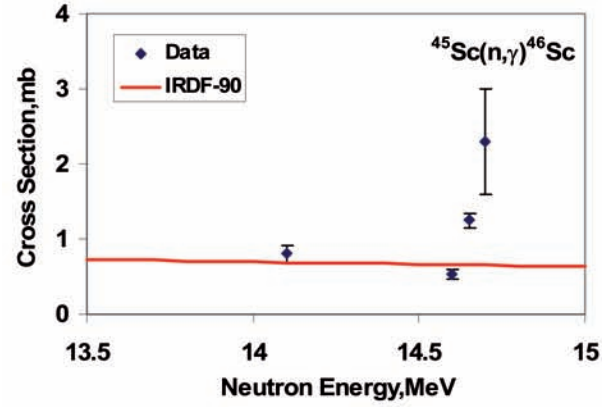
Data
IRDF-90
$^{45}Sc(n,\gamma)^{46}Sc$
Cross Section,mb
Neutron Energy,MeV
0
1
2
3
4
13.5
14
14.5
15

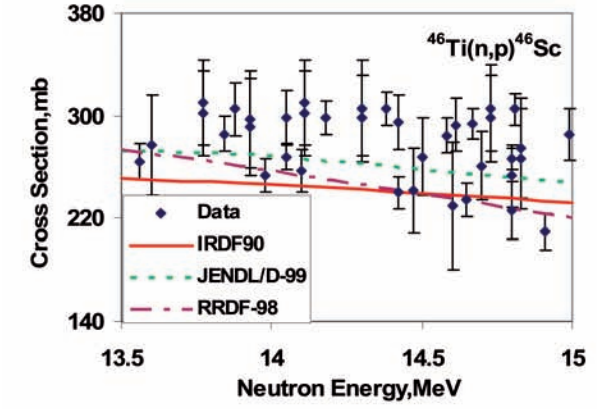
Data
IRDF90
JENDL/D-99
RRDF-98
$^{46}Ti(n,p)^{46}Sc$
Cross Section,mb
Neutron Energy,MeV
140
220
300
380
13.5
14
14.5
15

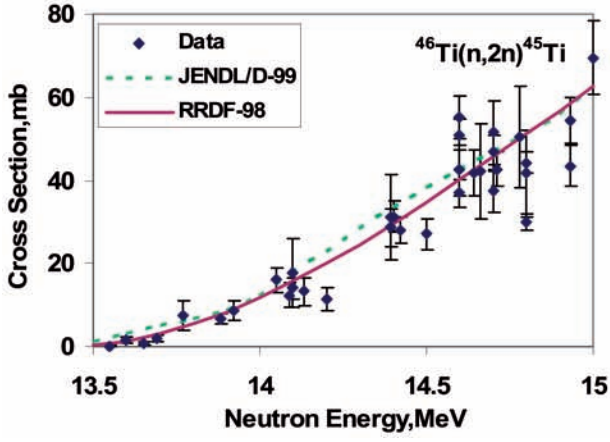
Data
JENDL/D-99
RRDF-98
$^{46}Ti(n,2n)^{45}Ti$
Cross Section,mb
Neutron Energy,MeV
0
20
40
60
80
13.5
14
14.5
15

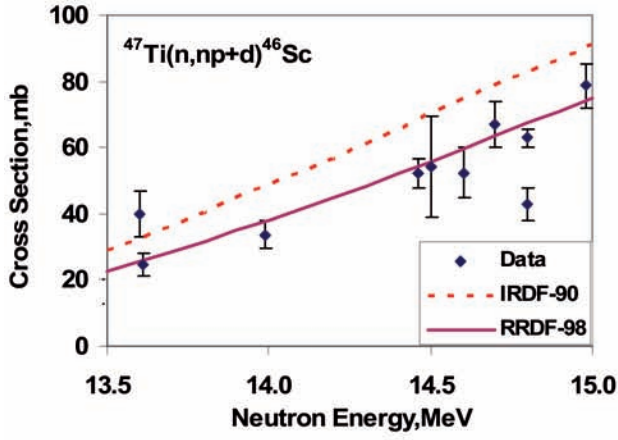
^{47}Ti(n,np+d)^{46}Sc
Cross Section,mb
Neutron Energy,MeV
Data
IRDF-90
RRDF-98
0
20
40
60
80
100
13.5
14.0
14.5
15.0

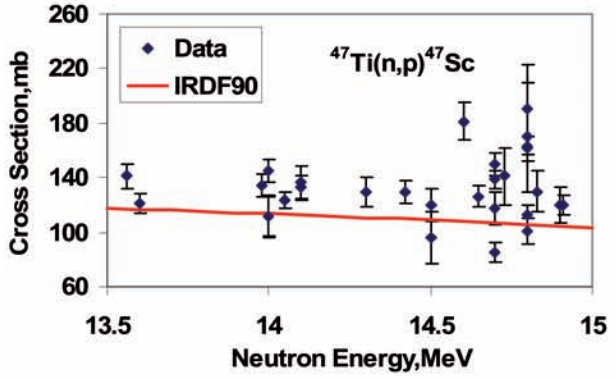
^{47}Ti(n,p)^{47}Sc
Cross Section,mb
Neutron Energy,MeV
Data
IRDF90
60
100
140
180
220
260
13.5
14
14.5
15

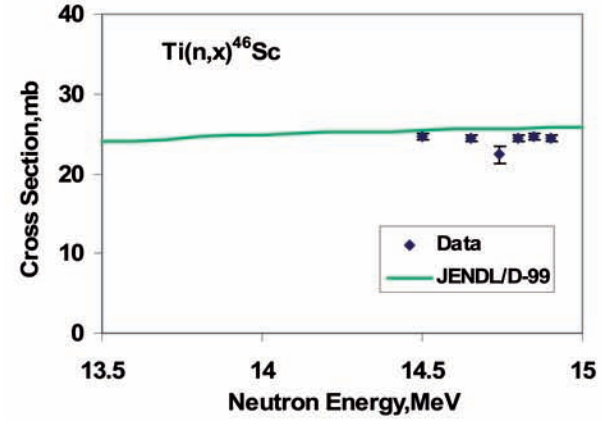
Ti(n,x)^{46}Sc
Cross Section,mb
Neutron Energy,MeV
Data
JENDL/D-99
0
10
20
30
40
13.5
14
14.5
15

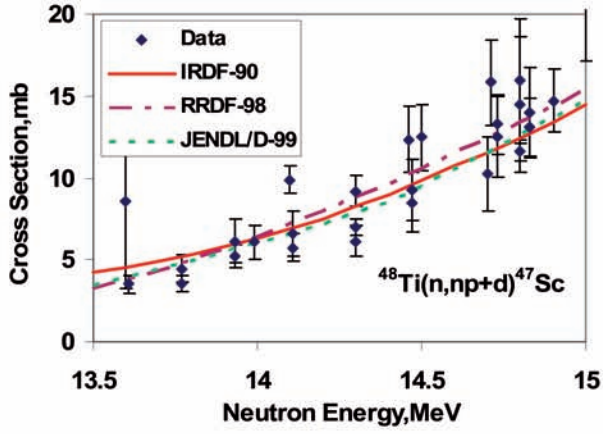
Data
IRDF-90
RRDF-98
JENDL/D-99
^{48}Ti(n,np+d)^{47}Sc
Cross Section,mb
Neutron Energy,MeV
0
5
10
15
20
13.5
14
14.5
15

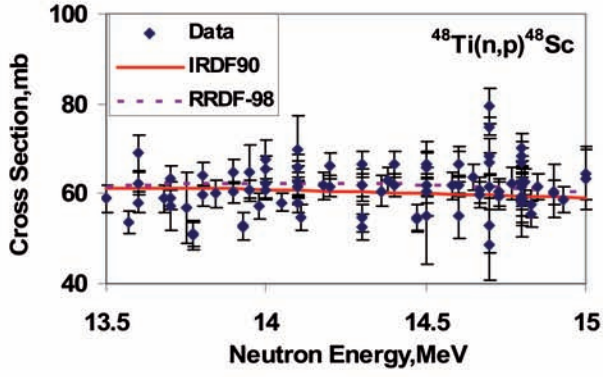
Data
IRDF90
RRDF-98
^{48}Ti(n,p)^{48}Sc
Cross Section,mb
Neutron Energy,MeV
40
60
80
100
13.5
14
14.5
15

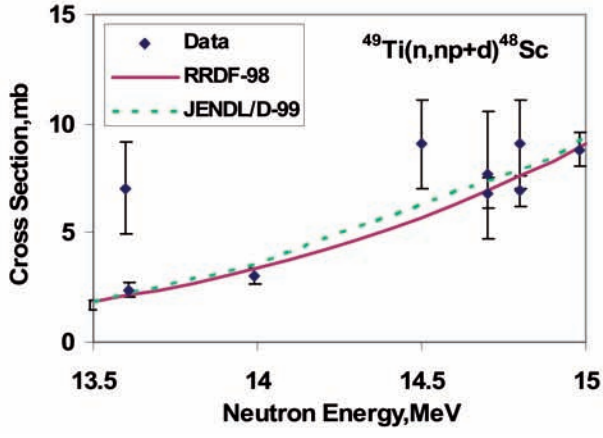
Data
RRDF-98
JENDL/D-99
^{49}Ti(n,np+d)^{48}Sc
Cross Section,mb
Neutron Energy,MeV
0
5
10
15
13.5
14
14.5
15

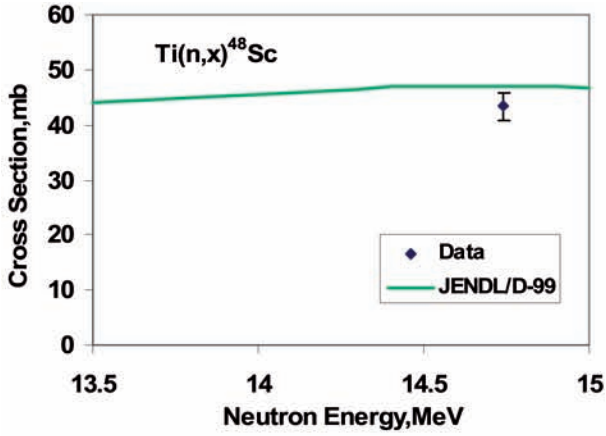
Ti(n,x)48Sc
Cross Section,mb
Neutron Energy,MeV
Data
JENDL/D-99
60
50
40
30
20
10
0
13.5
14
14.5
15

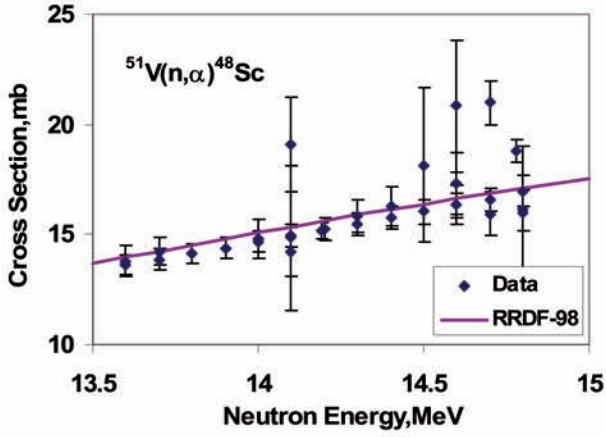
51V(n,α)48Sc
Cross Section,mb
Neutron Energy,MeV
Data
RRDF-98
25
20
15
10
13.5
14
14.5
15

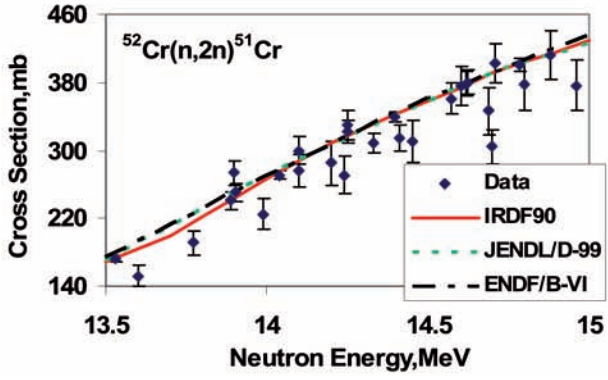
52Cr(n,2n)51Cr
Cross Section,mb
Neutron Energy,MeV
Data
IRDF90
JENDL/D-99
ENDF/B-VI
460
380
300
220
140
13.5
14
14.5
15

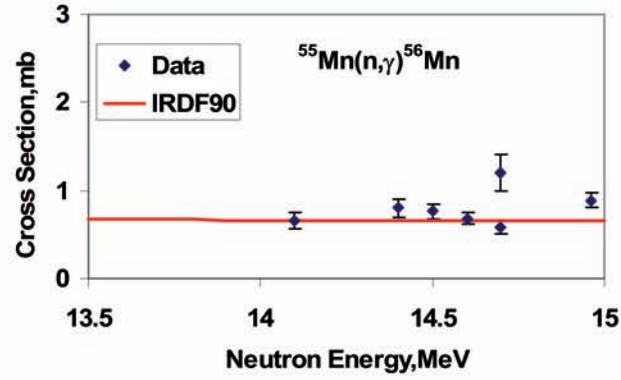
Cross Section,mb
3
2
1
0
Data
IRDF90
^{55}Mn(n,γ)^{56}Mn
13.5
14
14.5
15
Neutron Energy,MeV

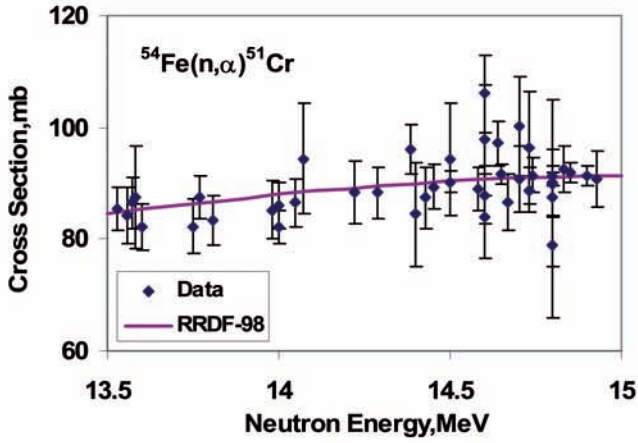
Cross Section,mb
120
100
80
60
^{54}Fe(n,α)^{51}Cr
Data
RRDF-98
13.5
14
14.5
15
Neutron Energy,MeV

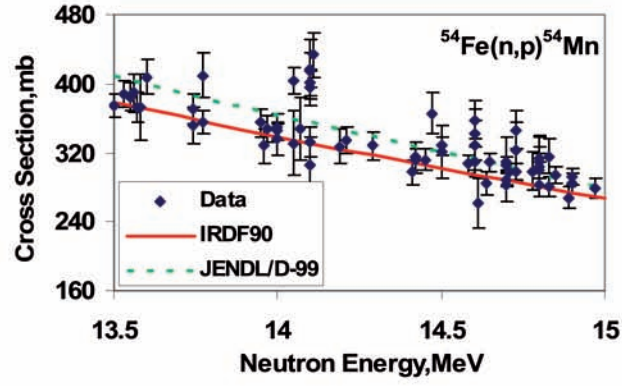
Cross Section,mb
480
400
320
240
160
^{54}Fe(n,p)^{54}Mn
Data
IRDF90
JENDL/D-99
13.5
14
14.5
15
Neutron Energy,MeV

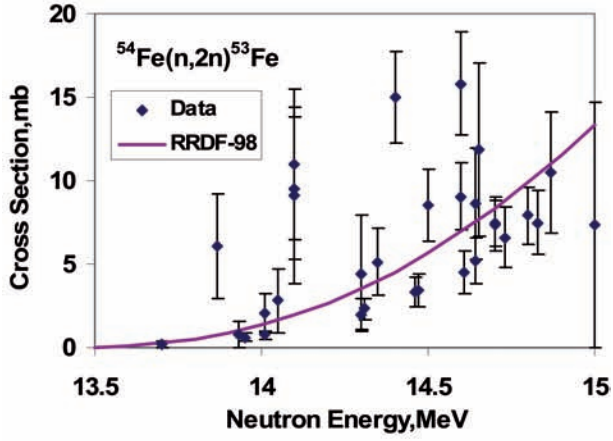
^{54}Fe(n,2n)^{53}Fe
Data
RRDF-98
Cross Section,mb
Neutron Energy,MeV
20
15
10
5
0
13.5
14
14.5
15

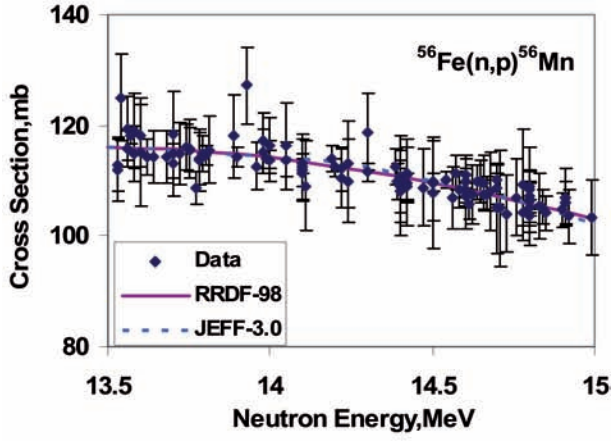
^{56}Fe(n,p)^{56}Mn
Data
RRDF-98
JEFF-3.0
Cross Section,mb
Neutron Energy,MeV
140
120
100
80
13.5
14
14.5
15

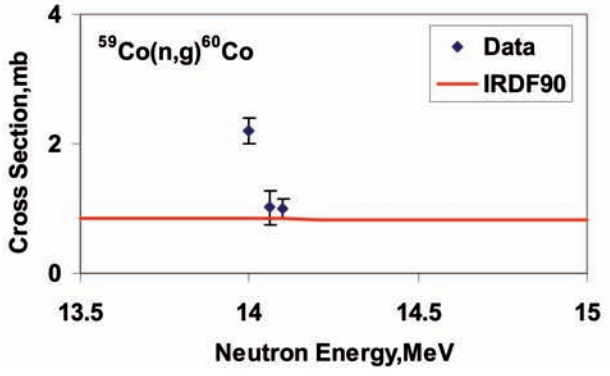
^{59}Co(n,g)^{60}Co
Data
IRDF90
Cross Section,mb
Neutron Energy,MeV
4
2
0
13.5
14
14.5
15

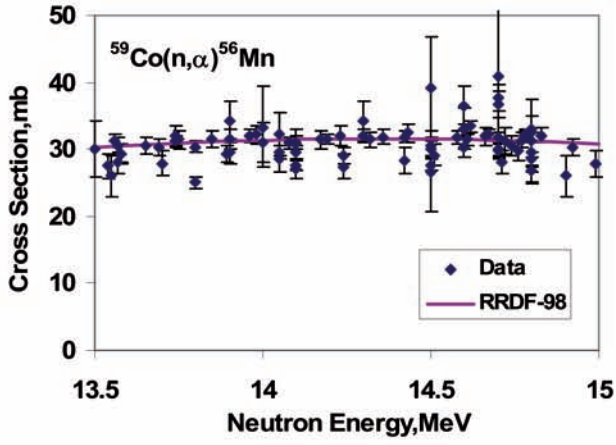
^{59}Co(n,α)^{56}Mn
Cross Section,mb
Neutron Energy,MeV
Data
RRDF-98
50
40
30
20
10
0
13.5
14
14.5
15

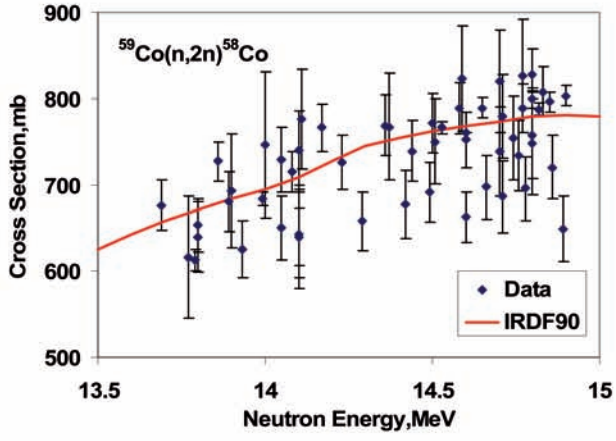
^{59}Co(n,2n)^{58}Co
Cross Section,mb
Neutron Energy,MeV
Data
IRDF90
900
800
700
600
500
13.5
14
14.5
15

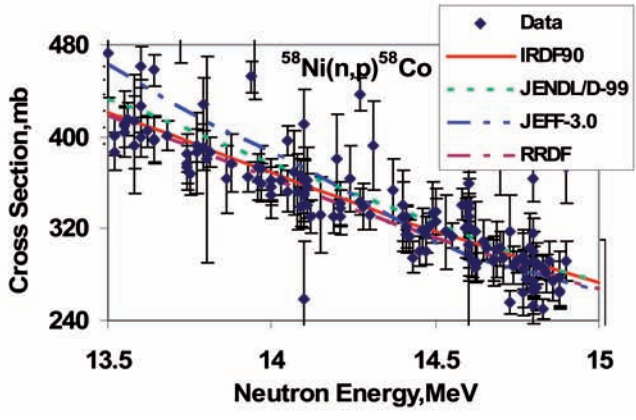
^{58}Ni(n,p)^{58}Co
Cross Section,mb
Neutron Energy,MeV
Data
IRDF90
JENDL/D-99
JEFF-3.0
RRDF
480
400
320
240
13.5
14
14.5
15

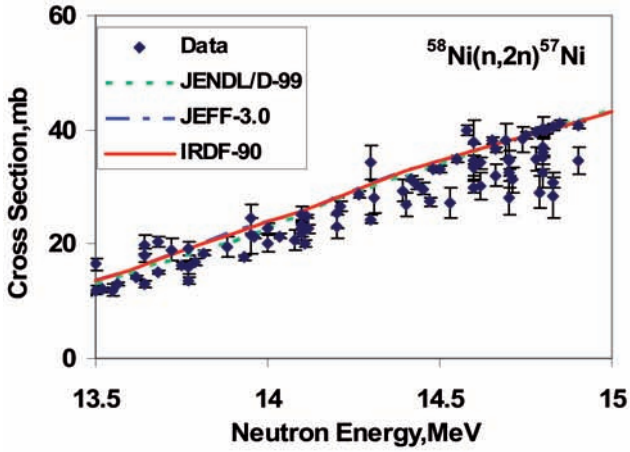
60
40
20
0
Cross Section,mb
Data
JENDL/D-99
JEFF-3.0
IRDF-90
58Ni(n,2n)57Ni
13.5
14
14.5
15
Neutron Energy,MeV

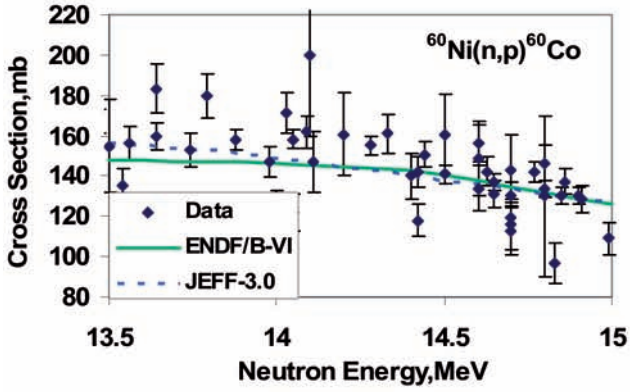
220
200
180
160
140
120
100
80
Cross Section,mb
60Ni(n,p)60Co
Data
ENDF/B-VI
JEFF-3.0
13.5
14
14.5
15
Neutron Energy,MeV

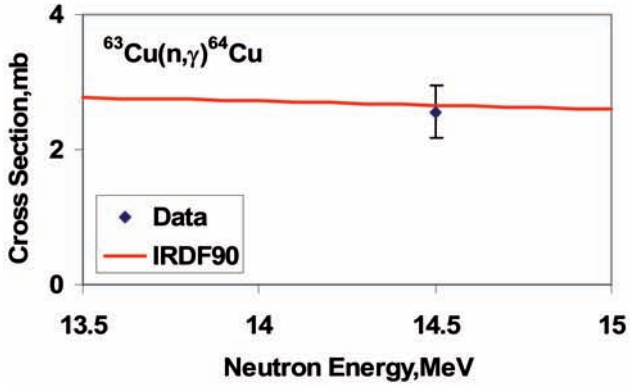
4
2
0
Cross Section,mb
63Cu(n,γ)64Cu
Data
IRDF90
13.5
14
14.5
15
Neutron Energy,MeV

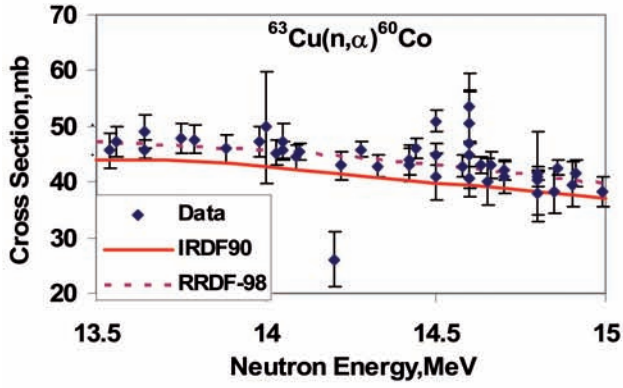
^{63}Cu(n,α)^{60}Co
Cross Section,mb
70
60
50
40
30
20
Data
IRDF90
RRDF-98
13.5
14
14.5
15
Neutron Energy,MeV

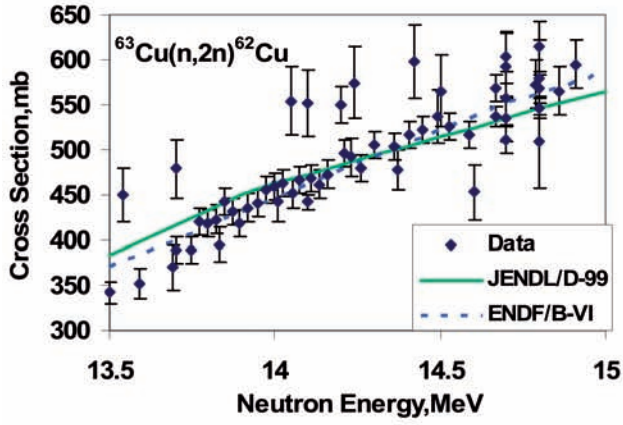
^{63}Cu(n,2n)^{62}Cu
Cross Section,mb
650
600
550
500
450
400
350
300
Data
JENDL/D-99
ENDF/B-VI
13.5
14
14.5
15
Neutron Energy,MeV

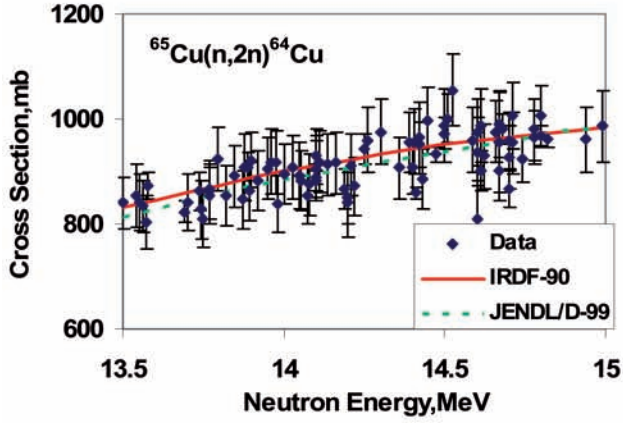
^{65}Cu(n,2n)^{64}Cu
Cross Section,mb
1200
1000
800
600
Data
IRDF-90
JENDL/D-99
13.5
14
14.5
15
Neutron Energy,MeV

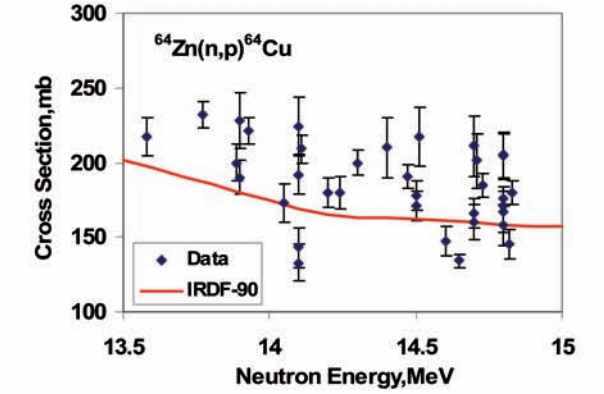
^{64}Zn(n,p)^{64}Cu
Cross Section,mb
Neutron Energy,MeV
Data
IRDF-90
300
250
200
150
100
13.5
14
14.5
15

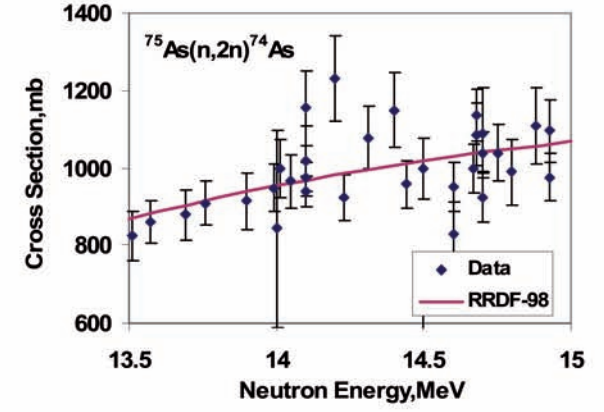
^{75}As(n,2n)^{74}As
Cross Section,mb
Neutron Energy,MeV
Data
RRDF-98
1400
1200
1000
800
600
13.5
14
14.5
15

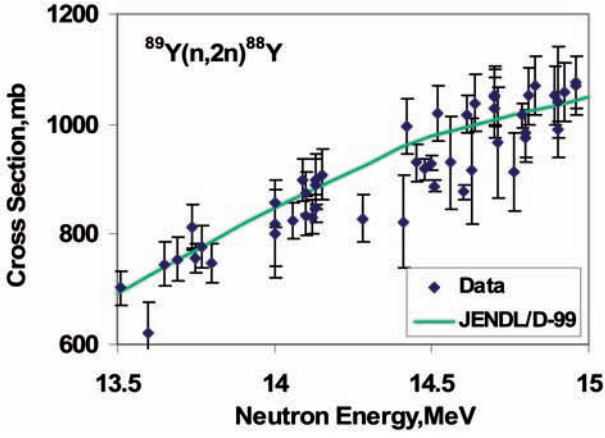
^{89}Y(n,2n)^{88}Y
Cross Section,mb
Neutron Energy,MeV
Data
JENDL/D-99
1200
1000
800
600
13.5
14
14.5
15

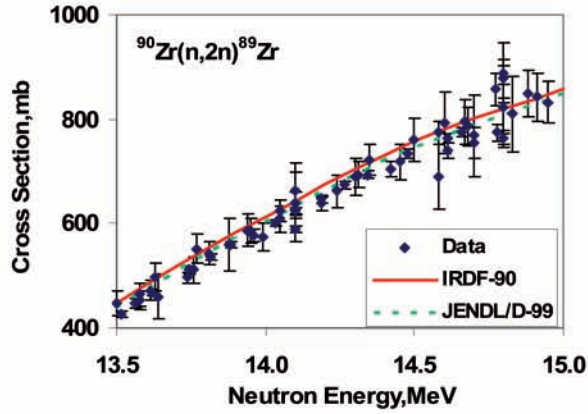
^{90}Zr(n,2n)^{89}Zr
Cross Section,mb
1000
800
600
400
13.5
14.0
14.5
15.0
Neutron Energy,MeV
Data
IRDF-90
JENDL/D-99

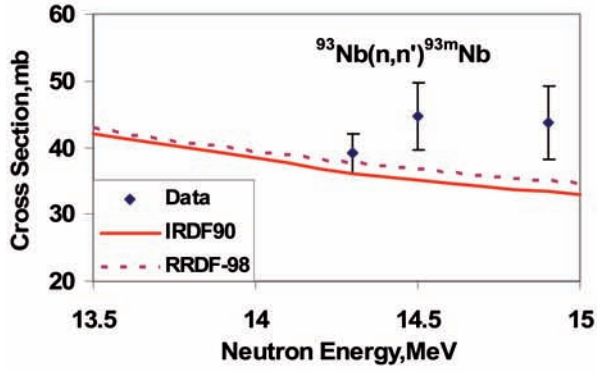
^{93}Nb(n,n')^{93m}Nb
Cross Section,mb
60
50
40
30
20
13.5
14
14.5
15
Neutron Energy,MeV
Data
IRDF90
RRDF-98

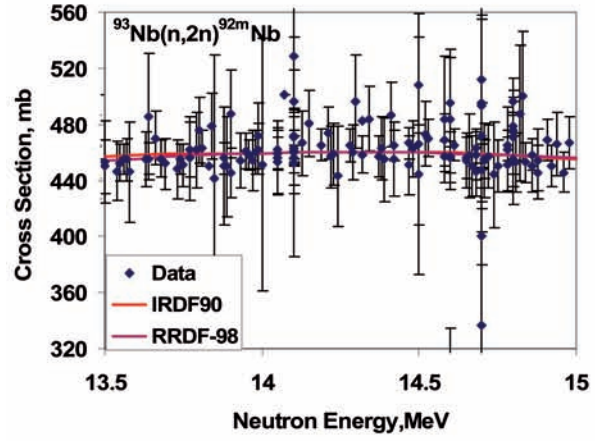
^{93}Nb(n,2n)^{92m}Nb
Cross Section, mb
560
520
480
440
400
360
320
13.5
14
14.5
15
Neutron Energy,MeV
Data
IRDF90
RRDF-98

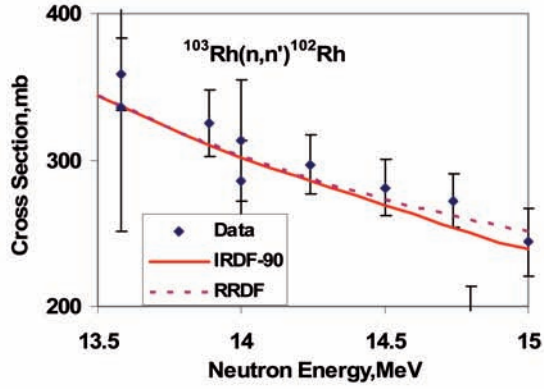
^{103}Rh(n,n')^{102}Rh
Cross Section,mb
400
300
200
13.5
14
14.5
15
Neutron Energy,MeV
Data
IRDF-90
RRDF

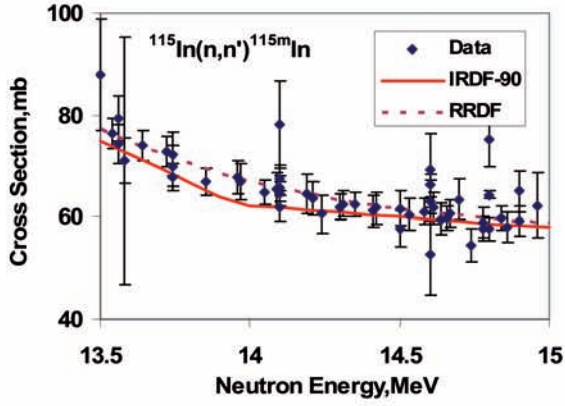
^{115}In(n,n')^{115m}In
Cross Section,mb
100
80
60
40
13.5
14
14.5
15
Neutron Energy,MeV
Data
IRDF-90
RRDF

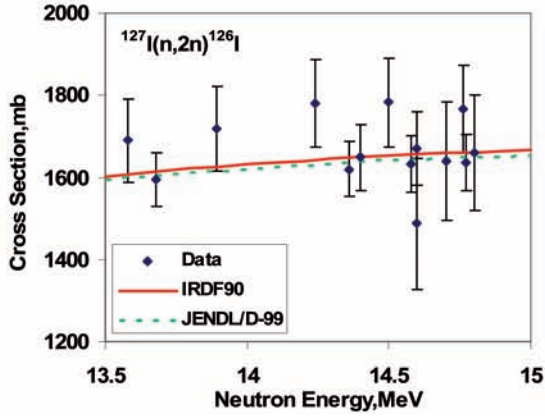
^{127}I(n,2n)^{126}I
Cross Section,mb
2000
1800
1600
1400
1200
13.5
14
14.5
15
Neutron Energy,MeV
Data
IRDF90
JENDL/D-99

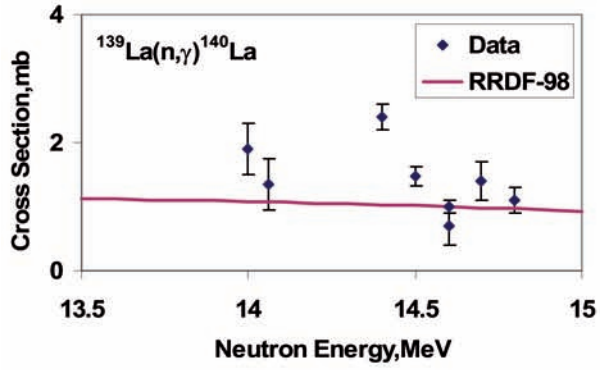
^{139}La(n,γ)^{140}La
Data
RRDF-98
Cross Section,mb
4
2
0
13.5
14
14.5
15
Neutron Energy,MeV

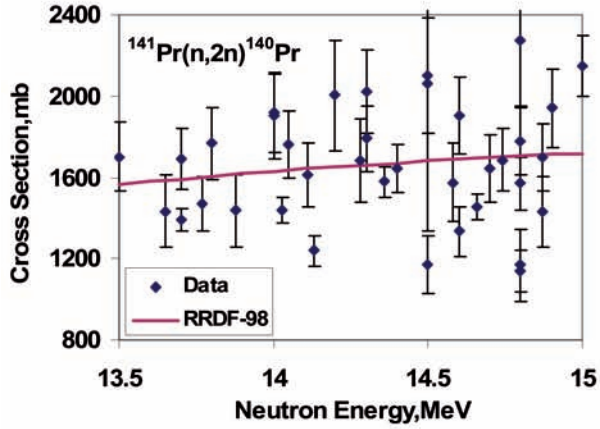
^{141}Pr(n,2n)^{140}Pr
Data
RRDF-98
Cross Section,mb
2400
2000
1600
1200
800
13.5
14
14.5
15
Neutron Energy,MeV

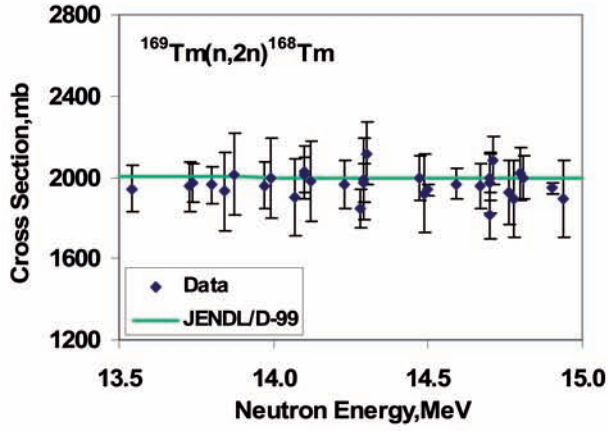
^{169}Tm(n,2n)^{168}Tm
Data
JENDL/D-99
Cross Section,mb
2800
2400
2000
1600
1200
13.5
14.0
14.5
15.0
Neutron Energy,MeV

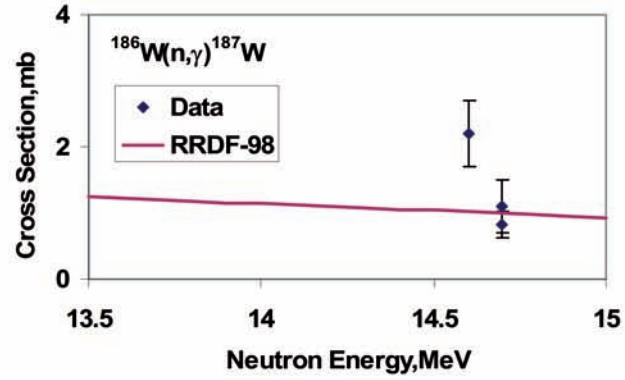
$^{186}W(n,\gamma)^{187}W$
Data
RRDF-98
Cross Section,mb
Neutron Energy,MeV
0
2
4
13.5
14
14.5
15

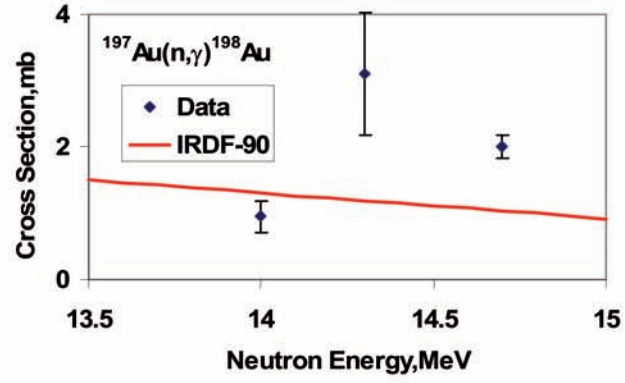
$^{197}Au(n,\gamma)^{198}Au$
Data
IRDF-90
Cross Section,mb
Neutron Energy,MeV
0
2
4
13.5
14
14.5
15

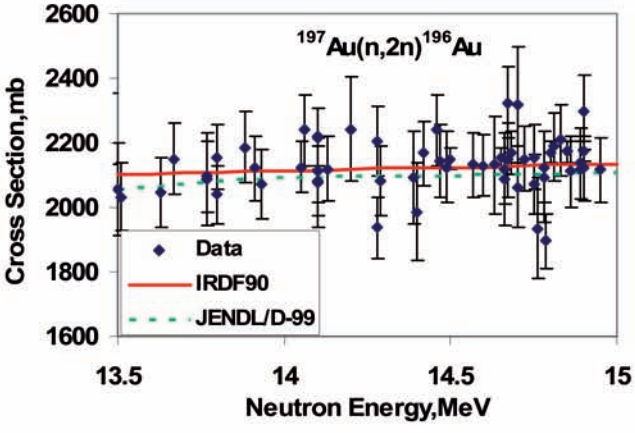
$^{197}Au(n,2n)^{196}Au$
Data
IRDF90
JENDL/D-99
Cross Section,mb
Neutron Energy,MeV
1600
1800
2000
2200
2400
2600
13.5
14
14.5
15

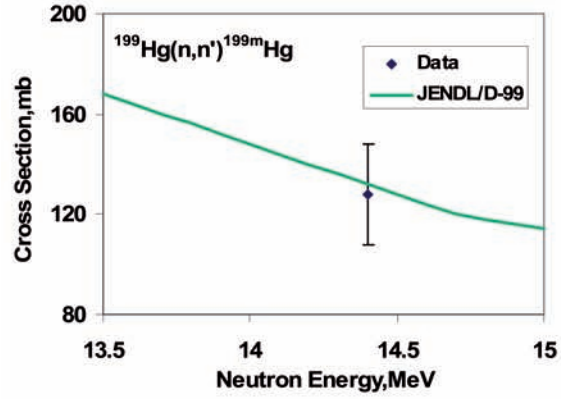
^{199}Hg(n,n')^{199m}Hg
Data
JENDL/D-99
Cross Section,mb
200
160
120
80
13.5
14
14.5
15
Neutron Energy,MeV

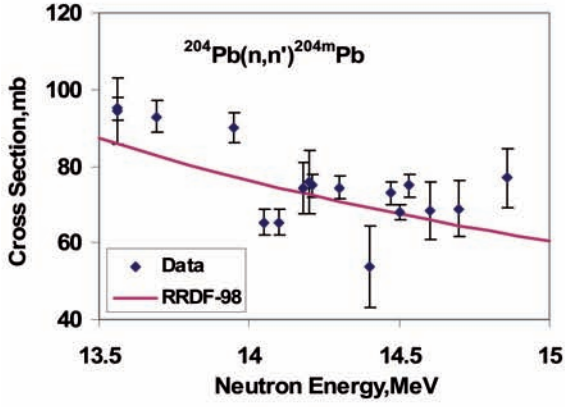
^{204}Pb(n,n')^{204m}Pb
Data
RRDF-98
Cross Section,mb
120
100
80
60
40
13.5
14
14.5
15
Neutron Energy,MeV

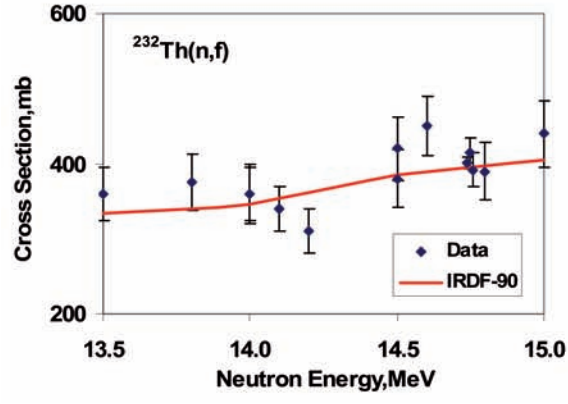
^{232}Th(n,f)
Data
IRDF-90
Cross Section,mb
600
400
200
13.5
14.0
14.5
15.0
Neutron Energy,MeV

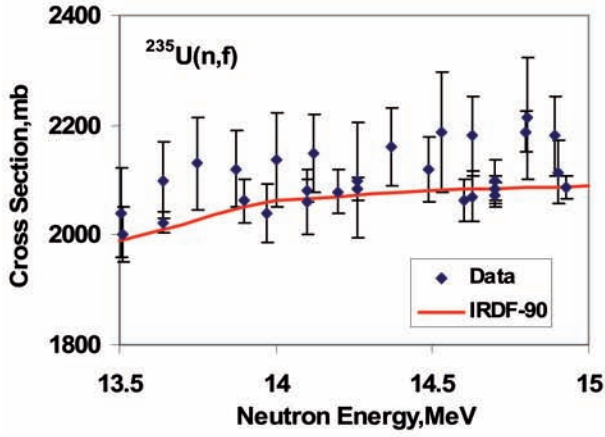
235U(n,f)
Cross Section,mb
2400
2200
2000
1800
13.5
14
14.5
15
Neutron Energy,MeV
Data
IRDF-90

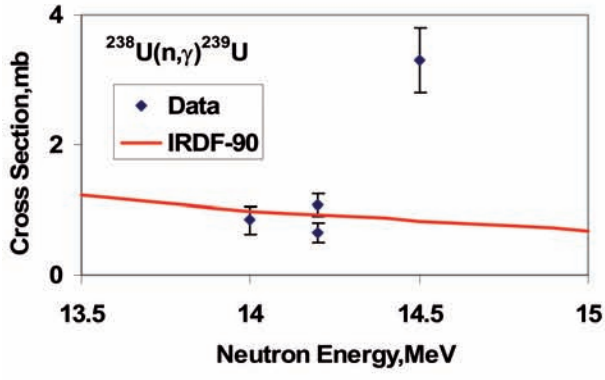
238U(n,γ)239U
Cross Section,mb
4
2
0
13.5
14
14.5
15
Neutron Energy,MeV
Data
IRDF-90

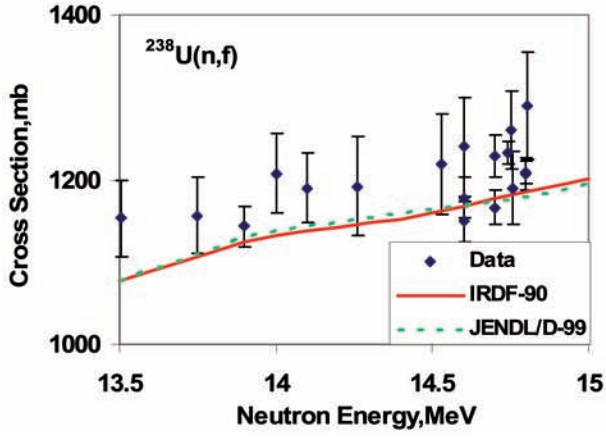
238U(n,f)
Cross Section,mb
1400
1200
1000
13.5
14
14.5
15
Neutron Energy,MeV
Data
IRDF-90
JENDL/D-99

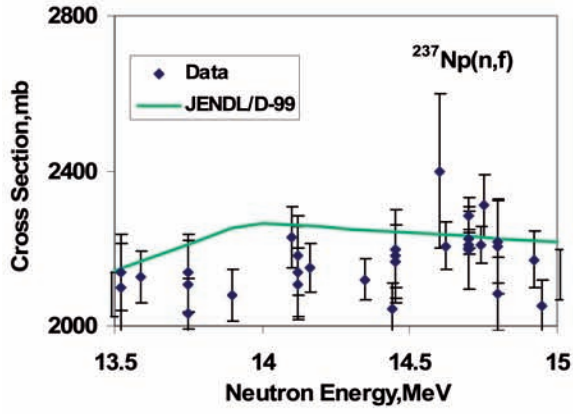
2800
2400
2000
Cross Section,mb
Data
JENDL/D-99
237Np(n,f)
13.5
14
14.5
15
Neutron Energy,MeV

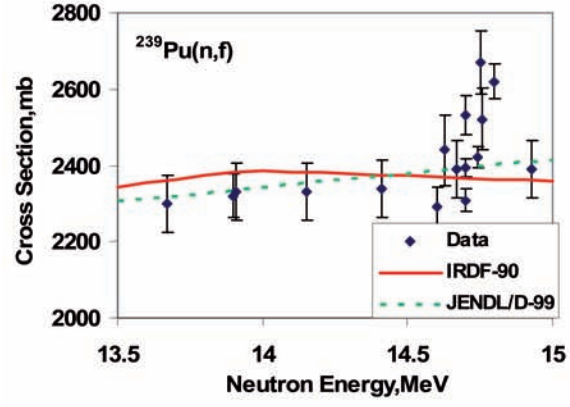
2800
2600
2400
2200
2000
Cross Section,mb
239Pu(n,f)
Data
IRDF-90
JENDL/D-99
13.5
14
14.5
15
Neutron Energy,MeV

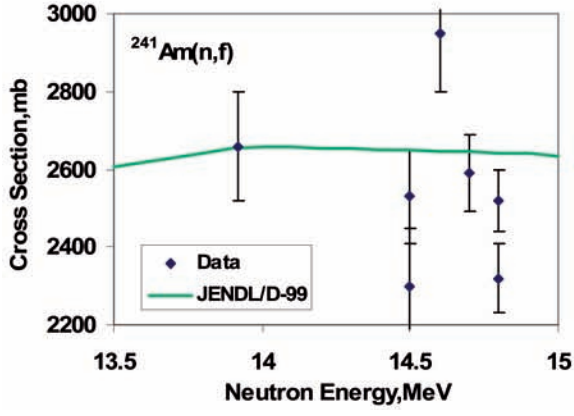
3000
2800
2600
2400
2200
Cross Section,mb
241Am(n,f)
Data
JENDL/D-99
13.5
14
14.5
15
Neutron Energy,MeV

CONTRIBUTORS TO DRAFTING AND REVIEW

Bersillon, O.	Commissariat à l'énergie atomique, France
Greenwood, L.R.	Pacific Northwest Laboratory, United States of America
Griffin, P.J.	Sandia National Laboratories, United States of America
Mannhart, W.	Physikalisch-Technische Bundesanstalt, Germany
McLaughlin, P.K.	International Atomic Energy Agency
Nolthenius, H.J.	Institute of Nuclear Techniques, Budapest University of Technology and Economics, Hungary
Nouri, A.	OECD Nuclear Energy Agency
Paviotti-Corcuera, R.	International Atomic Energy Agency
Shibata, K.	Japan Atomic Energy Agency, Japan
Trkov, A.	International Atomic Energy Agency
Zolotarev, K.I.	Institute of Physics and Power Engineering, Russian Federation
Zsolnay, E.M.	Institute of Nuclear Techniques, Budapest University of Technology and Economics, Hungary

INTERNATIONAL REACTOR DOSIMETRY FILE IRDF-2002 CD-ROM

The International Reactor Dosimetry File IRDF-2002 is an updated, standardized and benchmarked evaluated cross-section library of neutron dosimetry reactions with uncertainty information. This file has been assembled for lifetime management assessments of nuclear power reactors and other neutron metrology applications, such as boron neutron capture therapy, therapeutic uses of medical isotopes, nuclear physics measurements and reactor safety applications.

CONTENTS OF IRDF-2002 CD-ROM

This CD-ROM contains IRDF-2002 data and related information. The file 'index.html' provides a general description of the contents of the CD-ROM, and links both data and associated information:

1. Data files:
   - — Damage cross-sections;
   - — Decay data;
   - — Standard spectra;
   - — Dosimetry cross-sections in pointwise and groupwise ENDF-6 format;
   - — Codes for damage parameter and spectral adjustment calculations.
2. Plots that compare IRDF-2002 with other evaluated libraries and experimental data, including an interactive graphics package. Implemented via html, gif and pdf files — may need additional software.
3. Coordinated research project: general information, papers, reports and the final technical report.

ACCESS

Open 'index.html' under any browser on your computer and follow the links.
Type of computer: any (Windows, Linux, etc.).
Type of Internet browser: any (Internet Explorer, Netscape, Opera, etc.).
IRDF-2002 on the Web: http://www-nds.iaea.org/irdf2002/

An updated, tested and standardized reactor dosimetry cross-section database with associated uncertainty data and relevant decay data has been assembled to create a new data library for use in assessments of the service life of reactor pressure vessels. The resulting IRDF-2002 data library is available on CD-ROM and through the Internet; the selection procedure and contents are described in this publication. This set of recommended high quality data is also appropriate for use in other neutron metrology applications, such as boron neutron capture therapy, therapeutic uses of radioisotopes, nuclear physics measurements and reactor safety studies.

INTERNATIONAL ATOMIC ENERGY AGENCY
VIENNA
ISBN 92–0–105106–9
ISSN 0074–1914